Vol. 49 • No. 2

February 2006

Microwave Journal

RF Components and Systems

What's Hot in RF Components and Systems

UWB Low Loss Bandpass Filter

Salvan: Cradle of Wireless

horizon house

Founded in 1958

www.mwjournal.com

Microwave Journal

FEBRUARY 2006 VOL. 49 • NO. 2

FEATURES

COVER FEATURE

TECHNICAL FEATURES

Microwave Journal (USPS 396-250) (ISSN 0192-6225) is published monthly by Horizon House Publications Inc., 685 Canton St., Norwood, MA 02062. Periodicals postage paid at Norwood, MA 02062 and additional mailing offices.

POSTMASTER: Send address corrections to *Microwave Journal*, PO Box 3256, Northbrook, IL 60065-3256 or e-mail mwj@omeda.com. Subscription information: (847) 291-5216. This journal is issued without charge upon written request to qualified persons working in that part of the electronics industry, including governmental and university installation, that deal with VHF through light frequencies. Other subscriptions are: domestic, $120.00 per year, two-year subscriptions, $185.00; foreign, $200.00 per year, two-year subscriptions, $370.00; back issues (if available) and single copies, $10.00 domestic and $20.00 foreign. Claims for missing issues must be filed within 90 days of date of issue for complimentary replacement.

Posted under Canadian international publications mail agreement #0738654

Microwave Journal

FEATURES

DEPARTMENTS

STAFF

Publisher: Carl Sheffres
Associate Publisher: Edward Johnson
Editor: Harlan Howe, Jr.
Managing Editor: Keith W. Moore
Technical Editor: Frank M. Bashore
Associate Technical Editor: Dan Massé
Staff Editor: Jennifer DiMarco
Editorial Assistant: Barbara Walsh
Consulting Editor: Howard I. Ellowitz
Consulting Editor: Theodore S. Saad
Consulting Editor: Peter Staecker
Assistant to the Publisher: Kristen Dednah
Traffic Manager: Edward Kiessling
Traffic Administrator: Ken Hernandez
Director of Production & Distribution: Robert Bass
Design Director: R.A. Pike
DTP Coordinator: Janet A. MacDonald

EUROPE

Deputy Publisher: Michel Zoghob
European Editor: Richard Mumford
Office Manager: Eugenie Hardy

CORPORATE STAFF

Chairman: William Bazzy
President & CEO: Charles A. Ayotte
Executive Vice President: William M. Bazzy
Executive Vice President: Joan B. Egan
Senior Vice President & Group Publisher: David B. Egan

Executive Editorial Office:
685 Canton Street, Norwood, MA 02062
Tel: (781) 769-9750
FAX: (781) 769-5037
e-mail: mwj@mwjournal.com

European Editorial Office:
46 Gillingham Street, London SW1V 1HH, England
Tel: Editorial: +44 207 596 8730 Sales: +44 207 596 8740
FAX: +44 207 596 8749

www.mwjournal.com

Printed in the USA

What's Hot in RF Components and Systems

The 'information age' has seen the significant emergence of wireless applications mainly dedicated to improving the quality of people's lives (especially disabled and senior citizens), improving health, increasing the efficiency of air and road traffic, and bettering the environment. Over the last twenty years there has been a radical change from the days when communications were exclusively dedicated to military and governmental applications serving relatively few users to the situation today where the trend has been reversed with most applications devoted to the civilian market. The result is a huge increase in the number of customers, together with an increase in the number of applications, which results in an overcrowded frequency spectrum resulting from the continuous rise in the allocated frequencies and a radical change concerning the performance of the electronic modules required.

As is evident, there are various factors impacting on the development of RF components and systems that are being researched and investigated. For general communications systems, for example, there is the continuous movement towards smaller, secure systems that have increased functionality and reduced power consumption. These demands place severe constraints on circuit power dissipation and electromagnetic compatibility, and significantly increase the equipment design complexity, manufacturing costs and system weight.

One factor in particular that is gaining more and more importance is the noise exhibited by electronic modules. Today it is mandatory to realise high frequency receivers with very low noise behaviour. This requirement conflicts with the demand for increased operating frequencies, the reduction of power consumption and the rise in the number of users. Furthermore, the presence of several transmitters operating simultaneously on the same platform with multiple receivers requires very high dynamic range receivers, ultra-clean transmitters and careful attention to the overall electromagnetic compatibility design of the system. This usually requires filtering on both transmitters and receivers to ensure that they do not interfere with each other. Furthermore, the multiplication of the standard requires electronic modules to possess a certain degree of agility in order to optimise communication. The receiver or the transmitter has to switch to the standard or to the operator featuring the more efficient

Robert Plana
CNRS
Paris, France

characteristics. There are also similar requirements concerning battery and performance management. In fact, relating to the electromagnetic environment, the performance of the receiver/transmitter can be more or less relaxed in order to save energy, which is a key issue in the case of portable communications. In this case the system has to be smart enough to choose the best configuration by trading off the electrical performance (that is, linearity and noise figure) and the power consumption.

These requirements can be summarised by the statement: "The RF chip has to work properly anywhere, anytime and has to be as cheap as possible." The task of the system designers then can be tricky, as they have to identify the technology that will meet all of these requirements. To do so, the different ways that are being investigated today include:

- Miniaturisation
- Multifunctionality
- Heterogeneous integration
- Convergence between hardware and software technologies

These four main issues are explored through research at the material, technology, design, modeling and architecture level. With regards to the material level, competition now exists between the conventional approach that has been used in the past (GaAs, InP) and silicon-based materials (SiGe, MODFET, SiGe and HBT). For III-V based-materials, the more promising way seems to be the 'metamorphic' HEMT that combines the advantages of InP materials with those offered by GaAs. Furthermore, there is still research into heterogeneous epitaxy to grow III-V-based materials on silicon substrates and the emergence of a new family of nitride-based materials. GaN-based technology is showing very attractive capabilities for power applications in very harsh environments and has recently demonstrated interesting potential in the field of low noise applications, opening the way for very high integrated microwave systems in such conditions.

Concerning the silicon-based approach, SiGe-based technology (MODFET and HBT) is currently exhibiting frequency performance in the 400 GHz range. At the same time CMOS silicon-on-insulator (SOI) is showing significant potential with frequency performance above 100 GHz, thus opening up new paths for very highly integrated receivers featuring both analogue and digital processing potential offering more intelligence. CMOS for high frequencies necessitates research into dielectric materials in order to overcome the very high leakage current associated with reduced dimensions. This is achieved by using 'high k' material.

Finally, researchers are investigating an alternative approach that exploits nanomaterials and nanotechnologies. Some interesting results have already been produced that present the potential of carbon nano tubes, nanowires and the DOTFET approach that uses the quantum properties of a germanium-based island.

With regard to passive elements, the situation is becoming more complex as it is difficult to have materials featuring low insertion loss and a high quality factor from the microwave to millimetre-wave range. This is a major issue, particularly for miniaturisation, multifunctionality and heterogeneous integration. Here, we are seeing that III-V-based materials are still offering superior performance with respect to alternative silicon-based technology.

As for materials for passive elements, we are seeing that the multilayer approach results in an improvement in electromagnetic propagation. The use of polymer technologies (through thick layer) is an interesting alternative, especially as it is easily compatible with any other technology (such as GaAs, GaN, InP and SiGe).

Another solution that is emerging is the exploitation of the micromachining capabilities of semiconductor materials such as silicon, GaAs and InP. In particular, silicon is a very promising candidate as it is very easy to micromachine and all the technological processes are very mature. Additionally, these technologies will be compatible with the integrated circuits (IC) process (including digital ones) that will make it possible to realise high frequency modules featuring a high level of integration. Another attractive advantage of silicon-based technologies relates to its mechanical properties that make it possible to realise mobile regions through electrostatic, magnetic or thermal excitation that will result in devices featuring tuneable behaviour.

All these concepts come under the name of microelectromechanical systems (MEMS). MEMS technology offers the performance advantages of electromechanical components on size scales commensurate with single solid-state components. In many cases, a single MEMS component replaces and outperforms an entire solid-state circuit. In other cases, a judicious association of MEMS components with active devices will result in smart communicating devices. This defines a new concept for microwave and millimetre-wave systems that will combine MEMS technology with integrated circuits. This concept is referred to as MEMSIC and could be achieved in two different ways. One option is MEMS in IC, where all the devices are fabricated on the same chip and the appropriate micromachined process executed to improve the performance of the passive circuit, release the multifunctionality properties and have the antenna surrounding the chip. This approach is risky and probably will be developed in five to 10 years. A less risky approach consists of grafting the functionality on existing integrated circuits that is known as 'MEMS above IC.' Here, the system performance is tailored by grafting additional material and devices above the integrated circuits that could also include the antenna.

MEMS technology can also aid in the development of new transceiver architecture based on mechanical resonance properties, which today can be used in the 10 to 100 MHz range (the only limitation being related to the size of the component). However, moving to the 'nanoscale world,' specifically nano electromechanical system (NEMS) devices will see a transfer to resonance frequencies in the microwave range. The general belief today is that future telecommunications systems will encompass such devices. Nevertheless, it is important to assess their performance and to investigate the best technological process in terms of cost, reliability, performance and compatibility with integrated circuits. Besides these efforts at both the material and technology level, it is also important to assess the efforts that will be needed in the field of modeling, design, and component and system architecture.

As for the design and modeling, miniaturisation, multifunctionality and heterogeneous integration in relation to an increase in the multi-physic coupling and the multi-scale problems, which are currently not very well covered by commercial tools, it is important to develop research in this area. It is also understood that now we have to take into account all of these phenomena in the design process and it is important to develop a modeling strategy that will integrate these issues.

The requirements for the component architecture are on a different level. First of all, we need to define a component architecture that features high bandwidth characteristics in order to cover high bit rate requirements. Another important consideration is the power amplifier where it is crucial to feature high power-added efficiency and exhibit high reliability. In the field of low level signals and ultra stable signals and clocks, the key challenges are to fabricate low noise amplifiers that are not affected by the matching termination and feature ultra-low noise figures and high bandwidth. For RF and microwave sources, the phase noise is a quantity that determines the performance of the overall transceiver, and efforts are being made to propose architectures that minimize the phase fluctuations. Finally, for all these components, it is important to assess their potential for the reconfigurability that is achieved in different ways — the analogue approach using MEMS technologies and the digital one using the CMOS gates.

System architectures will need to be very compact, very secure and composed of the relevant building blocks in order to have a very robust design phase. This is a major issue in the effort to develop highly complex microwave and millimetre-wave systems featuring reconfigurability, and repair and testability functionalities. Here, the architecture should be revisited as there needs to be high convergence between analogue and digital technologies so as to better exploit the potential of each approach. Today, for instance, there is a tendency to avoid the testing of microwave and millimetre-wave systems by having the test facilities embedded in the chip itself. This is defining a new family of systems called millimetre-wave built in self-test (MWBIST) circuits. Another very promising application is the development of sensor networks deployed 'everywhere,' featuring a very high level of autonomy and intercommunication to carry out different missions. In this field, research is being instigated to develop ultra small intelligent systems utilising sensors, actuators, information processing and communication media through ad hoc networks. These ultra small systems will need to feature advanced architectures combining analogue and digital facilities and should have some software embedded.

These small communicating systems are known as 'smart dust' and represent a key challenge for microwave and millimetre-wave systems as they will combine hardware and software architectures in order to feature advanced functionalities and intelligence. They will be used in different applications in the industrial, civil and health sectors as well as the defence sector. This kind of RFID network is beginning to be implemented, although there is a strong need for networks featuring a high bit rate and then communicating in the millimetre-wave range.

This will necessitate research efforts at the material level in order to emphasize the heterogeneous integration, miniaturisation and multifunctionality. At the system level, research will be conducted in the design and architecture phase in order to define appropriate partitioning between hardware and software technologies to have intelligence embedded in these smart dusts.

As a final conclusion, future RF systems will result from a two-fold convergence in order to give some intelligence and autonomy to these systems — a convergence between different technologies and materials, and a convergence between hardware and software technologies. They should also be as small as possible to be transparent with respect to potential users that will be surrounded by billions of chips proposing services for different sectors. This will be the wireless revolution for ubiquitous communication that will be a strong economical challenge in the 21st century. ■

Robert Plana *was appointed director of the information and communication department at CNRS in 2005 and is now director of the engineering sciences department. In 2000, he became professor at Paul Sabatier University and Institut Universitaire de France, and started a research team at LAAS-CNRS in the field of micro and nanosystems for RF and millimetre-wave communications. Its main activities are in the technology, design, modeling, test, characterisation and reliability of RF MEMS for low noise and high power millimetre-wave applications, and the development of the MEMS IC concepts for smart microsystems. He has also built the AMICOM European Network of Excellence in this field, which encompasses 25 research groups.*

Harris Corp. Introduces Falcon Watch Remote Surveillance System

Harris Corp. unveiled an advanced sensor system product line that offers remote, unattended intrusion detection and surveillance capabilities ideally suited to the defense of military installations and perimeters, as well as for the protection of borders and other assets associated with homeland defense. The Harris Falcon Watch™ Remote Intrusion Detection and Surveillance system was developed by the Harris Sensor Systems Group, which is part of a new growth initiative within the Harris RF Communications Division, chartered to design products that are synergistic with the division's highly successful tactical radio business and adjacent markets. The Falcon Watch system includes the RF-5405 Intelligent Gateway, a communications node that receives alarms from multiple sensors and fuses the data into actionable reports for relay to command centers; and the RF-5400 Falcon® II Sensor Node, which is integrated with Harris Falcon® II tactical radios to provide situational awareness for the mobile user. The Harris Falcon Watch system utilizes seismic detectors, which detect ground vibration caused by vehicles or pedestrians; magnetic detectors, which detect the movement of metal objects such as weapons or vehicles; and passive infrared (PIR) sensors, which detect the movement of thermal signatures such as vehicles or pedestrians. The input is processed at the point of detection and then the resulting alarms are transmitted by radio to a monitoring point. Multiple radio relay nodes can be used to extend the system to protect larger-scale perimeters. The Harris Falcon Watch system is modular and configurable to address a broad range of threat or topographical environments. The system is specifically designed to withstand the rigors of harsh environments while operating in remote locations for very extended periods without battery replacement. The Harris Falcon Watch system detects the movement of vehicles and people while filtering out non-threatening, naturally occurring events. It transmits alarms to the Harris Falcon II RF-5400V-HH Advanced VHF Tactical Handheld Radio or the Falcon II RF-5800M-HH Advanced Multiband Tactical Handheld Radio. This allows the user to receive real-time sensor alerts directly, without carrying additional monitoring hardware. The sensor alarms can also be displayed by the Harris RF-6910 Situational Awareness System to provide a complete operational picture at a command center. The Falcon Watch Sensor system is available in various configurations. The Force Protection configuration is ideal for tactical, on-the-move missions by smaller squads and for temporary set-ups and deployments. It is small, lightweight, easy to use and features extended operational life as a result of its advanced low power techniques. Tactical radio integration results in less equipment that the soldier is required to carry and provides immediate notification of area intrusions. The Perimeter Surveillance of the Falcon Watch Sensor system is designed for applications requiring more complex detection and surveillance such as military installations, weapons depots and power-generation facilities. These extended deployment applications require more sophisticated security as provided by Harris Falcon II Tactical Radios, utilizing Harris Citadel® military-grade encryption and anti-jam technology. Falcon Watch also features capabilities for digital imaging and the option to display data and images on the Harris RF-6910 Falcon II Situational Awareness system.

Northrop Grumman Receives Joint STARS Upgrade Contract Worth $532 M

The US Air force has awarded Northrop Grumman Corp. a five-year, $532 M contract for the Joint Surveillance Target Attack Radar System (Joint STARS) System Improvement Program to provide system design and development improvements to the E-8C Joint STARS fleet. The contract covers the engineering, design, development, integration, test and delivery of various enhancements and upgrades to the Joint STARS fleet for the period of the contract. It also includes items such as technical orders, support equipment, initial spares and training and procurement of production and support system retrofit kits and documentation.

"This is an important step toward upgrading these low density, high demand aircraft to maintain their viability to the warfighter," said Dave Nagy, vice president of the Joint STARS program for Northrop Grumman. "Joint STARS will be the Defense Department's intelligence, surveillance and reconnaissance constellation for many years to come, so it is important that we can continue to add capability to this unique aircraft." The E-8C Joint STARS is the world's most advanced, wide-area airborne ground surveillance, targeting and battle management system. It detects, locates, classifies, tracks and targets hostile ground movements, communicating real-time information through secure data links with Air Force and US Army command posts.

All Joint STARS aircraft are assigned to the Georgia Air National Guard's 116th Air Control Wing, a "total force blended wing," based at Robins Air Force Base, Warner Robins, GA. The wing comprises active-duty Air Force, Army and Air National Guard personnel.

AACER System Would Detect Ground Targets

Development of an airborne radar that can search broadly for ground targets while transmitting data about them at Ka-band is the objective of the Affordable Adaptive Conformal ESA Radar (AACER) program awarded to Raytheon by the Defense Advanced Research Project Agency (DARPA). Raytheon was selected to proceed with Phase II of a planned three-phase, four-year program after a competitive down-select at the end of Phase I with Northrop Grumman Electronics Systems. The AACER system is a DARPA funded program being administered by the US Army Research Laboratory in Adelphi, MD. Intended for use on rotary, unmanned aerial vehicles in development by DARPA and the Army, the AACER system will feature ground moving target detection and track, dismount detection, synthetic aperture radar imaging and high data rate communications capability at Ka-band. The technology for electronic processing combines elements of Raytheon's APG-79 electronically scanned array radar for the F/A-18 and seeker technology from the company's Advanced Medium Range Air-to-Air Missile with innovative new low cost millimeter-wave hardware designs.

Raytheon Standard Missile-3 Intercept Challenging Ballistic Missile Target

A Raytheon Co.-produced Standard Missile-3 (SM-3) destroyed a ballistic missile target outside the earth atmosphere during a Missile Defense Agency/Aegis Ballistic Defense (BMD) Program flight test over the Pacific Ocean. It was the sixth successful intercept for the Aegis BMD program using the SM-3. The November 17 mission was the first test against a separate ballistic missile target. The SM-3 Block I initial deployment round used in the test was an operational missile delivered by Raytheon last year for testing and availability for emergency deployment. In the operationally realistic scenario, the SM-3 was launched from the USS Lake Erie, an Aegis BMD cruiser, and hit the target missile that had been launched from the US Navy's Pacific Missile range facility on Kauai, HI. The ship's crew was not informed of the target launch time and operational testers observed the exercise to ensure a realistic wartime environment. "SM-3 continues to perform flawlessly in increasingly challenging scenarios. This test, using a missile right from the Navy's inventory, was conducted in operational conditions," said Edward Miyashiro, Raytheon Missile Systems vice president, Naval Weapons Systems. "Continued success provides confidence that the nation can increase the number of systems deployed and make missile capability improvements. We are even seeing our international allies taking a closer look at SM-3 for their homeland defense. Sea-based ballistic missile defense provides a global capability." Japan has decided to procure SM-3 and the Aegis system for its Kongo class ships. Raytheon's Missile Systems business in Tucson, AZ, is developing SM-3 and leads the integrated team effort, which includes Alliant Techsystems, Aerojet and the Boeing Co. ■

European Ministers Formulate Space Strategy

Following a two-day meeting of the European Space Agency's (ESA) ruling Council the Ministers responsible for space in the ESA's 17 Member States and Canada formulated a coherent plan for discovery and competitiveness for Europe in space. They accordingly endorsed the continuation of a set of ongoing programmes and agreed to undertake major new initiatives designed to give Europe a clear vision and tangible means to further strengthen its space exploration and exploitation activities. They emphasised the need for Europe to maintain a competitive space sector able to lead the search for new discoveries, guarantee access to strategic data and new services, and consolidate its share of the global commercial market.

The Ministers reaffirmed the strategic importance of Europe continuously improving its scientific, technological and industrial capabilities in the field of space so as to enable it to better respond to the expectations of its citizens concerning the environment, quality of life and security. They also noted the increase in the volume and quality of the Agency's relations with its international partners. The Ministers recognised that the global scenario in the space sector is evolving rapidly, in particular with increasing numbers of players mastering major space technologies and offering competitive conditions for civil and dual-use applications.

A major political step was achieved with the approval of an overall European launcher policy ensuring coherence between the launcher and satellite fields. The Ministers also recognised that it is crucial to continuously foster European cooperation on space activity by further developing an overall European Space Policy encompassing ESA, the European Union, plus national and industrial programmes, and to allocate the available resources and capabilities to common European initiatives, so as to achieve the critical mass needed to face the worldwide competition.

Intel and QinetiQ Announce Chip Technology Breakthrough

As a result of research undertaken in conjunction with QinetiQ, Intel Corp. has announced development of a new, ultra-fast, yet very low power prototype transistor using new materials that could form the basis of its microprocessors and other logic products beginning in the second half of the next decade. The two companies' researchers have jointly demonstrated an enhancement-mode transistor using indium antimonide (InSb) to conduct electrical current. Intel anticipates using this new material to complement silicon, further extending Moore's Law.

InSb is a III-V compound semiconductor. This class of semiconductor is used for a variety of discrete and small-scale integrated devices such as radio-frequency amplifiers, microwave devices and semiconductor lasers. Although researchers from Intel and QinetiQ have previously announced transistors with InSb channels the new prototype transistors have a gate length of 85 nm, which is half the size of those previously disclosed. This is the first time that enhancement mode transistors have been demonstrated.

Ken David, director of components research for Intel's Technology and Manufacturing Group, commented, "By providing 50 percent more performance while reducing power consumption by roughly 10 times, this new material will give us considerable flexibility because we will have ability to optimise for both performance and power of future platforms."

Avago Emerges from Agilent Semiconductor Group Acquisition

Avago Technologies has begun operations as the world's largest privately held independent semiconductor company. Its creation follows the completion of the acquisition of Agilent Technologies Inc.'s Semiconductor Products Group by Kohlberg Kravis Roberts & Co. (KKR) and Silver Lake Partners in a $2.66 B transaction. Its heritage of technical innovation dates back to its Agilent/Hewlett-Packard roots.

The new company serves three primary product categories comprising RF/microwave components, optoelectronics and enterprise ASICs. It boasts an extensive portfolio of more than 5500 products, which are sold into a broad set of applications and end markets, including wireless and wired communications, industrial, automotive, consumer electronics, and storage and computing. Products are sold to more than 40,000 customers through both a worldwide distributor network and direct sales force.

Avago Technologies is co-headquartered in Singapore and San Jose, CA, US. It had net revenue of $1.8 B in fiscal 2005 and begins with 6500 employees of which 1000 are analogue design engineers. The company has over 35 years of operating history in Asia, where approximately three-quarters of its employees are located and where a significant portion of its products are produced.

Avago Technologies, Europe starts with a total of 220 employees in seven different countries. Sales and Marketing is headquartered in Boeblingen, Germany, and all 108 employees there have transferred from Agilent to the new company. Avago Technologies, Europe has an R&D site in Turin, Italy, a design centre in Germany and one in the UK as well as a sales presence in seven countries. Globally it maintains highly collaborative design and product development engineering resources, including five design centres in Asia, four in the United States, together with the two in Europe.

Galileo Concessionaire Maps Out Key Locations

In what is a major step forward for the Galileo European satellite radio navigation project, the future Galileo Concessionaire has agreed upon the locations of the various facilities under its responsibility that are required for the successful deployment of the programme.

Under the agreement the Headquarters of the Galileo Concessionaire will be located in Toulouse, France, with the Operations Company to be located in London, UK. The two Control Centres (Constellation and Mission) will be located in Germany and Italy as well as the two Performance Evaluation Centres supporting the concessionaire headquarters. Spain will host facilities that include redundancy for the Control Centres, and are related to Galileo safety critical applications. Furthermore, a new consortium of German companies will join the team, adding core competencies to the Concessionaire.

Following on, as it does, from the recent budgetary consensus, this landmark agreement clears the way for the efficient implementation of the programme supporting a commercial and best value for money approach to the Galileo Public Private Partnership.

Chipcon Acquired by Texas Instruments

Chipcon, a designer of short-range, low power wireless transceiver devices, has been acquired by Texas Instruments (TI) Inc. in a transaction valued at approximately \$200 M. At the time of going to press the transaction was expected to be completed during January 2006.

Under the agreement Chipcon, which employs about 120 people, becomes a wholly-owned subsidiary of TI and continues to operate from its Oslo, Norway headquarters. Its other facilities include a software design centre in San Diego, CA, and sales offices in New Hampshire, Germany, Hong Kong and Tokyo. Chipcon's president and CEO, Geir Forre, will lead TI's group integrating short-range wireless personnel and products from both Chipcon and TI.

It is envisaged that combining Chipcon's design experience in RF transceiver and System-on-Chip devices with TI's advanced analogue silicon technologies and broad systems expertise will enhance TI's ability to offer customers complete short-range wireless solutions for consumer, home and building automation applications. ■

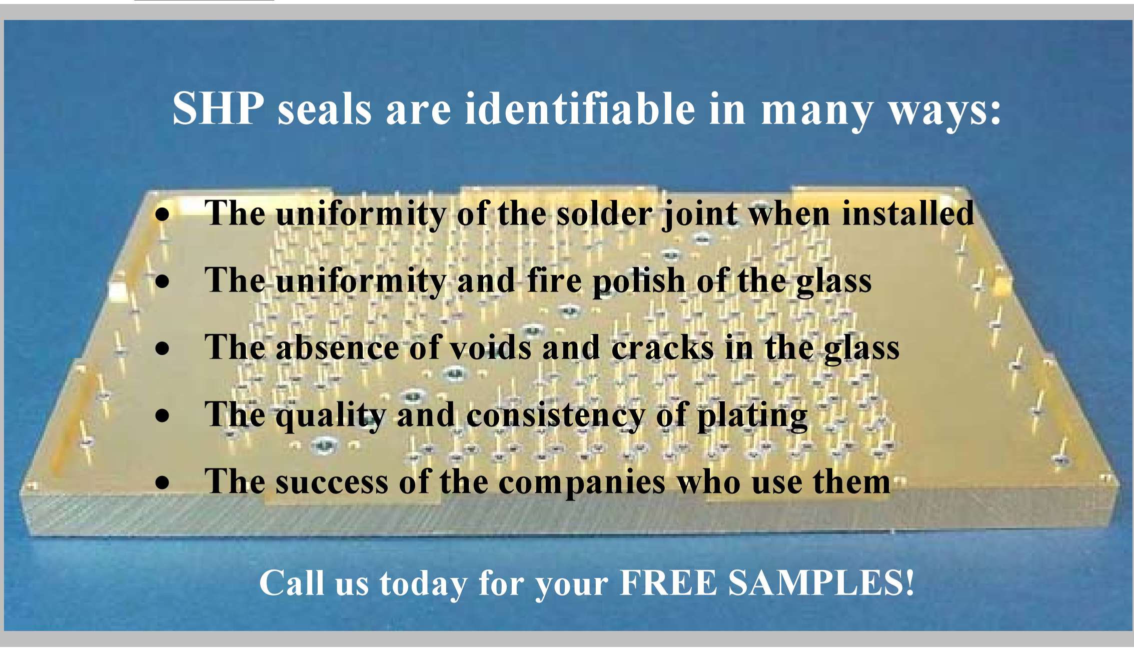

New Hope on the Horizon for 802.11n

The Enhanced Wireless Consortium indicated last month that its proposals for the draft 802.11n standard are now substantially aligned with the work of the IEEE's working group. This is good news for most of the stakeholders in the process. ABI Research has reported on this process before, most notably when a group of companies led by Intel formed the EWC, apparently in opposition to the groups (TGn Sync and WWiSE) responsible for the so-called "joint proposal" for the new standard. When EWC was formed, observers suggested it was a spoiling action aimed at Airgo, the innovative chipmaker whose MIMO designs — never claimed as "pre-n" — were already in wide use. Some also feared that the new group would create a stalemate with the IEEE standard working group. ABI Research disagreed that this development would derail the process. The just-released update to its comprehensive 'Wi-Fi Research Service' notes "While this has led to media reports suggesting the IEEE process has been 'hijacked' by the EWC and is now irrelevant, ABI Research believes this view is far-fetched." That view now appears justified. "It looks as if the EWC's proposals and the existing 'joint proposal' dove tail well," says senior analyst Sam Lucero, "and we hear that a draft standard may appear as early as January." Does this development hurt Airgo? If so, they are putting on a brave face. "They say that they have all the fundamental technical pieces to do what EWC is recommending," Lucero notes. "But they had a good 18 to 24 month lead on the rest of the market in terms of pushing this MIMO-based technology out. Suddenly that has been erased. If EWC's proposals are accepted, tiny Airgo will be up against Atheros, Marvell, Intel and others." On the positive side, ratification of a standard would move the whole market forward, benefiting everyone. Either way, we will see real "11n" and "pre-11n" chipsets on the market by the end of 2006.

Alcatel Selected by M/A-COM for New York State Public Safety Communications

Alcatel announced it has signed a subcontract with M/A-COM Inc., a leader in critical communications technologies, to equip the State of New York with an advanced public safety communications network to enhance communications interoperability among public safety first responders. The Statewide Wireless Network, for which M/A-COM will act as prime with the State of New York, will improve data transmission and quality of service, and enable faster emergency response and increased public safety. "The state of New York will now have the most advanced public safety communications network of its kind, ensuring reliable and secure communications among the various state agencies," said John Vaughan, vice president and general manager, M/A-COM Wireless Systems. "Working together with a team of partners that includes Alcatel, we are proud to provide the State with a turnkey system that addresses the critical needs of public safety and homeland security communications." The state-funded communication network features Alcatel microwave digital radio system and cross-connects that will be used for backhaul transmission at more than 300 sites in New York State. The Alcatel MDR-8000 microwave digital radio provides point-to-point wireless communications links, while Alcatel 1630-GSX cross connect streamlines narrowband and broadband capabilities into a single platform. This combination simplifies operation and maintenance requirements, offers unparalleled bandwidth and security, and insures consistent portable and mobile communications among essential personnel. "Deploying public safety communications networks has become an important priority for Alcatel," said Hubert de Pesquidoux, president of Alcatel's North American activities. "Alcatel's comprehensive solution, as part of M/A-COM's overall network solution, will provide the State of New York with a robust network that ensures maximum uptime and reliability."

Mesh Network Market May See Tenfold Growth in Five Years

Wireless mesh networking looks set to achieve a stellar growth rate by the end of the decade, but most of the growth will be in market segments not served by existing infrastructures. According to a new study from ABI Research, the increase will mostly come from deployment by alternative service providers and municipalities, rather than incumbent service providers. There will also be some "campus" style deployments in academic, corporate and resort environments, as well as temporary rollouts at conferences or fairs. The new study, "Wireless Mesh Networking: Technology and Deployment Strategies for Metropolitan and Campus Networks," examines the trends for both metro-scale and campus-scale wireless mesh networking technology on a worldwide basis. "I think that the growth rate will be dramatic," says Sam Lucero, senior analyst of wireless connectivity. "It is an interesting market that has a lot of potential for alternative service providers such as Earthlink — ISPs who do not have their own facilities at present. It is an essential means for them to remain viable in the provision of services. Wireless mesh networking allows them a relatively cost-effective way to deploy their own facilities within targeted areas. But they are not positioning this as directly competitive to triple-play services." Incumbents — both cable operators and telcos — have not significantly embraced the mesh concept, but it is noteworthy that several of them have invested in mesh networking companies. The announcement by Cisco Systems of new wireless mesh solutions also supports ABI Research's optimistic view of this market. Lucero comments, "Cisco's

introduction of a wireless mesh networking product family represents further validation for an already fast-growing metro-scale wireless mesh networking market. In addition, with the company's significant customer base for enterprise WLAN equipment and its emphasis on centralized control of unified indoor WLAN/outdoor wireless mesh networks, Cisco may be able to jumpstart the campus-scale wireless mesh networking market in a way that its competitors have largely been unable to do to date."

Near Field Communications Approaches Three Critical Years

Near Field Communications (NFC) applications will transform consumer commerce, connectivity and content consumption, beginning with trials through 2006 and volume deployments into 2007, according to a new study from ABI Research. NFC, a short-range contactless communication protocol, enables easy-to-use, secure Bluetooth and Wi-Fi connectivity between devices. It provides high bandwidth content acquisition and transfer, contactless payment capability and smart object interaction. That means, for instance, interactive advertising posters and kiosks, instant ticketing and transmitting audio, video and pictures. NFC brings convenience to increasingly connected digital customers. "Near Field Communications" details NFC's global business applications, market players and opportunities. According to Erik Michielsen, the firm's director of RFID and ubiquitous networks, the story of NFC's growth from 'infancy' to 'young adult' status will play out over three years. 2005, he says, has seen the groundwork laid. The NFC forum industry association now counts 60-plus members and this year has demonstrated the critical ability of many players — wireless carriers, handset OEMs, application developers, payment processors, infrastructure providers, content owners, card issuers, bank and merchants — to collaborate. "2006 will be a year of trials and trial data digestion," says Michielsen. "NFC standards, licensing and interoperability will solidify. Commercial NFC products will reach market." By 2007, the research indicates, higher volume NFC deployments will be common, first in wireless handsets, then in other kinds of consumer electronics, from PCs to cameras, printers, set-top boxes and more. However, certain conditions are essential to NFC's success. Michielsen states: "Open, interoperable, standards-based NFC environments are critical to stabilizing NFC ecosystem working relationships and commitments, especially with wireless carriers seeking clarity on NFC business benefits. 2005 and 2006 NFC trials will be important to help them understand how the numbers add up." ■

INDUSTRY NEWS

■ On October 21st, 2005, **Bill Reich**, marketing and communications manager for Narda Microwave East, an L3 Communications company, passed away at the age of 62. A Narda employee for 25 years, Reich initially headed the organization's publications department, and later oversaw the company's sales activities. "Bill Reich was both my long-term customer and friend," said Ed Johnson, associate publisher, *Microwave Journal*. "He was the most knowledgeable MARCOM I knew. He was cognizant of all aspects of his company's operations. He is sorely missed, and will live on in the hearts and minds of all who knew him."

■ **SciTech Publishing Inc.**, Raleigh, NC, and **Noble Publishing**, Thomasville, GA, have reached an agreement whereby SciTech will acquire all assets of Noble. Closing is subject to standard terms and conditions. SciTech assumed operation of Noble as of January 2, 2006.

■ **EMS Technologies Inc.** announced the signing of a definitive agreement for the sale of its Satellite Networks (SatNet) division to **Advantech Advanced Microwave Technologies Inc.**, a manufacturer of satellite and terrestrial wireless communication equipment, with corporate headquarters in Montreal, Canada. The parties are seeking to close the transaction as soon as possible, subject to certain customer and supplier consents.

■ **Andrew Corp.** has signed a definitive agreement to acquire **Skyware Radio Systems GmbH**, Krefeld, Germany, a producer of state-of-the-art electronic products for broadband satellite communications networks. Under terms of the agreement, which is subject to review by German antitrust authorities, Andrew will pay approximately $9 M in cash, with additional cash consideration possible if certain financial performance goals are reached over a two-year period. Privately-held Skyware generated approximately $12 M in sales during its fiscal 2004. Its products are in use primarily within the Europe, Middle East and Africa markets. In related news, Governor Mike Easley announced that Andrew Corp. will move into a new facility in Wayne County, NC, in 2006 adding 204 new jobs and retaining and relocating 232 existing jobs from the company's Smithfield, NC facility. The project represents an investment by Andrew of $11.5 M over six years.

■ **TECOM Industries Inc.**, a Smiths Interconnect company, and **Rockwell Collins** have entered into a long-term purchase agreement for the HGA-2100 high gain antenna to meet the Boeing 787 SATCOM high gain antenna requirement. The HGA-2100 is the latest addition to TECOM's line of SATCOM antenna products.

■ **TriQuint Semiconductor Inc.** has announced the opening of a new design and support center in Chelmsford, MA. The facility, known as the New England Design Center (NEDC), is part of the company's ongoing efforts to work more closely with strategic partners and customers on development of next generation wireless modules and components. The 15,000 square foot NEDC, located in the Boston suburbs, consolidates design and engineering support activities previously handled at locations in Lowell, MA and Nashua, NH.

■ **Trilithic Inc.**, a designer and manufacturer of RF and microwave passive components and filters, announced the opening of a new sales office in Europe. With this expansion, Trilithic will provide local sales support for all customers and sales agents in Europe as well as initiating new business development projects. Located outside of London, Trilithic Europe's office is managed by David O'Connell (doconnell@trilithic.com) and sales support is provided by Amanda O'Connell (aoconnell@trilithic.com).

■ **Taconic**, Petersburgh, NY, recently held a ribbon cutting ceremony at the site of its new manufacturing facility in Cheonan, Korea. Awards for outstanding performance were handed out to key contributors who made the opening possible including a local construction company as well as several Korea Taconic employees.

■ **RF Micro Devices Inc.** (RFMD) announced that the company's board of directors has approved the expansion of RFMD's assembly operations in China. The expansion, which is projected to be on-line during the June quarter of 2006, is expected to increase RFMD's internal assembly capacity by approximately 50 percent, representing approximately 25 percent of the company's assembly requirements.

■ In line with its multidomestic strategy, **Thales** has established commercial representation in Bratislava, under the management of Marc Duflot. The intention is for this office to become a Central Office for the region and capitalize on opportunities arising throughout Central Europe. The company's increased presence follows the strong development of the Slovak Republic, which is a member of both the European Union and NATO. The new office demonstrates Thales' strategy to cooperate with local industry partners in order to create a solid basis for a mutually beneficial relationship through a progressive transfer of advanced technical know-how.

■ **Rohde & Schwarz** has taken an important step forward towards further growth and innovation with the opening of a 16,000 m^2 Technology Center in Munich, Germany. In doing so it claims to have created an optimum work environment that supports the creativity of its employees. The center will also be a major recipient of the company's recruitment drive as it aims to attract 200 new employees — mainly engineers — in Germany alone, the majority of them for research and development.

■ **M2 Global Technology Ltd.** has announced that it will be moving to a new 25,000 square foot facility by March. The new facility will allow the local company to bring all of its operations, including electronics manufacturing, welding, mechanical assembly and sheet-metal services under one roof. The company will be moving into an existing building, located at 5714 Epsilon Drive, San Antonio, TX 78249.

■ **Polytec Inc.**, a provider of advanced, light-based vibration, speed and length, and topography measurement systems to North America, has opened a dedicated east coast regional office in Hopkinton, MA. The new office will service customers from the southeastern United States north to the New England states and eastern Canada. In addition, an engineering lab facility will soon be completed, permitting characterization of customer-supplied structures and MEMS devices.

■ **Aeroflex** and **Centro de Tecnología de las Comunicaciones** (Cetecom Spain) have entered into a long-term, global distribution partnership under which Aeroflex will become the sole worldwide sales and support channel for Cetecom's mobile communications integrated tester (MINT) RF conformance test platform for 2G/2.5G/3G mobile handsets.

■ **TestMart** announced an agreement with **XL Microwave** (now **Pendulum Instruments Inc.**). The deal provides the US government and federal contractor a marketplace with special pricing on select frequency counters and standards, wireless test instrumentation and other products.

■ **AMI Semiconductor**, a designer and manufacturer of state-of-the-art integrated mixed-signal and structured digital products, and **Mentor Graphics® Corp.** have partnered to offer a state-of-the-art analog/mixed-signal technology design kit containing comprehensive and proven building blocks at the device level. This kit enables semiconductor companies and electronic systems manufacturers to jump-start their design cycles on AMI Semiconductor's foundry process using Mentor's analog/mixed-signal IC flow, thereby cutting time-to-market and ensuring manufacturing success of analog, low data rate wireless, mixed-signal and system-on-chip ICs.

■ **Summitek Instruments** has announced a licensing agreement with **Willtek Communications**, a provider of test and measurement solutions to the wireless industry. Summitek Instruments, a manufacturer of software products designed to automate spectrum management as well as S-parameter measurements, has signed an agreement to license the OASIS Spectrum Monitoring software to Willtek as an option for its line of 9101 and 9102 handheld spectrum analyzers.

■ **Technical Research and Manufacturing** (TRM), Bedford, NH, has announced a new low cost, quick turn coupler and divider/combiner program. On selected products, TRM is guaranteeing less than two-weeks delivery for quantities of one to five, with low, monolithic pricing for these same quantities.

■ **UltraSource Inc.**, a manufacturer of custom thin film circuits and ceramic interconnect devices, has achieved ISO 9001:2000 registration. The successful completion of the certification culminated months of intense activity that resulted in the rewriting of the company's Quality Manual, redefining the company Quality Policy and documenting the Quality Management Systems.

■ **Merrimac Industries Inc.**, a designer and manufacturer of RF microwave components, has been granted a patent for its Multi-Mix® Microtechnology from the United States Patent and Trademark Office entitled "Method of Manufacturing Multilayer Microwave Couplers Using Vertically-connected Transmission Line Structures." This patented technology reduces the size of surface-mount RF couplers and enables low loss implementation of RF interconnects between layers in multilayer stripline structures leading to further miniaturization of integrated module designs.

■ **QUALCOMM Inc.** announced that the company has shipped two billion chips since 1996 when it delivered its first commercial CDMA solutions to wireless handset and infrastructure customers. QUALCOMM marked the shipment of its first billion chips in 2003.

■ **Avago Technologies** announced that it has shipped its 200 millionth film bulk acoustic resonator (FBAR) filter. Strong demand by handset manufacturers has driven Avago to increase its shipments to more than 15 million per month. FBAR filters are used in mobile phones, data cards and other wireless products.

■ **Tyco Electronics** has named **TTI Inc.** its North American Distributor of the Year for 2005. The award was presented in Fort Worth, TX, where executives from both companies were meeting.

CONTRACTS

■ **Agilent Technologies Inc.** announced it has been awarded a $19.73 M contract by the **US Air Force** to provide Agilent microwave measuring receivers to the Air Force Metrology and Calibration Lab (AFMETCAL). Agilent also has received a $2.3 M contract to deliver low noise signal generators to the lab. The microwave measuring receiver, which provides frequency coverage up to 50 GHz, will be used by AFMETCAL for calibrating signal generators and step attenuators to meet stringent government and commercial accuracy requirements.

■ **L-3 Communications Cincinnati Electronics** (CE) has been selected by **General Dynamics Land Systems** (GDLS) Division to provide the advanced infrared thermal imager for the Stryker Mobile Gun System (MGS). CE has begun delivery of 72 thermal imagers to be installed in the Commander's Panoramic Viewer that provides situational awareness and target assessment for the Stryker MGS.

■ **TiaLinx Inc.**, a developer of wafer scale antenna arrays, announced that it has received a Small Business Innovative Research (SBIR) Phase 1 award from the **Defense Advanced Research Project Agency** (DARPA). The objective of this program with DARPA is to address feasibility of using TiaLinx's proprietary integrated RF beamforming technology, focusing on ultra-wideband modulation operating at extreme frequencies for Giga-band signaling applications. The device will require low power to operate and offers a substantial reduction in mass and volume.

PERSONNEL

■ Hittite Microwave Corp. announced that **Stephen G. Daly**, president and chief executive officer and a director of the company, has been elected to the additional office of chairman of the board. He succeeds the company's founder, Yalcin Ayasli, who will remain on the board and serve as chairman emeritus. Daly joined the company in 1996, has served as president since January 2004 and chief executive officer since December 2004.

■ **Alec Reader** and **Philip Nelson** have been appointed to the board of directors of Innos, the UK research and development company for innovations in nanoscale technology. The appointment of Reader coincides with his promotion to the role of sales and marketing director. Nelson was previously director of the Institute of Sound and Vibration Research and was appointed deputy vice-chancellor of the University of Southampton in 2005. He brings a proven pedigree in acoustics — currently serving as president of the International Commission for Acoustics — and an in-depth knowledge of creating industry sponsored research grants.

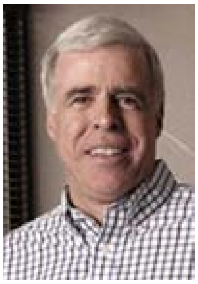

▲ *Rick Thompson*

■ Interconnect Devices Inc. (IDI) announced the appointment of **Rick Thompson** to the position of chairman of the board and CEO. Thompson will lead both IDI and its sister company Synergetix.® Thompson, one of the original founders of the company, served as IDI's first president from 1979 to 1985. He has served as a member of the IDI board of directors since its beginning. Thompson returned to the CEO position with the recent departure of Edward J. Schifman, who served as IDI's president and CEO since 1985.

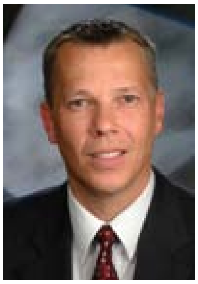

▲ *Lars Marcher*

■ **Lars Marcher** took up the position as chief financial officer of Terma A/S with the title of executive vice president and CFO. Since 2004, he has held the position of president and CEO of Dataram Corp., which manufactures memory modules for large computer systems and complex simulation projects. He has a broad international management experience, attained over 19 years of key management positions in a number of companies, which include Purup Electronics, The East Asiatic Co. and Apple Computers.

▲ Guy Petignat

■ **Guy Petignat** has joined Huber + Suhner as COO Fiberoptic + Cable Technology, and member of the Executive Group Management. He is a Swiss and Australian citizen with a master's degree in mechanical engineering from the Swiss Federal Institute of Technology (ETH), and an MBA from Harvard Business School. He was previously COO for Kaba Key + Ident Systems Europe and Asia Pacific. Petignat has a genuine industrial background and a proven track record with several years of experience with the Kaba group, as well as among others, more than 10 years with Ascom.

■ Silicon Laboratories Inc. announced the appointment of **Necip Sayiner** as president and chief executive officer. Sayiner replaces interim chief executive officer Nav Sooch, who will continue to play an active role in the company as chairman of the board of directors. Prior to joining Silicon Laboratories, Sayiner held various leadership roles at Agere Systems.

■ WJ Communications Inc. announced that it has appointed **Morteza Saidi** as vice president of engineering. Saidi brings over 25 years of successful experience in managing and developing RF products. He served most recently as founder and CEO at S-Communications, a fabless semiconductor company. Prior to that, he was the co-founder, CTO/VP of RF and Analog for Resonext Communications (acquired by RF Micro Devices in 2002).

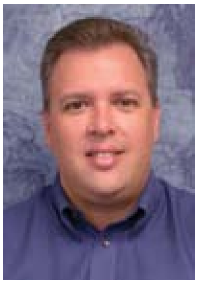

▲ Michael J. Kujawa

■ TRAK Microwave Corp. has appointed **Michael J. Kujawa** as vice president of sales and marketing in Tampa, FL. Kujawa will be responsible for marketing communications, new business development and all worldwide sales efforts. Kujawa joins TRAK from MI Technologies where his last position was vice president sales. His career spans 20-plus years of experience in the RF/microwave industry, including entrepreneurial ventures and leadership experiences focused on business development and operations management.

▲ Kirk Anderson

■ MI Technologies announced the appointment of **Kirk Anderson** to the position of strategic account manager. Prior to his appointment at MI Technologies, Anderson held key positions at Hewlett Packard and Agilent Technologies, first as an RF/microwave applications engineer from 1984 to 1988 and later as a principal project manager for systems and services from 1994 to 2005.

■ AR Worldwide Modular RF, a division of AR Worldwide, welcomes senior RF engineer, **Charles Ohiri**. Ohiri's expertise will enable the company to expand its engineering capabilities above 1 GHz. He brings 19 years of hands-on experience in radio and RF design and system application. His most recent focus has been on highly linear wireless communication base station amplifier design.


▲ Sheenu Chacko-Thomas

■ Renaissance Electronics Corp. announced the appointment of **Sheenu Chacko-Thomas** as sales and marketing specialist for the Ferrite Product Group. Chacko-Thomas will focus primarily on the New England and eastern North American territories. Chacko-Thomas, who graduated from Loyola University Chicago with a degree in marketing, will also be marketing products for Renaissance. She comes to the company with extensive experience in both marketing and sales. She can be reached at (978) 772-7774 x13 or via e-mail: schacko-thomas@rec-usa.com.

REP APPOINTMENTS

■ **Renaissance Electronics Corp.** announced the appointment of **Wavelength RF Supply**, Colleyville, TX. Wavelength RF Supply will service the Texas territory and will represent all product lines of Renaissance. Ryan Krier of Wavelength RF Supply can be contacted at (817) 428-3506 or e-mail: sales@wavelengthsupply.com.

■ **MITEQ Inc.**, a supplier of RF and microwave components, has appointed **Associated Technical Sales LLC**, Tustin, CA, as its exclusive sales representative for southern California. Associated Technical Sales can be contacted at (877) 287-1737.

■ **G.T. Microwave Inc.**, Randolph, NJ, has appointed BT Gu of **Weisher Technologies Co. Ltd.** to represent the company in China. Weisher Technologies is a privately owned vendor for RF and microwave products and services. The company has offices in Beijing, ShenZhen, Nanjing and Chengdu. Weisher Technologies' main office is located at Room 1602-1604, Huaying Building Nanshang Road, Nanshan District, ShenZhen, P.R. China 518054 and the e-mail address is botao.gu@weisher.com.

■ **Sullins Electronics**, a designer and manufacturer of connectors and interconnect systems, announced the signing of a distribution agreement with **Bisco Industries Inc.**, an international distributor of specialty fasteners and electronic components. The agreement, effective immediately, allows Bisco to promote, supply and support both the Sullins and Micro Plastics lines of connectors and interconnect systems throughout North America.

WEB SITE

■ **ANADIGICS Inc.**, a supplier of wireless and broadband solutions, announced that the company's web site now includes an on-line store to provide a convenient channel for ordering product samples. Users can easily order samples of the company's GSM/GPRS and WCDMA power amplifiers, base station amplifiers and RF switches at www.anadigics.com.

KU-BAND MMIC POWER AMPLIFIERS DEVELOPED USING MSAG MESFET TECHNOLOGY

This article presents the design approach and test results of 1, 1.5, 2 and 5 W, Ku-band MMIC power amplifiers developed using the high performance MSAG MESFET technology. Both single-ended and balanced topologies were used. A minimum power-added efficiency (PAE) of 27 percent, an output power (P_{out}) of 5 W and an associated gain of 21.5 dB were achieved over the 12.5 to 14.5 GHz frequency range. To the author's best knowledge, these results represent the state-of-the-art in MESFET-based MMIC Ku-band power amplifiers.

TABLE I

SUMMARY OF Ku-BAND REACTIVELY MATCHED MEDIUM POWER AMPLIFIERS

Frequency Range (GHz)	No. of Stages	Gain (dB)	P_o (W)	PAE (%)	Device Technology	Year Reference
8 to 13.5	2	–	2.5	38	0.2 μm pHEMT	1996[1]
8 to 14	2	15	2.8	36	HBT	1998[2]
13 to 15.0	2	–	6.0	–	0.15 μm pHEMT	2002[3]
Ku/K	3	22	6.0	30	0.25 μm pHEMT	2003[4]
13.5 to 15	3	22	8.0	22	0.25 μm pHEMT	2004[5]
14.0 to 14.5	2	15	1.8	22	0.25 μm pHEMT	2004[6]
12.5 to 14.5	3	19	7.0	27	0.4 μm MESFET	this work

During the past decade, there has been significant progress in monolithic Ku-band power amplifiers operating over both narrow and broad bands. Many different technologies, including MESFET, HBT and HEMT, are being pursued to develop MMIC power amplifiers[1–6] in order to obtain the maximum output power (P_{out}) and power-added efficiency (PAE) from a single chip. Progress in this area, for Ku-band MMIC power amplifiers, has been summarized in ***Table 1***. The performance listed is the minimum over the frequency range. MMICs with greater than 1 W output power were selected for comparison. The gain shown is taken at the minimum power level. Although MIC technology can be used to develop broadband power amplifiers, power MMIC amplifiers, in general, offer smaller size and lightweight, higher gain, wider bandwidth, higher reliability, lower cost and much better unit-to-unit amplitude and phase tracking capability, when manufactured in large volume. MMIC power amplifiers have the following potential advantages as compared to commonly available internally matched power amplifiers:

INDER J. BAHL
M/A-COM, Roanoke, VA

- Multistage designs have higher gain (20 to 30 dB)
- Higher overall power-added efficiency (PAE)
- Compact in size and lightweight
- Lower parts count, higher reliability and lower cost
- No external biasing chokes are required

Several high efficiency C- and X-band power MMIC amplifiers have been developed successfully using the high performance, low cost and highly reliable multifunction self-aligned gate (MSAG) MESFET IC process[7–16] at the M/A-COM facility in Roanoke, VA. These amplifiers have demonstrated PAEs in excess of 55 and 40 percent with associated output powers of 14 and 12 W, at C- and X-band, respectively, over approximately a 15 percent bandwidth.[12,13] These results represent the state-of-the-art power amplifier performance at C- and X-band and the MSAG MESFET technology provides a low cost solution to the power section of active aperture phased-array T/R modules.

In this process, the ion-implanted active devices use 0.4 μm gates, deposited by employing low cost optical lithography, leading to higher throughput and lower cost. The MSAG process has unique features: it does not use air bridges, has polyimide scratch protection, multi-level plating capability[15] for low loss passive components, no hydrogen poisoning susceptibility and is very reproducible unit to unit. These features all lead to a mean time to failure (MTTF) greater than 100 years at a channel temperature of 150°C, higher assembly yields with MSAG chips and provide cost-effective solutions.

The MSAG process also uses three layers of polyimide (ε_r = 3.2): inter-level dielectric (3 μm thick), inductor crossover layer (7 μm) or low loss microstrip (10 μm thick) and a scratch protection buffer layer (7 μm thick) for mechanical protection of the finished circuitry. Three metal layers are used: metal 1 (0.5 μm thick), first plated gold (4.5 μm thick) and second plated gold (4.5 μm thick). The multi-level plating (MLP) process allows a reduction in the chip size and lowers the resistive loss in passive components. Low capacitance metallization crossovers are achieved by a polyimide intermetal dielectric layer. The front side processing is completed by depositing a polyimide buffer layer. The buffer layer provides mechanical protection of the circuit structures during backside processing, dicing and subsequent assembly operations. Finally, the wafers are thinned to their final thickness of 75 μm, through-wafer vias are etched and the backside is metallized.

This article describes the design and test results of several fully monolithic, class AB, Ku-band MMIC power amplifiers, designed to operate at a nominal power supply voltage of 8 V. The amplifiers described include a high gain, high PAE and linearity 1.5 W amplifier; a broadband 1.5 W amplifier; a 2 W balanced amplifier; and a 5 W high power amplifier. The general design approaches, along with salient features of each design, are also discussed.

GENERAL DESIGN APPROACH

The MSAG MESFET technology was selected to develop Ku-band power amplifiers because of its high across-the-wafer uniformity, excellent linearity and low cost capabilities. One of the basic requirements for achieving high power output and PAE on a single MMIC chip is the high across-the-wafer uniformity of the saturated drain-source current (I_{DSS}) and device cut-off frequency (f_T) in order to combine all unit FET cells efficiently. The high across-the-wafer uniformity for efficient power combining becomes more important at higher frequencies. The MSAG transistors, based on a self-aligned gate approach, have a planar channel structure contributing to better across-the-wafer uniformity, reproducibility and manufacturability.

FET Size

The design of the MMIC power amplifier starts with the selection of the number of stages and unit FET sizes required, based on the gain, PAE/linearity and output power requirements. The choice of FET cell size impacts the matching networks, combining topology, chip size and electrical performance. Larger FET cell sizes reduce the chip area because fewer combiners are required. However, they have lower input and output impedances, which increase the impedance matching ratio of the matching networks, increasing circuit mismatch loss and reducing bandwidth. In addition, there is a reduction in the FET's performance due to increased parasitic reactances and resistances. This latter effect is minimized with careful FET design.

Except for the 5 W HPA, the unit FET's gate periphery was restricted to less than 0.8 mm. The Ku-band MMICs have demonstrated power densities of 0.6 W/mm at V_{DS} = 10 V and 0.48 W/mm at V_{DS} = 8 V, which are used to determine the total FET periphery needed in the design of these power amplifiers. This translates to eight 1.8 mm gate periphery FETs with offset vias arranged edge-to-edge creating effectively an eight-feed 14.4 mm FET to achieve 5 W output power at V_{DS} = 8 V. The large gate periphery 1.8 mm FET shown in ***Figure 1*** uses offset vias and has a lower source inductance (higher gain) than in-line via FETs of similar gate periphery. FETs with a smaller than 0.8 mm gate periphery have in-line source vias. A binary corporate feed combining, that is two FETs, driving four FETs, which finally drive eight FETs, was used to realize better linearity and to maintain good layout

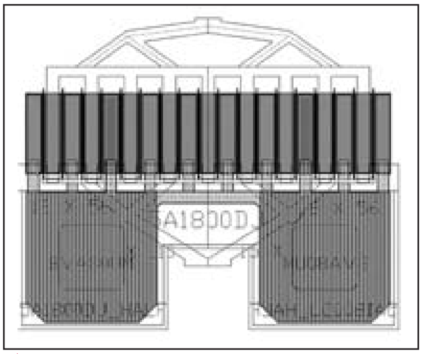

▲ *Fig. 1 Physical layout of the 1.8 mm FET with offset vias.*

TABLE II

SUMMARY OF THERMAL ANALYSIS OF Ku-BAND FETs

FET Size (mm)	No. of Fingers	Gate-Gate Pitch (μm)	Thermal Resistance R_{TH} (°C/W)	Net Power Dissipated (W) Based on 0.5 W/mm	ΔT (°C)
0.3	4	30	267.9	0.15	40.2
0.625	6	30	132.2	0.313	41.3
0.625	6	20	146.8	0.313	45.9
0.75	6	30	110.2	0.375	41.3
1.80	18	24	51.0	0.90	45.9
14.4	144	24	6.5	7.2	46.8

symmetry to obtain maximum possible performance.

After the selection of FET sizes, the FET's gate periphery, the number of fingers in each FET cell and gate-to-gate pitch are finalized. The unit gate width for each FET is the FET size or periphery, divided by the number of fingers, and is a function of device type and frequency of operation. The gate pitch determines the area over which the FET dissipates power; a larger pitch reduces the FET channel temperature. The design of the output FETs is key in reducing the chip area. Keeping in mind the electrical, physical and thermal design requirements for each design, appropriate physical dimensions were selected for each FET.

Thermal Design

The thermal modeling of semiconductor devices can be performed by using numerical techniques such as the finite difference and finite element analyses or by using simple analytic methods such as the Cooke model.[17] Based on published data and the measurements carried out at M/A-COM, it is believed that the Cooke model predicts FET channel temperature accurately. The first step is to calculate the thermal resistance (R_{TH}) of each FET used in the designs. The thermal resistance is calculated, based on the FET structure (gate-to-gate pitch, unit gate width and FET size) and the substrate properties. The maximum channel temperature rise can then be obtained, knowing the power dissipated in the device. ***Table 2*** summarizes the thermal resistance calculations for several FETs used in the designs. The GaAs substrate thickness and thermal conductivity at room temperature are 75 μm and 0.46 W/cm°C, respectively. The difference in the temperature, ΔT, from the bottom surface (carrier) to the top surface (channel) of the MMIC chip is calculated using $\Delta T = R_{TH} \times P_{DC}$, where P_{DC} is the net power dissipated in the device. For these calculations, the thermal resistance goal is chosen based on the maximum allowed junction temperature of 150°C.

Consider a FET having a 100 μm unit gate width and a 24 μm gate-to-gate spacing. According to Cooke's model, the incremental increase in

R_{TH} value per unit width of a FET from fingers 1 to 2, 2 to 4, 4 to 18 and 18 to 144 fingers is 19, 14, 9 and 2 percent, respectively. This means that the R_{TH} value for closely spaced heat sources is about 45 percent higher than the isolated heat source. Thus, any physical separation between the FETs helps in lowering the R_{TH} value. In the Ku-band amplifiers, all FETs are isolated, except the 1.8 mm FET used in the output stage of the 5 W HPA. In the 5 W HPA, the output stage eight FETs are treated as one FET of 14.4 mm gate periphery for thermal resistance calculations.

The next step is to calculate the net power dissipation in the FETs under RF drive. An in-house program was used to calculate the power delivered to each FET and the power delivered out of each FET in order to calculate the net power dissipated in the devices. Based on these calculations and the measured hybrid FET performance data, an average value of 0.5 W/mm power dissipation was used to calculate the value of ΔT for each FET.

Load Impedance

A unit cell of 625 µm FET was characterized at 10 V and 14 GHz using a load pull technique. The measured load for this FET is equivalent to the parallel combination of a 90 Ω resistor (R_L) and a –0.10 pF capacitor (C_L). In the design, for other FET peripheries, the load impedance was obtained by using the following scaling relationships

$$R_L = \frac{90 \times 0.625 \times V_{DS}}{Wg \times 10}\,\Omega \quad (1)$$

$$C_L = -\frac{0.19 \times Wg}{0.625}\,\text{pF} \quad (2)$$

where

Wg = total FET periphery in mm
V_{DS} = operating drain voltage in volts

As a first-order approximation, the reactive part of the load is assumed to be independent of the drain voltage. The negative sign in Equation 2 represents an inductive reactance. For example, for a 1 mm FET, operating at 8 V, the values of R_L and C_L are

$$R_L = 45\ \Omega$$
$$C_L = -0.304\ \text{pF}$$

This scaling method for obtaining the load impedance works reasonably well for a 6 to 10 V operation, for gate peripheries less than 3 mm and up to 20 GHz, when the FET's output feed is designed or scaled accordingly.

Hybrid amplifiers at 14.5 GHz were designed using the aforementioned load pull data. Typical measured performance obtained for the 0.625 mm FET biased at 10 V and 20 to 30 percent I_{DSS} is shown in ***Table 3***.

TABLE III
SUMMARY OF MEASURED PERFORMANCE AT 14.5 GHz OF A 0.625 MSAG FET BIASED FOR CLASS AB OPERATION

Parameter	Value @10 V	Value @8 V
Power gain (dB)	8.4	8.5
Power output (dBm)	27	26
PAE (%)	60	62
V_{GS} (V)	–2	–1.8

TABLE IV

SIMULATED DATA FOR SEVERAL MSAG FETs USING NONLINEAR MODELS AT 12 GHz, BIASED AT 10 V

FET Size (mm)	Gate-Gate Pitch (μm)	No. of Fingers	G_{max} (dB)	P_o (dBm)	G_A (dB)	PAE (%)
0.625	30	6	13.8	27.1	9.5	64
0.94	30	10	13.4	28.5	9.3	60
1.50	30	14	12.5	30.6	8.4	58
1.8	24	18	11.5	31.5	8.0	57
2.50	20	24	10.4	32.7	7.5	55

Linear and Nonlinear Models

The design of Ku-band amplifiers was based on both the linear and nonlinear MSAG FET models. For linear simulations, equivalent circuit (EC) models and small-signal S-parameters obtained over 0.5 to 40 GHz at the operating bias point were used. The EC model topology used is typical of most FET models in the commercial simulators. The Q-point of the FETs was selected for class AB operation (approximately 30 percent I_{DSS}) of the device, in order to obtain the maximum P_{out}, PAE and linearity. Four sets of S-parameter data, corresponding to device low gain, high gain, low current and high current, were used in the amplifier designs.

The nonlinear FET model used to simulate the Ku-band amplifiers is based on a modified Materka model,[18] optimized to predict accurately the output power and PAE. The nonlinear model has I-V equations along with improved capacitance equations compiled into a commercial CAD tool. The model parameters were extracted using extensive S-parameter data, load pull data and pulsed I-V data. The nonlinear model was verified for the standard 0.625 mm FET using extensive hybrid measurements at 14.5 GHz.

Table 4 summarizes the electrical performance of MSAG FETs at 12 GHz calculated using the nonlinear model. The device gain and PAE are reduced significantly by increasing the device size from 0.625 to 2.5 mm.

AMPLIFIER DESIGN CONSIDERATIONS

In this section, a summary of design considerations, used in the design of Ku-band power amplifiers, is described. This includes chip size, loss in matching networks, electromigration requirements and stability considerations.

Chip Size

In general, larger sizes used in power amplifier MMICs perform better in terms of RF parameters and thermal design. However, reducing the chip area will be a significant cost saving requirement, provided that all other characteristics such as reliability and RF yield are almost the same. Reducing the chip area contributes to MMIC cost reduction in two ways: a larger number of chips per wafer, and higher visual and functional yields. For example, M/A-COM's yield model for MSAG processing predicts that reducing the chip area from 40 mm^2 to 20 mm^2 will improve MMIC visual and functional yields by a factor greater than 1.2. Thus, reducing the chip area of power amplifiers is an important factor to reduce their costs. An 18 mm^2 chip area was selected for the 5 W HPA to achieve a goal of better than 0.3 W/mm^2 power density at 10 V.

Low Loss Matching Networks

It is desirable to lower the dissipative loss in the power amplifier's output matching network (using lumped inductors and microstrip lines) in order to improve the P_{out} and PAE performance. The dissipation loss in the microstrip matching networks was improved by using the modified microstrip structure shown in ***Figure 2***. This structure is compatible with MMIC fabrication using a multi-level plating (MLP) process.[15] The strip conductor is fabricated on a thin polyimide dielectric layer, which is placed on top of the GaAs substrate. This allows more of the electric flux lines in the air and thus resembles a suspended microstrip line, which has a much lower dissipation loss than a conventional microstrip. Another way to think of this is that instead of inserting 50 to 75 µm of additional GaAs beneath the line, a thinner layer of 10 µm thick polyimide (a material with lower permittivity) has been inserted in order to reduce the dissipative loss by half.[19] The impedance of such lines can be increased by 40 to 60 percent as compared to standard lines on the given base substrate. This modified structure also helps in the fabrication of the feed structure of the offset via FETs.

The additional thick metallization layer available in the MLP process offers benefits as well, mostly in the area of DC current routing/high power design and extending the usage of passive components to lower frequencies. Most straightforwardly, the designer now has the flexibility to use 9 µm thick transmission lines. The current handling for such lines is 20 mA/µm.[20–22]

A second benefit of the additional thick metal layer is the option to create high current structures, such as spiral inductors. Previously, spiral inductors could be current limited, based on the width of the thin metallization underpass to get from the center of the spiral, typically 2 mA/µm as compared to 10 mA/µm for 4.5 µm thick lines. With MLP, a spiral inductor can be fabricated with 4.5 µm thick spirals and 4.5 µm thick underpasses.

In this design, low loss microstrip lines on a 10 µm thick polyimide layer[19] are used to lower the loss, es-

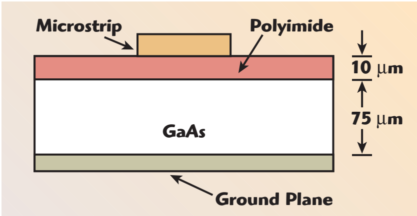

▲ *Fig. 2 Multilayer microstrip configuration.*

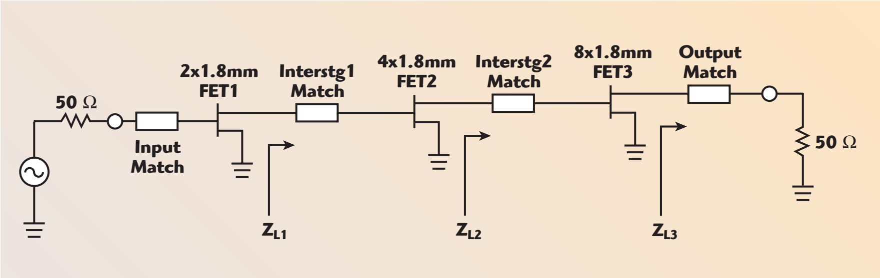

▲ *Fig. 3 Three-stage power amplifier configuration depicting the load required at the drain of each FET stage.*

pecially in the output matching network. Since the lines on polyimide have poor thermal conductivity, a thermal design for such lines is also performed.[23,24]

Electromigration Requirements

Electromigration requirements dictate the microstrip and inductor line widths carrying DC current. A conservative current density of 2.2×10^5 A/cm^2 is used as an electromigration limit for the 4.5 µm thick gold conductors. This translates to a maximum allowed current per unit line width of 10 mA/µm. The maximum current expected in the output FET for this design is approximately 2A. This dictates that, in the output matching network, dual drain bias lines should be used, and each line must be 100 µm wide. The requirement for such wide, low impedance shunt lines complicates efforts to shrink the chip area, and also gives rise to unbalance in the output feed lines due to junction discontinuity effects, impacting significantly the circuit bandwidth. Compact lumped elements are used in the earlier stages where power and current densities are less.

Stability

For MSAG FETs, the experience has been that the standard even mode ($K > 1$) and odd mode stability analyses are adequate to avoid microwave oscillations. However, under a large-signal condition and pulsed operation, it is necessary to design a worst-case K-factor greater than 1, based on S-parameter data for various bias conditions from $V_{DS} = 3$ V and 50 percent I_{DSS} to $V_{DS} = 10$ V and 25 percent I_{DSS}, to ensure the amplifier's stability. This approximately replicates the envelope a full cycle of the input signal experiences during the large signal and pulsed operation. It was found that imposing a $K > 2.0$ condition for $V_{DS} = 10$ V and 25 percent I_{DSS} small-signal S-parameters is adequate to ensure unconditional stable operation under all conditions. Exercising special care in maintaining the symmetry in the amplifier's layout and properly selecting isolation resistors prevents odd mode oscillations.

Design Methodology

Traditionally, a power amplifier can be designed based on the load line method.[25–28] The design of Ku-band MMIC power amplifiers was based on a design methodology using small signal and nonlinear FET models and load pull data obtained at the operating bias point. In this method, initially, the load line technique[25,26] is used to optimize the circuit parameters. For example, in a three-stage, 5 W power amplifier, the optimum load impedances Z_{L1}, Z_{L2} and Z_{L3} at the drain of the first, second and third stage FETs, respectively, which are necessary to realize maximum output power and PAE, are shown in ***Figure 3***. Then the design is simulated using the nonlinear model to calculate the power compression of each stage and the output power and PAE as a function of input power. Since it is very difficult to realize the required load impedances over wide bandwidths and to optimize a circuit using a nonlinear model, the above design process is repeated so that an optimum solution for simultaneous match for load impedances at the drain of each FET and best gain, power and PAE are achieved.

The Ku-band amplifiers were designed using a low loss matching (LLM) design technique.[29] This technique has been successfully applied to the design of power amplifier drivers and high power amplifiers at M/A-COM's Roanoke facility. In this scheme, both the resistive or dissipative loss (DL) and mismatch loss (ML) for each stage are calculated and controlled as required in the design. Generally, DL and ML for the output match are kept at a minimum and the ML for each interstage is minimized. The controlling factors for DL and ML for each interstage include stability criteria and electrical performance. This also helps in optimizing the FET aspect ratios. The dissipative loss is for the individual passive stage, that is interstage, output, etc., and the mismatch loss is the difference between the required device's optimum load impedance and the transformed 50 Ω output impedance at the drain terminal of the FET. The previously described method is based on the assumption that the device input impedance depends strongly on the load connected at the drain terminal rather than its large-signal parameters. For FETs and HEMTs, this assumption is fairly accurate and is the cornerstone of the multistage Ku-band designs.

In the matching networks, a reactive binary matching topology was used, employing low pass and high pass networks that provide higher power output and PAE. Both lumped elements and distributed circuit elements were used for impedance matching networks. In the design optimization using the load line technique, four sets of S-parameter data, corresponding to low gain, high gain, low current and high current, were used. These data files represent the possible fabrication changes and allow a design to be realized that is more tolerant to process variations.

The input stage, which has a limited gain compensation network, was designed for good input match as well as for maximum power transfer at the high frequency end. The interstage matching networks were designed to provide a flat gain response and enough output power to the succeeding stage FETs for achieving maximum output power and PAE. The output matching elements were selected to provide an optimum load match with minimum possible insertion loss, since the efficiency is reduced to a greater extent by a given amount of loss due to decreased power out, gain and available DC power at the FET drain pads. Each stage as well as the complete amplifier were designed to be unconditionally stable over a 3 to 10 V drain power supply

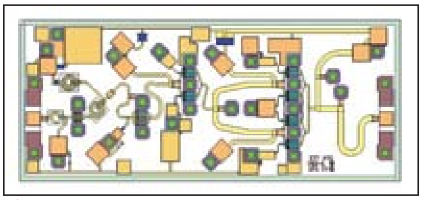

▲ *Fig. 4 Layout of the Ku-band linear power amplifier (chip size is 4.3 x 1.8 mm).*

and 25 to 50 percent I_{DSS} drain current. EM simulations were used extensively during circuit optimization for closely packed passive circuit components and discontinuities.

HIGH GAIN, PAE/LINEARITY POWER AMPLIFIER

The four-stage design consists of a 0.3 mm, a 0.625 mm, two 0.625 mm and four 0.625 mm FETs in the first, second, third and fourth stages. All FETs have a 30 μm gate-to-gate pitch. The FET 2:1 aspect ratio maintains a better linearity. The circuit was designed for high 1 dB power compression (P1dB) and high gain. Single drain pad and single gate pad supply operations were used. The first three stages use small resistors in the drain bias lines for stabilization. The values of the resistors and their sizes were selected so that the voltage drop across them is less than 0.5 V and they also meet the electromigration requirements. In the gate bias lines, the isolation resistors values were 200 Ω per mm of FET periphery. The nominal drain supply voltage is 8 V and the gate voltage is –2 V. ***Figure 4*** shows the physical layout of the MMIC amplifier.

BROADBAND POWER AMPLIFIER

The three-stage design comprised of a 0.625 mm FET at the input driving two 0.625 mm FETs and driving four 0.625 mm FETs at the output. The FET 2:1 aspect ratio, in this case, is required to obtain high power and PAE over a larger bandwidth. This design also uses a single drain pad and single gate pad supply operation. ***Figure 5*** shows the layout of the three-stage broadband amplifier.

BALANCED 2 W POWER AMPLIFIER

The 2 W power amplifier uses a balanced configuration, as shown in ***Figure 6***. In this design, Wilkinson divider/combiners with 90° phase offset 50 Ω lines were used instead of Lange couplers. In this case, the reflected signals from the two single-ended amplifiers have a 180° phase difference across the 100 Ω isolation resistor. Thus, the out-of-phase reflected signals are absorbed in the isolation resistor. This topology minimizes the reflected signals at both the input and output terminals and pro-

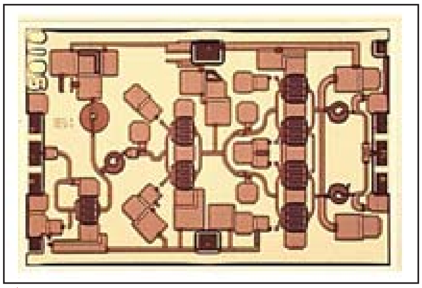

▲ *Fig. 5 Layout of the broadband power amplifier (chip size is 3.0 x 1.8 mm).*

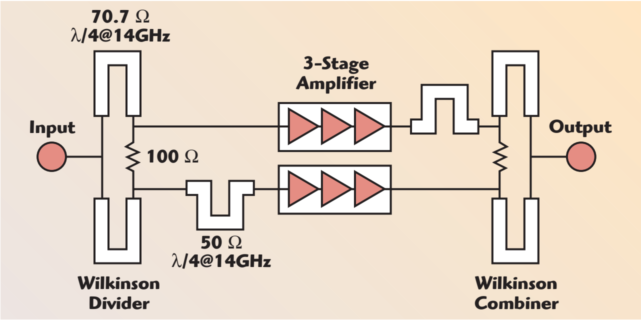

▲ *Fig. 6 2W, Ku-band, balanced power amplifier configuration.*

vides good VSWR. Also, the effect of mismatch on the output power and PAE, due to bond wires and package lead frame, is minimum.

The single-ended amplifier's FET topology is the same as for the broadband amplifier using a 2:1 FET aspect ratio. This design requires a bias supply from both sides. ***Figure 7*** shows a photograph of the balanced 2 W amplifier.

5 W HPA

The 5 W HPA design uses two 1.8 mm FETs driving four 1.8 mm FETs and driving eight 1.8 mm FETs. Here, the FET aspect ratio is 2:1 and the circuit is designed for maximum P_{out} and PAE under saturation. The matching circuit microstrip lines are on 10 μm polyimide. ***Figure 8*** shows a photograph of the 5 W MMIC HPA. This design requires a bias supply from both sides.

TEST DATA FOR THE KU-BAND MMIC CHIPS

Several MMIC amplifier chips for each design were assembled on gold-plated Elkonite (Cu-W alloy) carriers for RF characterization after "on-wafer" pulsed power screening. The Elkonite material was chosen for its good thermal conductivity and good

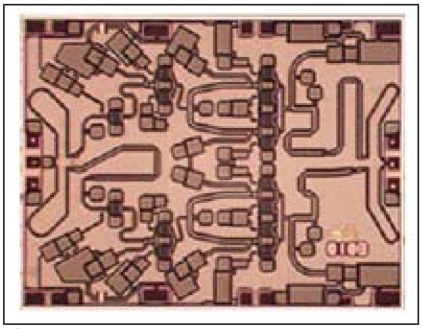

▲ *Fig. 7 Photograph of the Ku-band balanced 2W amplifier (chip size is 4.4 x 3.4 mm).*

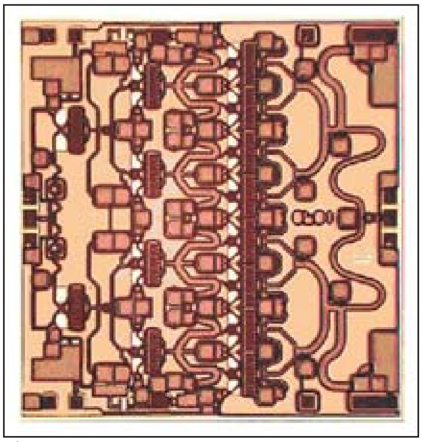

▲ *Fig. 8 Photograph of the Ku-band 5W amplifier (chip size is 4.2 x 4.4 mm).*

thermal expansion match to GaAs and alumina. The ICs were die attached on a pedestal, using gold-tin (AuSn) at 300°C, in order to keep the bond wire lengths to a minimum between the chip and the input and output microstrip feed lines, which were printed on 15-mil thick alumina substrates. The test fixtures were fitted with high performance microstrip-to-coaxial connectors having return loss better than 20 dB up to 18 GHz. All chips were tested under CW conditions.

High Gain, PAE/Linearity Power Amplifier

The average measured performance of the four-stage linear power amplifier at V_{DS} = 8 V is shown in ***Figure 9***. The gain was approximately 32.5 ±1 dB over the 14 to 14.5 GHz frequency range. At P1dB the output power was greater than 31.5 dBm and the PAE greater than 28 percent. The output third-order intercept point (TOI) was greater than 39.5 dBm. The noise figure and second harmonic levels were also measured. Their values were less than 5 dB and -48 dBc, respectively.

Broadband Power Amplifier

The typical measured P_{out} and PAE for the three-stage broadband amplifier MMIC at V_{DS} = 8 V and P_{in} = 18 dBm are shown in ***Figure 10***. The amplifier has an output power

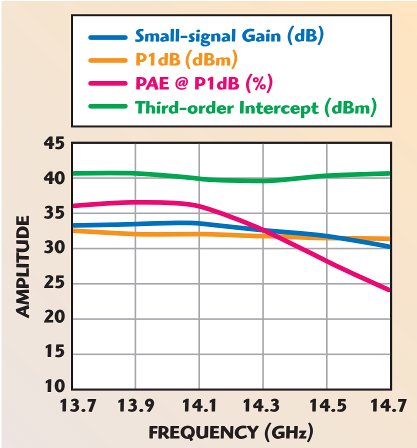

▲ *Fig. 9 Typical measured gain, P1dB, PAE and output third-order intercept versus frequency.*

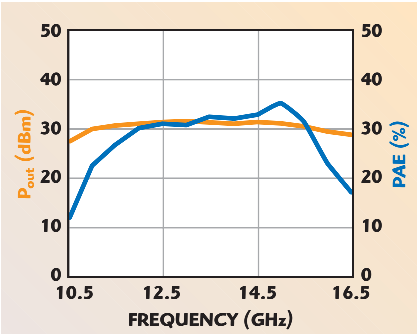

▲ *Fig. 10 Output power and power-added efficiency vs. frequency at V_{DD} = 8V and P_{in} = 18 dBm.*

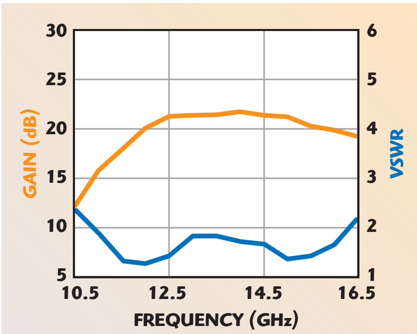

▲ *Fig. 11 Small-signal gain and VSWR vs. frequency at V_{DD} = 8V.*

greater than 31 dBm and a PAE better than 30 percent, over the 12 to 15.5 GHz frequency range. Over 11 to 16 GHz, the output power was better than 30 dBm. The output power was increased to 32 dBm at V_{DS} = 10 V. The variations of small-signal gain and input VSWR as a function of frequency are shown in ***Figure 11***. The input VSWR is better than 2:1 over the 10.9 to 16.4 GHz range.

Balanced 2 W Power Amplifier

Figure 12 shows the typical measured P_{out} and PAE for the balanced amplifier MMIC at V_{DS} = 8 V and P_{in} = 18 dBm. The amplifier has an output power greater than 33 dBm and a PAE better than 22 percent over the 12 to 15.5 GHz frequency range. When the supply voltage was increased to 10 V, the output power was better than 34.5 dBm. ***Figure 13*** shows the small-signal gain and input VSWR versus frequency. The input

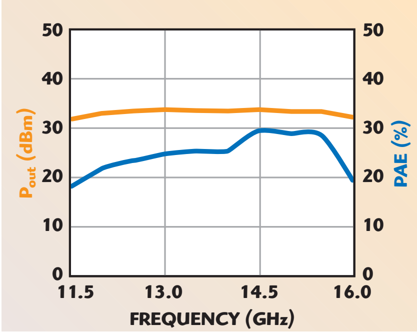

▲ *Fig. 12 Output power and power-added efficiency vs. frequency at V_{DD} = 8V and P_{in} = 18 dBm.*

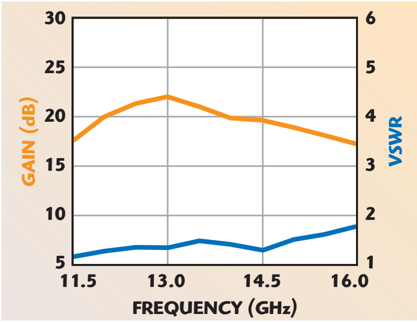

▲ *Fig. 13 Small-signal gain and input VSWR vs. frequency at V_{DD} = 8V.*

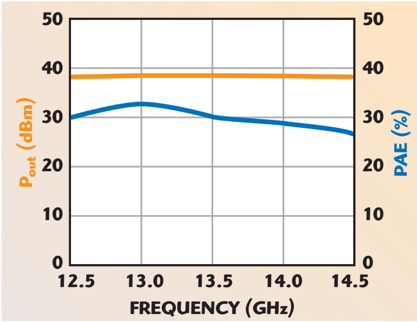

▲ *Fig. 14 Output power and power-added efficiency vs. frequency at V_{DD} = 8V and P_{in} = 23 dBm.*

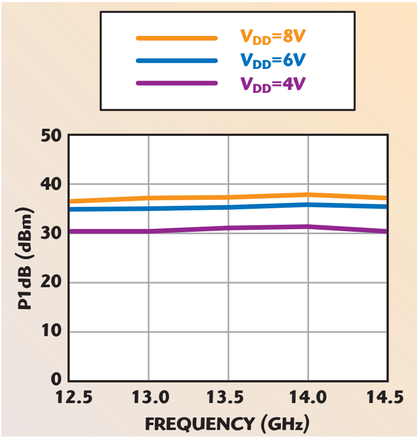

▲ *Fig. 15 1 dB compression point vs. drain voltage.*

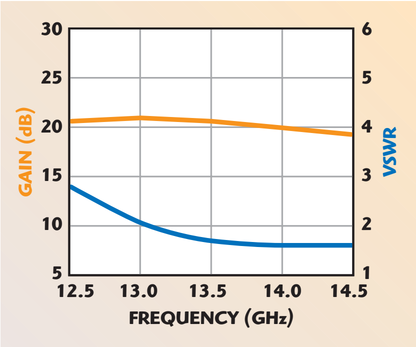

▲ *Fig. 16 Small-signal gain and input VSWR vs. frequency at V_{DD} = 8V.*

VSWR is better than 1.5:1 over the 11.5 to 15 GHz range.

5 W HPA

The typical measured P_{out} and PAE for the 5 W amplifier MMIC at V_{DS} = 8 V and P_{in} = 23 dBm are shown in ***Figure 14***. The amplifier has an output power greater than 38.5 dBm and a PAE better than 27 percent over the 12.5 to 14.5 GHz frequency range. ***Figure 15*** depicts the P1dB power levels at various drain voltages. The variations of small-signal gain and input VSWR as a function of frequency are shown in ***Figure 16***. The input VSWR is better than 2:1 over the 13.1 to 14.8 GHz range. The measured second- and third-harmonic power levels at V_{DS} = 8 V and P_{in} = 23 dBm were below –40 and –75 dBc, respectively.

CONCLUSION

A variety of Ku-band power amplifier MMICs has been developed using M/A-COM's MSAG MESFET technology. The power amplifiers have demonstrated excellent power performance: greater than 5 W output power with power-added efficiency of 32 percent at 13 GHz for the 5 W amplifier, and an outstanding PAE (36 percent) and linearity (TOI = 40 dBm) at P1dB compression and 14 GHz for the 1.5 W amplifier. This outstanding power performance was only possible because of high across-wafer uniformity of saturated drain-source current (I_{DSS}) and cut-off frequency (f_T) for the MSAG process. ■

ACKNOWLEDGMENT

The author wishes to acknowledge the support of M/A-COM's layout, test, standard microwave products and wafer-processing groups in the successful development of the above MMICs.

References

1. M. Cardullo, et al., "High Efficiency X-Ku-band MMIC Power Amplifiers," *1996 IEEE MTT-S International Microwave Symposium Digest*, Vol. 1, pp. 145–148.
2. M. Salib, et al., "A Robust 3 W High Efficiency 8 to 14 GHz GaAs/AlGaAs Heterojunction Bipolar Transistor Power Amplifier," *1998 IEEE MTT-S International Microwave Symposium Digest*, Vol. 2, pp. 581–584.
3. J. Komiak, W. Kong and K. Nichols, "High Efficiency Wideband 6 to 18 GHz PHEMT Power Amplifier MMIC," *2002 IEEE MTT-S International Microwave Symposium Digest*, Vol. 2, pp. 905–907.
4. T. Shimura, et al., "A High Power Density, 6 W MMIC for Ku-/K-band Applications," *2003 IEEE MTT-S International Microwave Symposium Digest*, Vol. 2, pp. 851–854.
5. Q. Zhang and S.A. Brown, "Fully Monolithic 8 W Ku-band High Power Amplifier," *2004 IEEE MTT-S International Microwave Symposium Digest*, Vol. 2, pp. 1161–1164.
6. J.G. Kim, et al., "A 2 W Balanced Power Amplifier MMIC for Ku-band Satellite Communications," *Microwave and Optical*

Technology Letters, Vol. 42, August 2004, pp. 342–344.
7. A.E. Geissberger, et al., “Refractory Self-aligned Gate Technology for GaAs Microwave FETs and MMICs,” *Electronic Letters*, Vol. 23, September 1987, pp. 1073–1075.
8. A.E. Geissberger, I.J. Bahl, E.L. Griffin and R.A. Sadler, “A New Refractory Self-aligned Gate Technology for GaAs Microwave Power FETs and MMICs,” *IEEE Transactions on Electron Devices*, Vol. 35, No. 5, May 1988, pp. 615–622.
9. I.J. Bahl, et al., “Class-B Power MMIC Amplifiers with 70 Percent Power-added Efficiency,” *IEEE Transactions on Microwave Theory and Techniques*, Vol. 37, No. 9, September 1989, pp. 1315–1320.
10. I.J. Bahl, et al., “C-band 10 W MMIC Class-A Amplifier Manufactured Using the Refractory SAG Process,” *IEEE Transactions on Microwave Theory and Techniques*, Vol. 37, No. 12, December 1989, pp. 2154–2158.
11. I.J. Bahl, et al., “Multifunction SAG Process for High Yield Low Cost GaAs Microwave Integrated Circuits,” *IEEE Transactions on Microwave Theory and Techniques*, Vol. 38, No. 9, September 1990, pp. 1175–1182.
12. W.L. Pribble and E.L. Griffin, “An Ion-implanted 13 W C-band MMIC with 60 Percent Peak Power-added Efficiency,” *1996 IEEE Microwave and Millimeter Wave Monolithic Circuits Symposium Digest*, pp. 25–28.
13. E.L. Griffin, “X-band GaAs MMIC Size Reduction and Integration,” *2001 IEEE MTT-S International Microwave Symposium Digest*, Vol. 2, pp. 709–712.
14. I.J. Bahl, “Design of a Generic 2.5 W, 60 Percent Bandwidth, C-band MMIC Amplifier,” *Microwave Journal*, Vol. 45, No. 9, August 2002, pp. 54–70.
15. M. Ashman and I.J. Bahl, “High Performance Wideband MSAG Gain Block/Driver Amplifier MMICs Using MLP Technology,” *Microwave Journal*, Vol. 47, No. 12, December 2004, pp. 74–88.
16. I.J. Bahl, “MESFET Process Yields MMIC Ka-band PAs,” *Microwaves and RF*, Vol. 44, No. 5, May 2005, pp. 96–112.
17. H.F. Cooke, “Precise Technique Finds FET Thermal Resistance,” *Microwaves and RF*, August 1986, pp. 85-87; correction of this paper in *Microwaves & RF*, February 1987, p. 13.
18. A. Materka and T. Kacprzak, “Computer Calculation of Large-signal GaAs FET Amplifier Characteristics,” *IEEE Transactions on Microwave Theory and Techniques*, Vol. 33, No. 2, February 1985, pp. 129–135.
19. I.J. Bahl, et al., “Low Loss Multilayer Microstrip Line for Monolithic Microwave Integrated Circuits Applications,” *International Journal of RF and Microwave Computer-aided Engineering*, Vol. 8, November 1998, pp. 441–454.
20. I.J. Bahl, “High Current Capacity Multilayer Inductors for RF and Microwave Circuits,” *International Journal of RF and Microwave Computer-aided Engineering*, Vol. 10, March 2000, pp. 139–146.
21. I.J. Bahl, “High Q and Low Loss Matching Network Elements for RF and Microwave Circuits,” *IEEE Microwave Magazine*, Vol. 1, September 2000, pp. 64–73.
22. I.J. Bahl, *Lumped Elements for RF and Microwave Circuits*, Artech House Inc., Norwood, MA, 2003.
23. KELDIST, M/A-COM’s Internal Software.
24. I.J. Bahl, “Average Power Handling Capability of Multilayer Microstrip Lines,” *International Journal of RF and Microwave Computer-aided Engineering*, Vol. 11, November 2001, pp. 385–395.
25. S.C. Cripps, *RF Power Amplifiers for Wireless Communications*, Artech House Inc., Norwood, MA, 1999.
26. E.L. Griffin, “Application of Loadline Simulation to Microwave High Power Amplifiers,” *IEEE Microwave Magazine*, Vol. 1, June 2000, pp. 58–66.
27. K. Chang, I.J. Bahl and V. Nair, *RF and Microwave Circuit and Component Design for Wireless Systems*, John Wiley & Sons Inc., Hoboken, NJ, 2002, Chapter 11.
28. I.J. Bahl and P. Bhartia, *Microwave Solid State Circuit Design*, Second Edition, John Wiley & Sons Inc., Hoboken, NJ, 2003, Chapter 10.
29. I.J. Bahl, “Low Loss Matching (LLM) Design Technique for Power Amplifiers,” *IEEE Microwave Magazine*, Vol. 5, December 2004, pp. 66–71.

BUILDING A 3.3 TO 3.8 GHZ 802.16A WIMAX LNA ON FR4 MATERIAL

This article presents the design of a 3.3 to 3.8 GHz LNA, suitable for IEEE 802.16a WiMAX customer premise equipment (CPE) and base transceiver stations (BTS), built on inexpensive FR4 copper laminate epoxy glass board material using the Agilent Technologies ATF-54143 E-pHEMT (enhancement-mode pseudomorphic high electron mobility transistor).

The high loss tangent (tan δ) and relatively variable dielectric constant (ε_r) of the FR4 copper laminate epoxy glass material (tan δ = 0.04, ε_r = 4.6) generally limits its use to applications below 3 GHz.[1] For higher frequencies, designers usually use more expensive materials such as the Rogers RO4350B glass-reinforced hydrocarbon/ceramic laminate[2] with tan δ = 0.003 and ε_r = 3.48. Normally, the insertion loss for the FR4 board will increase rapidly when the operating frequency goes above 3 GHz, and designing 3 GHz circuits using FR4 material is usually not recommended. When using high performance devices such as the ATF-54143, however, circuits designed on FR4 material can meet the customer's requirements for noise figure, gain and linearity. The biggest benefit to customers is the lower cost of the FR4 material. This is a critical concern for customers' main production. With the increasing acceptance of WiMAX as a substitute for the existing broadband wire-line infrastructure in the last mile, people are now designing and testing WiMAX CPE and BTS operating at around 3.5 GHz. Properly designed circuits on a FR4 board can help to reduce the transceiver cost. Based on theoretical analysis and ADS simulation, this article presents a successful WiMAX LNA built on a FR4 board using the ATF-54143 E-pHEMT.

TARGET ANALYSIS

With a single 3.6 V supply, the E-pHEMT LNA delivers a measured 0.82 dB noise figure (NF), 12.8 dB gain, +19 dBm output power at 1 dB gain compression (P1dB), 36.7 dBm third-order output intercept point (OIP3), –20 dB input return loss (IRL) and –12 dB output return loss (ORL) at 3.5 GHz.

To arrive at a balance between noise figure, gain and linearity, the device drain source current (I_{ds}) was chosen to be 60 mA with a 3 V drain-to-source voltage; the gate-to-source voltage was 0.59 V. According to the ATF-54143 data sheet,[3] this transistor

XIAO LU
Agilent Technologies Inc.
Shenzhen, China

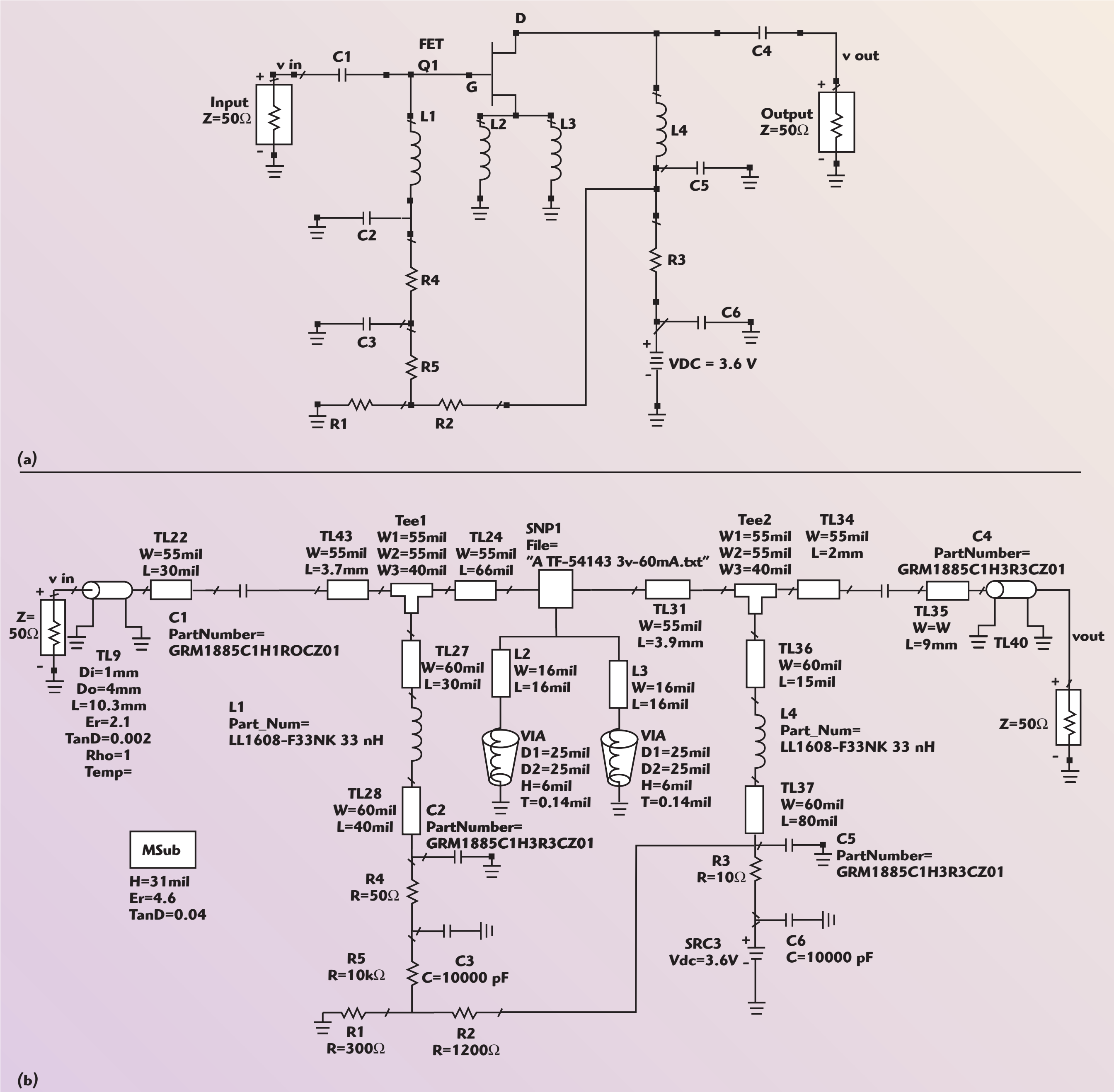

Fig. 1 ATF-54143 low noise amplifier's (a) circuit schematic and (b) ADS simulation.

has the following typical features at 3.5 GHz: F_{min} = 0.65 dB, G_a = 14.5 dB, OIP3 = +37.2 dBm, S_{11}=0.608 ∠149.6^0 (VSWR≈4.1), Γ_{opt} = 0.32 ∠–170^0.

The circuit can be simulated in both linear and nonlinear operation modes by using the Agilent EEsof Advanced Design System (ADS) software. A two-port S-parameter file in the Touchstone format was used to simulate the gain, noise figure and input/output return loss; an ADS model based on the data sheet[3] was applied to simulate the bias conditions and linearity. Accurate equivalent models for the resistors, inductors, capacitors and microstrip lines are critical for exact simulation because they determine the tuning elements on the circuit board. Thus, device models from Toko and Murata are adopted to model the capacitors and inductors from these two vendors, and board properties provided by the FR4 vendor are adopted to model the microstrip lines. ***Figure 1*** shows the circuit schematic and the corresponding ADS simulation file that includes all the models.

RF INPUT MATCHING

The RF input matching always plays a key role in an LNA design. It is not only a way to achieve a low NF, it is also the way to obtain higher IIP3, higher gain and better input return loss. In addition, since a filter exists before the LNA in some transceiver systems, a poor input return loss will degrade the performance of the filter, and thus impact the total performance of the system. Therefore, the goal for the input matching is to achieve good return loss and noise figure while maintaining ac-

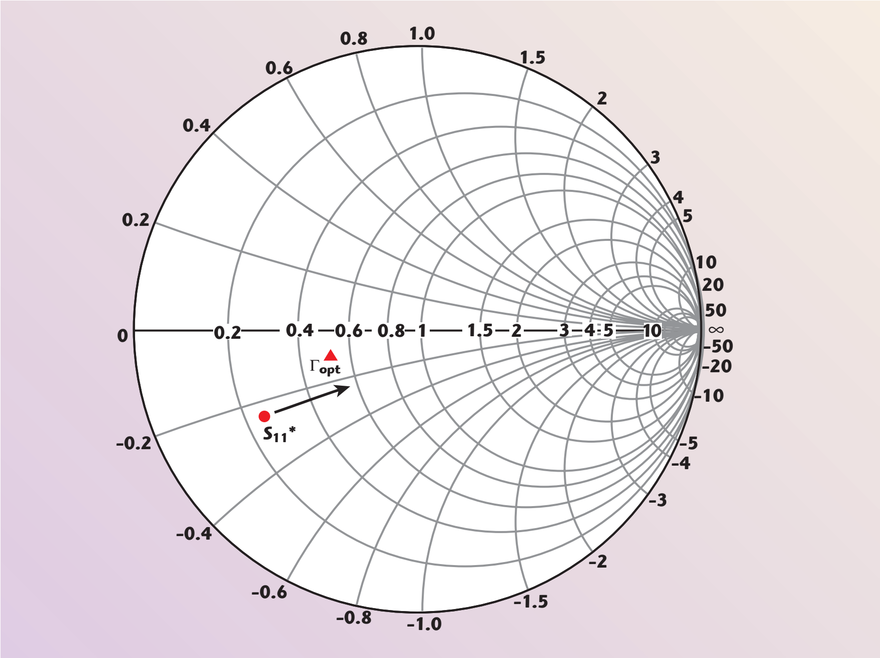

▲ *Fig. 2 Input S_{11}^* and Γ_{opt} for the ATF-54143 transistor.*

ceptable gain and IIP_3. According to ***Figure 2***, the transistor has an $S_{11}^* = 0.608 \angle -149.6^0$, which is a little far away from $\Gamma_{opt} = 0.32 \angle -170^0$. This means that if a good input return loss is desired, the noise figure will be high; if a good noise figure is desired, the VSWR will be high. The best way to resolve these opposing requirements is to obtain good noise figure and good return loss by pulling S_{11}^* close to Γ_{opt} by using a feedback network.

NEGATIVE FEEDBACK TO PULL S_{11}^* CLOSER TO Γ_{opt}

According to Nyquist theory, the noise from any impedance is determined by its resistive component,[4] and an ideal lossless element will not impact the NF_{min} if it is applied as the feedback network.[5]

In ***Figure 3***,

$$Z_{in} = R_g + \frac{1}{j\omega C_{gs}} \tag{1}$$

In ***Figure 4***, when adding a source inductance L_s in the FET's source lead, the input voltage can be rewritten as

$$V_g = I_g\left(R_g + \frac{1}{j\omega C_{gs}}\right) + \left(I_g + g_m V_c\right) j\omega L_s \tag{2}$$

Since

$$V_c = \frac{I_g}{j\omega C_{gs}} \tag{3}$$

Then V_g can be expressed as

$$V_g = I_g\left(R_g + \frac{1}{j\omega C_{gs}}\right) + \left(I_g + g_m \frac{I_g}{j\omega C_{gs}}\right) j\omega L_s$$

$$= I_g\left(R_g + \frac{1}{j\omega C_{gs}} + j\omega L_s + \frac{g_m L_s}{C_{gs}}\right) \tag{4}$$

Thus, the equivalent input impedance is

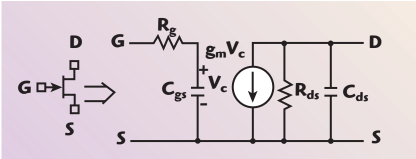

▲ *Fig. 3 Simplified FET model.*[6]

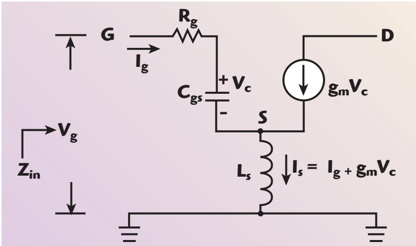

▲ *Fig. 4 FET model with an external source inductance.*

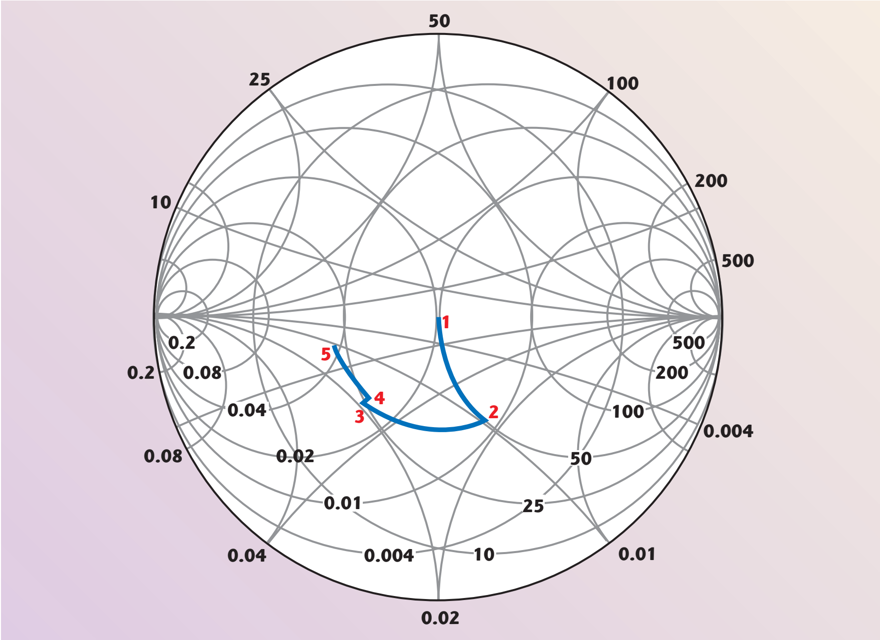

▲ *Fig. 5 Implementation of the input matching.*

$$Z'_{in} = \frac{V_g}{I_g} = \left(R_g + j\omega L_s\right) + \left(\frac{1}{j\omega C_{gs}} + \frac{g_m L_s}{C_{gs}}\right) \quad (5)$$

In Equation 5, the term

$$\frac{g_m L_s}{C_{gs}} + j\omega L_s$$

is an "added" input impedance introduced by the source inductor, and the added resistive and reactive component both help to pull the S_{11}^* closer to Γ_{opt}.

Normally, L_s should be a small inductor optimized according to Equation 5. Based on the analysis above, a small microstrip line (width = length = 16 mil) together with a via-hole was introduced on both of the source leads to work as a small inductor. According to the measured results, the microstrip lines actually pull the S_{11}^* closer to Γ_{opt} while not changing the value for Γ_{opt} (necessary for NF_{min}). Since the feedback is negative, there is an accompanying decrease in gain with increasing feedback. In this circuit, the gain did not decrease too much.

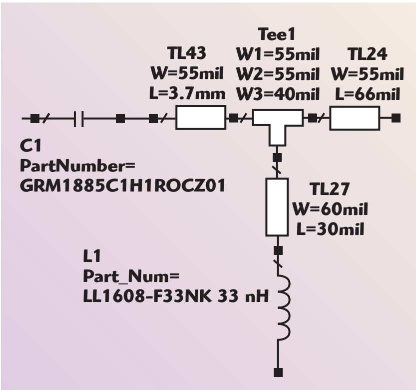

▲ *Fig. 6 Simulation of the input circuit matching.*

INPUT MATCHING NETWORK DESIGN

Since the LNA operates around 3.5 GHz, a high pass filter is required for input matching. When pulling S_{11}^* closer to $\Gamma_{opt} = 0.32 \angle -170°$, the matching network should also maintain the gain.

In **Figure 5**, the input conjugate S_{11} is 0.38 $\angle$–162° after proper allocation of the capacitor, inductor and microstrip lines. **Figure 6** is the equivalent circuit. According to the measured results, this input matching network will lead to S_{11} = –20 dB and NF = 0.82 dB. The measurement results are in line with the theoretical analysis and ADS simulation.

PASSIVE DC BIASING

Once the RF input matching has been established, the next step is to establish the DC biasing. Since the DC biasing conditions are V_{gs} = 0.59 V, V_{ds} = 3 V and I_{ds} = 60 mA, it is easy to determine the DC biasing

TABLE I
COMPONENT PART LIST FOR THE ATF-54143 WiMAX AMPLIFIER

Devices		Vendor's Part No.
C1	1 pF	Murata GRM1885C1H1R0CZ01D
C4	3.6 pF	Murata GRM1885C1H3R6CZ01D
L1	33 nH	Toko LL1608-FH33NJ
L4	10 nH	Toko LL1608-FH10NJ
C2,C5	3.6 pF	Murata GRM1885C1H3R6CZ01D
C3,C6	10 nF	Murata GRM188R71E103KA01D
J1,J2	SMA connectors	E.F. Johnson 142-0701-881
Q1	E-pHEMT	Agilent Technologies ATF-54143
R1	300 Ω chip resistor	
R2	1200 Ω chip resistor	
R3	10 Ω chip resistor	
R4	50 Ω chip resistor	
R5	10 kΩ chip resistor	
L2,L3	strap each source pad to the ground pad with 16 mil width and 16 mil length	

$$R3 = \frac{V_{dc} - V_{ds}}{I_{ds}} = \frac{3.6 - 3}{60 \times 10^{-3}} = 10\Omega$$

$$\frac{R1}{R1 + R2} = \frac{V_{gs}}{V_{ds}} = \frac{0.59}{3} \approx \frac{1}{5} \qquad (6)$$

where

V_{dc} = power supply voltage, 3.6 V
V_{ds} = device drain to source voltage, 3 V
V_{gs} = device gate to source voltage, 0.59 V
I_{ds} = device drain to source current, 60 mA

DETERMINING DEVICE VALUES

To achieve low input return loss, low noise figure and high gain, the values for C1, TL43, L1 and TL24 in the simulation are established according to the analysis of the input matching network design. The width and length of L2 and L3 are determined according to the ADS simulation. The SRF (series resonant frequency) for C5 is selected to be 3.5 GHz to terminate the frequency around 3.5 GHz and thus help improve linearity. C3 and C6 are used as a low frequency bypass to terminate the high frequency second-order harmonics and thus help improve linearity. The resistor R5 helps terminate the low frequencies, and can improve the in-band stability by preventing resonant frequencies between the two bypass capacitors. ***Table 1*** summarizes the bill of material for the LNA board.

MEASURED PERFORMANCES OF THE ATF-54143 LNA AT 3.5 GHz

With a drain current of 60 mA, the measured and simulated performances of the LNA are compared with good agreement. ***Figure 7*** shows a gain of 12.8 dB at 3.5 GHz and a noise figure of 0.82 dB is achieved (see ***Figure 8***). ***Figure 9***

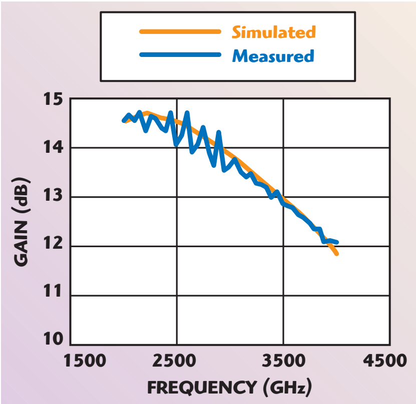

▲ *Fig. 7 Comparison of the measured and simulated gain of the LNA.*

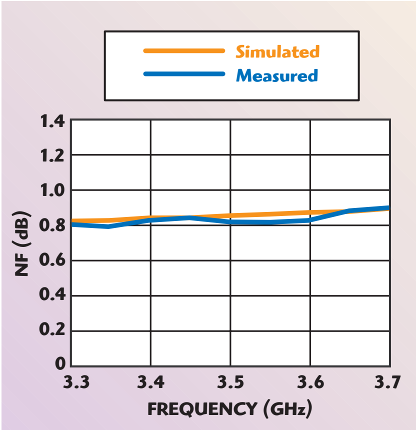

▲ *Fig. 8 Comparison of the measured and simulated noise figure of the LNA.*

shows the comparison between the simulated and measured input return loss, both of which are 20 dB at 3.5 GHz. The simulated and measured output return loss are shown in ***Figure 10***, both of which are greater than 11 dB. The response is wide enough to cover the operating frequency range from 3.3 to 3.8 GHz. ***Figure 11*** depicts the comparison for the isolation (S_{12}), while ***Figure 12*** is the comparison for OIP3.

CONCLUSION

Based on theoretical analysis and ADS simulation, this article demonstrates a 3.3 to 3.8 GHz WiMAX LNA built on a FR4 board material. Since it has a high linearity (P1dB > +19 dBm, OIP3 > +36 dBm), this LNA can also be used as a PA driver for radio cards and CPE. The measured RF results verify the feasibility of 3.5 GHz WiMAX designs built on a FR4 board. Over the 3.3 to 3.8

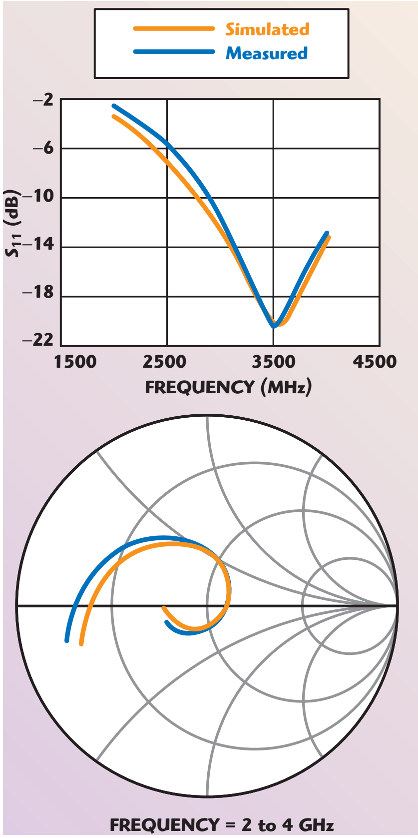

▲ *Fig. 9 Comparison of the measured and simulated input return loss of the LNA.*

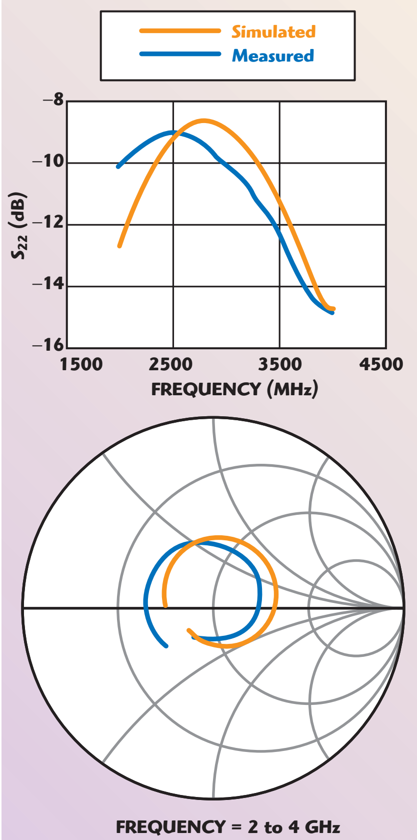

▲ *Fig. 10 Comparison of the measured and simulated output return loss of the LNA.*

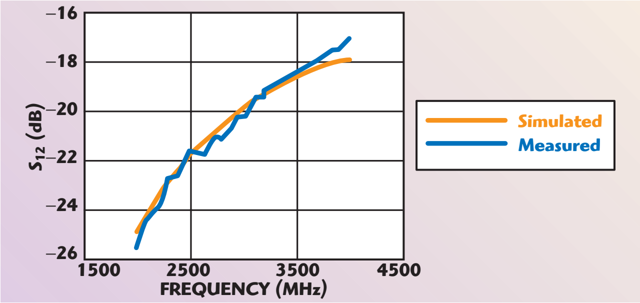

▲ *Fig. 11 Comparison of the measured and simulated isolation (S_{12}) of the LNA.*

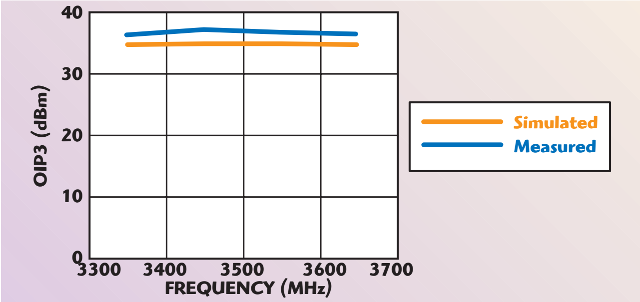

▲ *Fig. 12 Comparison of the measured and simulated OIP3 of the LNA.*

GHz operating frequency range, the FR4 board does not significantly impact the noise figure and gain. ■

ACKNOWLEDGMENTS

The author would like to thank Eric Chan, Lim Chin-Liang and Abdullah Asrul-Sani of Agilent Technologies, Malaysia, for their valuable help and comments during the circuit tuning and validation.

References

1. I. Bahl, *Lumped Elements for RF and Microwave Circuits*, Artech House Inc., Norwood, MA, 2003, Chapter 13.
2. Data Sheet, "RO4000® Series High Frequency Circuit Materials," Rogers Corp., 2002.
3. Data Sheet, "Agilent ATF-54143 Low Noise Enhancement-mode Pseudomorphic HEMT in a Surface-mount Plastic Package," Agilent Technologies Inc., 2003.
4. I. Bahl and P. Bhartia, *Microwave Solid State Circuit Design*, John Wiley & Sons Inc., Hoboken, NJ, 1988, Chapter 7.
5. J. Engberg and T. Larsen, *Noise Theory of Linear and Nonlinear Circuits*, John Wiley & Sons Inc., Hoboken, NJ, 1995, Chapter 6.
6. S.A. Maas, *Nonlinear Microwave and RF Circuits*, Artech House Inc., Norwood, MA, 2003, Chapter 8.

Xiao Lu *received his BSc and MSc degrees in electrical engineering from Zhejiang University, China. He joined STMicroelectronics in 2003, working in DVB-S tuner development. He joined Agilent Technologies Inc. (formerly Hewlett Packard) in 2004 and is currently working as an application engineer. His design experience includes LNAs, mixers, VCOs and PAs for wireless applications.*

A SPECIALIZED LOW LOSS 8 dB COUPLER

A coupler with a through loss of less than 1.45 dB from 5 to 900 MHz was needed in a 75 Ω system and only commercial couplers of 10 dB (or more) could offer this low through loss, particularly at the highest frequencies. Unfortunately, another requirement was to produce a very high RF level at the input port when the coupled port was driven. This required a high power driver with very high linearity on the coupled port. The greater the coupling loss, the higher the power required to drive the coupled port so it was advantageous to have an 8 dB coupler rather than a 10 dB coupler. It was also found that the amplifier could drive more power into a 50 Ω load than a 75 Ω load because of voltage swing limitations. The coupler described in this article gave some freedom not available on commercial couplers. For example, the isolated port was not used, so it could be buried inside the coupler.

Fig. 1 Schematic of the 8 dB coupler.

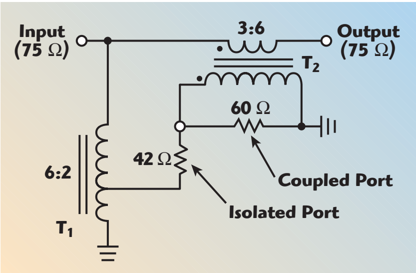

THE BASIC COUPLER

Using ideal transformers, the circuit shown in ***Figure 1*** is an 8 dB coupler, which has a 50 Ω impedance looking in the coupled port. It also has a theoretical insertion loss of 0.83 dB and a return loss of nearly 21 dB. In addition to having different turns-ratios on the transformers, the interconnections are somewhat different than for a conventional coupler. Since there is no need to access the isolated port, it is made floating. This allows the shunt transformer T1 to be an autotransformer, which simplifies construction and improves performance. This ideal 8 dB coupler has a theoretical loss of 0.83 dB, whereas the requirement allows a loss of 1.45 dB, which leaves about 0.6 dB to account for core losses, skin-effect losses and any reflection mismatches within the windings themselves. As it turns out, this 0.6 dB extra loss is a tough requirement; ordinary commercial 8 dB couplers have nearly twice this extra loss.

HIGH FREQUENCY DESIGN

Since the high frequency loss is the hardest to meet, extensive modeling and measurements were done to minimize the losses and the reflective mismatches. To make the transformers perform well at high frequencies, the

CECIL W. DEISCH
Tellabs
Naperville, IL

windings must be modeled as coupled transmission lines. The total length of the windings is restricted by the phase shifts at the highest frequency, which limits the core size and the number of turns. This, in turn, limits the wire size to fine magnet wire so skin and proximity losses alone contribute a little over 0.1 dB. Even if reflective mismatches are eliminated at high frequencies, this leaves only 0.5 dB total loss for the two cores. A clever way was found to wind the cores to give overall good performance and still provide an insertion loss of approximately 1.35 dB at 900 MHz. Although more exacting to wind (extra cost), no tuning is required. The construction details and rationale follow.

THE SHUNT TRANSFORMER: MODELING TURNS AS TRANSMISSION LINES

Consider the two-turn helix (in air) shown in ***Figure 2***. It can be modeled as a simple two-wire transmission line, which is folded back upon itself. If the spacing between the turns is known, the Z_0 of the line is known. The electrical length of the line is simply the length of one turn modified by ε_r, the relative dielectric constant. Knowing just these two characteristics, high frequency modeling can quite accurately predict the performance. This assumes an air core and that there is no radiation. Even though the coil may be wound on a ferrite core, at the highest frequencies, the ferrite can be substituted with air (except for core losses). Since most of the winding anomalies show up at high frequencies, this is an excellent modeling tool. For a multi-turn helix, the assumption is that only the next adjacent turns have significant effect on high frequency performance. Under this assumption, a helix is simply the composite of multiple double-coupled transmission lines. A six-turn helix, with a tap at two turns from ground, can thus be modeled, as shown in ***Figure 3***.

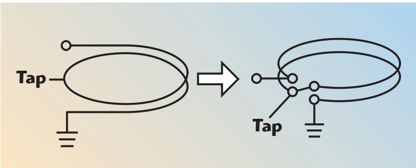

Fig. 2 Shunt transformer modeled as transmission lines.

SKIN AND PROXIMITY EFFECTS

At 900 MHz, the skin effect restricts the current flow in the wires to a thin layer less than 2.54 μm thick. Additionally, the current is highly concentrated on the sides of the wire that are in close proximity to other conductors. The net result is that at approximately 0.1 dB, the copper conductor losses are approximately twice that predicted by skin effect alone. The copper losses might be slightly reduced by using a larger wire — #34 wire, for example — but core losses may increase in the series transformer because the wires are forced to be closer to the lossy ferrite in the tightly packed core hole.

TWISTED PAIR TRANSMISSION LINES

In the 50 to 75 Ω range, the characteristic impedance, Z_0, of the twisted pair is quite sensitive to the tightness of the twist because even a few spots of slight wire separation significantly change (increase) Z_0. The primary function of twisting the wires is to assure intimate tight spacing of the wires, even as the pair (or triple) is wound around the core. Within reason, the tighter the twist, the lower Z_0, and the more securely the wires of the pair are held in intimate contact. Instead of twisting, the same result might be accomplished if the pair (or triple) was co-extruded with insulation that held the spacing of the wires constant. The presence of the magnetic core affects the Z_0 of the twisted pair. That is, a twisted pair may have a Z_0 of 70 Ω in air, but may increase to 75 Ω when wound about a ferrite core. The reason is that the core allows more flux linkages, which increases the effective inductance of each wire. Increased inductance means a higher Z_0. The increase in Z_0 and the increase in core loss are closely related.

CORE LOSSES

It is obvious that the core material should have low losses for a fixed number of turns. For cores with roughly equal cross-section area with six turns, the losses of commercial cores range from approximately 0.2 to 0.4 dB in a 75 Ω system. Another core requirement is that it has a high enough inductance at the lowest frequencies so as to maintain high return loss and low insertion loss. A third requirement (in the present system) is that it has about 110 dB of linearity for 65 dBmV signals at the coupled port up to approximately 70 MHz. If a core is wound with a fixed number of turns and is placed across a voltage source, to a close approximation, the core losses are proportional to $(Bf)^2$, where B is the magnetic flux density in the core and f is the frequency. At a fixed frequency, B increases linearly with applied voltage, so the core losses are proportional to B^2 and hence to V^2, just the same as for an ordinary resistor. If the applied voltage is held constant while the frequency is increased, B decreases as 1/f. The net result is that core losses of the shunt transformer tend to be constant with frequency, which is borne out by network analyzer measurements. At high frequencies especially, current-carrying wires that lie close to the ferrite material cause core losses. This applies especially to the series transformer.

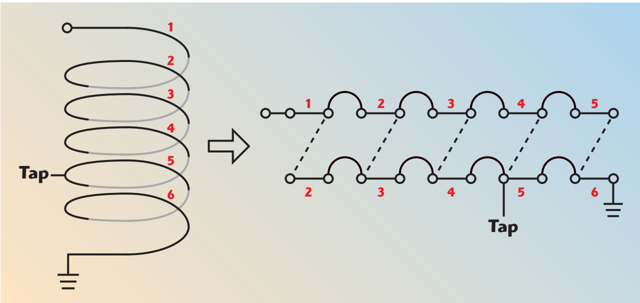

Fig. 3 A six-turn helix model.

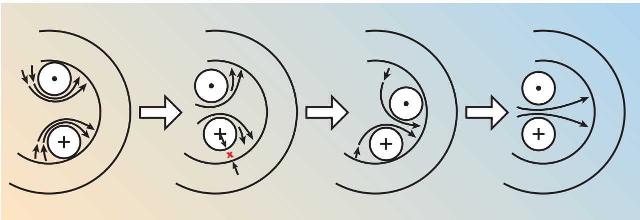

Fig. 4 Two wires with opposite current direction in a ferrite core.

Even if there is no net magnetic flux encircling the hole in the core, there are locally intense magnetic fields around the current-carrying wires, which cause losses in the ferrite. Consider the case of just two wires passing through the hole in a core, each of which carries identical current in opposite directions (see ***Figure 4***). Clearly, there is no net flux around the core because the canceling currents create no net H field. Yet, as shown, there are local H fields in the close vicinity of the wires, which set up local B fluxes in the core. Wherever there are B fluxes in the ferrite, there are losses, and since the currents in the wires of the series transformer tend to be constant, the local H field tends to be constant. As stated before, the core losses tend to increase as $(Bf)^2$, so although the permeability of ferrite decreases with frequency, the local B fluxes do not drop fast enough to make up for the higher ferrite losses at higher frequencies. The net result is that core losses in the series transformer are very low at low frequency, but rise rapidly at high frequency. The skin-effect losses also rise with frequency, but rise relatively slowly as $\sqrt{f}$.

If the two wires are moved away from the ferrite, the core losses are reduced because the local H field drops off as 1/x. Instead, if the two wires are closely paired but still touching the ferrite, local H fields are reduced and core losses are also lowered, but are still significant. Finally, if the two wires are paired and moved away from the ferrite, core losses are dramatically reduced because the H field tends to drop off as $1/x^2$. For lowest core losses, the lesson is to pair the wires with opposite currents and keep them away from the core surfaces.

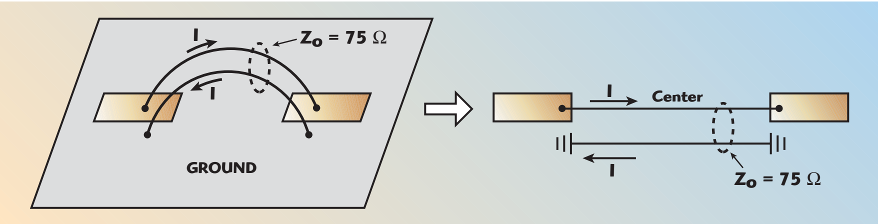

Fig. 5 Series transformer modeling.

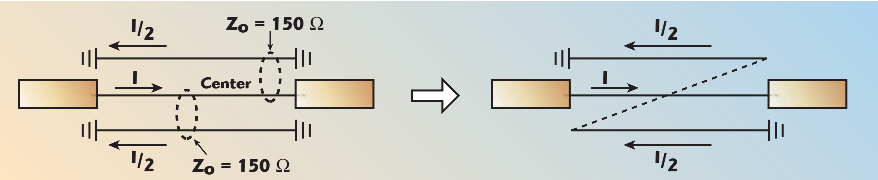

Fig. 6 Series transformer with two outer conductors in series.

MODELING THE SERIES TRANSFORMER

The series transformer monitors current in the main transmission path, has a turns-ratio of 3:6 and must have an isolated secondary. To set up the transmission line model, consider the diagram shown in ***Figure 5***. The main transmission path is broken and a 75 Ω, two-wire transmission line is inserted. Except for additional phase shift, the main path is not affected. However, the RF current in one conductor is of the same magnitude but opposite polarity to the current in the other conductor. Now assume that the center conductor has a wire on either side of it, each of which has a Z_0 of 150 Ω. The center conductor still sees a net Z_0 of 75 Ω, but each of the outer conductors carries only one half of the current of the center conductor. Next, connect the two outer conductors in series, as shown in ***Figure 6***. If the lines are electrically short enough, the result is an isolated 2:1 current transformer. Finally, one end can be lifted from ground and a resistor to ground can be inserted (see ***Figure 7***). Although the resulting current transformer is no longer "perfect" because of the phase shift between the two series sections and the imperfect ground at the resistor end, it is still good enough for this coupler application. Instead of grounding one end of the series connection, the center connection can be grounded and a resistor can be placed at each end of the series connection. This now makes a push-pull output, which may have great benefit in certain applications.

The end view of this three-wire arrangement is shown in ***Figure 8***. Simulations indicate that the high frequency performance is somewhat improved if the outer two wires are tightly coupled to each other. In fact, simulations indicate that the Z_0 of the two "outer" wires should be about 25 Ω, although in practice it is difficult to get lower than approximately 40 to 50 Ω, which, fortunately, still gives good performance. The "center" conductor still needs to have a Z_0 of 75 Ω between itself and the pair of tightly coupled outer conductors.

These two Z_0 requirements can be met by pre-twisting three #36 AWG magnet wires as follows: Two of the wires are first tightly twisted (about 16 twists per inch) in the clockwise direction. This forms the two "outer" wires, which need tight coupling. Next, the "center" wire is twisted (about 8 twists per inch) about the first pair, but in a counterclockwise direction (see ***Figure 9***). This gives a Z_0 close to 75 Ω between the center wire and the tightly

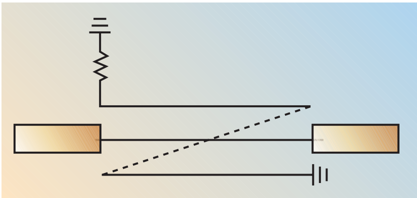

Fig. 7 Series transformer with one end of the secondary loaded.

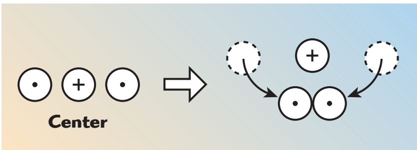

Fig. 8 Three wire arrangement.

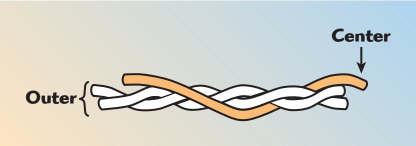

Fig. 9 Twisted wire configuration.

twisted outer pair. If the center wire is twisted in the same direction around the outer pair, Z_0 is much lower than 75 Ω because it tends to lie close to the outer pair throughout the spiral. Twisting in the opposite direction allows the center wire to just touch the outer pair in a few spots and hence produces an acceptably higher Z_0.

This specially made twisted triple should not be tightly wound on the series transformer so as to keep the current-carrying wires away from the lossy ferrite core. Ideally, the twisted triple should touch the ferrite at only four corners for each turn. This adds slightly to the turn length, but the benefits of lower core loss at high frequency outweigh the detriment of extra phase shifts.

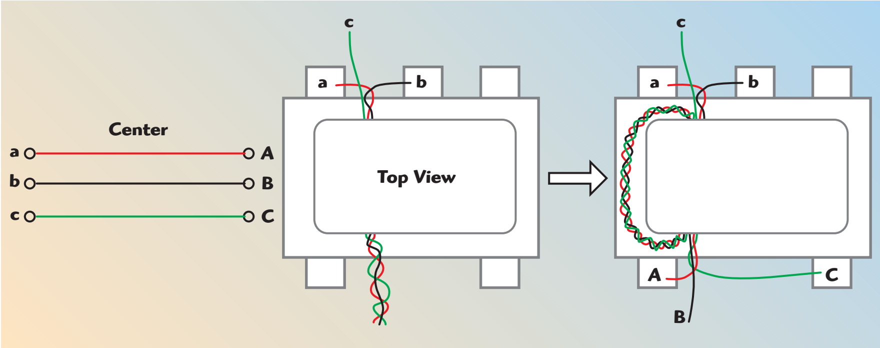

Fig. 10 Winding the series transformer in the ferrite core.

WINDING THE TWO-HOLE CORE

The Series Transformer

Take the #36 pre-twisted triple with "center" wire a-A and two "outer" wires b-B, c-C and insert it in the left-hand hole of the ferrite core, as shown in ***Figure 10***. Connect ends a and b to the solder tabs shown. Make sure there is a least one twist of a and b between the tabs and the entrance hole; do not widely space these wires. Leave end c free and unconnected for the moment. Wind two more turns (for a total of three turns) of the triple through the left-hand hole. Do not tightly wind the triple against the core in order to minimize core losses. Connect ends A and C on the tabs as shown. Again, make sure there is at least one twist of A and C between the tabs and the core hole. Now take ends c and B and snugly pull them against the existing windings, twist together and solder the connection, as shown in ***Figure 11***.

The Shunt Transformer

Take a single #36 wire and attach it to tab e, as shown in ***Figure 12***. Wind four turns through the right-hand hole as a single-layer, closely bunched winding. As the wire exits from the fourth turn, wrap one turn around tab f then continue winding two more turns. Connect the end at

G as shown. This winding has six turns with a tap at two turns from ground. This winding may be wound tightly against the core because this winding nominally carries no current. It is all right (probably advantageous) to wind the last two turns in contact with the first turn in order to slightly increase the capacitance.

MODIFICATIONS TO IMPROVE PERFORMANCE

In the real world, there are always parasitic impedances, which, to some extent, can be compensated. Experimentation shows that the best overall performance is obtained by adding components and changing impedances, as shown in ***Figure 13***. At high frequencies, the apparent turns-ratio of T_1 is slightly changed by adding a small capacitor (0.2 to 0.4 pF) between the top and the tap of T_1. This capacitor does not change the phase shift of T_1 much, but does lower the Thevenin voltage at the tap by canceling part of the inductive impedance looking back into the tap. This extra capacitance may be incorporated into the winding arrangement of the turns of the shunt transformer. Conversely, if a small capacitor is placed between the tap and ground, the apparent Thevenin voltage at the tap is raised at high frequencies. Note also that the impedance on the isolated port has been changed to an RC network. ■

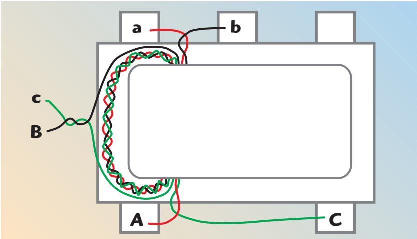

Fig. 11 Series transformer connections.

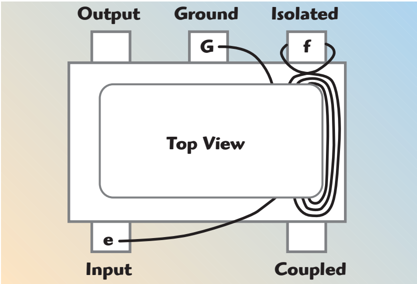

Fig. 12 Winding a shunt transformer on the ferrite core.

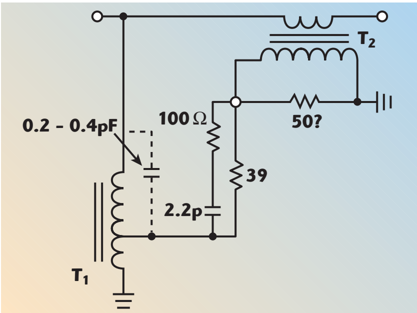

Fig. 13 Final configuration of the 8 dB coupler.

Cecil W. Deisch received his MSEE degree from New York University and has spent most of his career at AT&T Bell Labs, concentrating mostly on magnetics and analog circuit design. In addition to being awarded several patents, he has published many technical papers in various branches of electrical engineering and is an AT&T fellow. During his career, he has designed circuits covering the frequency range from 20 Hz (telephone ringing voltage) to 1 GHz. He now works for Tellabs, where he developed this new low loss coupler configuration.

DESIGN OF A UWB LOW INSERTION LOSS BANDPASS FILTER WITH SPURIOUS RESPONSE SUPPRESSION

This article describes a new ultrawideband (UWB) microstrip bandpass filter based on a dual-mode ring resonator with spur-line structures placed at the input and output ports. This type of filter is characterized by its compact size, sharp rejection, low insertion loss and wide stopbands. The spur-line structure generates a band rejection to suppress the spurious response without changing the prototype design. In addition, the resonance frequency of the spur-line bandstop filter can be accurately and conveniently calculated. The highest attenuation of the spurious levels in the proposed filter is greater than 33 dB without degradation of the performance of the bandpass filter.

Recently, more attention has been paid to applications of ultrawideband (UWB) technology on wireless communication. It offers advantages of decreased cost and increased capabilities, compared with other conventional radio technologies. Standards activities for UWB systems are promoting a global perspective for not only technology but also regulations. UWB has the characteristics of low cost, bulk data transmission rate and very low power consumption that make it attractive in local area networks, position location and tracking, and radar systems. Planar bandpass filters, with a wide bandwidth of 3.1 to 10.6 GHz, are highly suitable for integration of UWB front-ends. A planar bandpass filter, based on a microstrip structure, can provide the advantages of easy design, lower fabrication cost and compact size, and has been widely used. In addition, a dual-mode resonator is often built into the microstrip related bandpass filter design to improve the passband and rejection. Planar dual-mode filters have been introduced, which offered significant size, weight and cost advantages over cavity and dielectric resonator designs.[1] Several authors, dealing with the advances of novel materials and fabrication technologies,[2–5] have discussed the filtering characteristics of different configurations. These types of filters were ideally suited for narrow bands. A new generation of microwave dual-mode filters, using square ring resonators with enhanced L-shaped coupling arms, was later discussed.[6] Advantages of low insertion loss, sharp rejection band and wide passband were obtained. Subsequently, the area of the overall filter structure was reduced and a sharper passband

CHU-YU CHEN
Southern Taiwan University of Technology
Tainan, Taiwan
CHENG-YING HSU
SUE-TE University
Kaoshiung, Taiwan

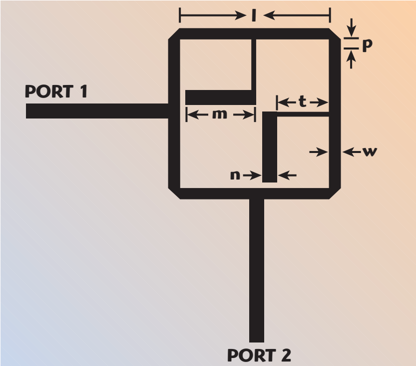

▲ *Fig. 1 Dual-mode, wideband bandpass filter.*

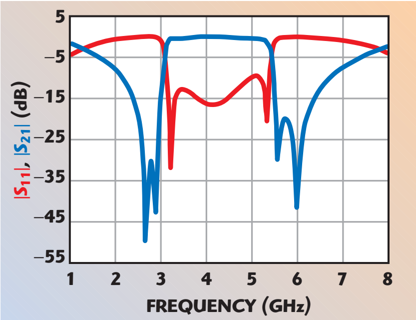

▲ *Fig. 2 Simulated results for the dual-mode, wideband bandpass filter.*

was provided. However, the presence of spurious harmonics was a fundamental drawback.[7] A number of improved structures, such as an I/O taping line, defected ground structure (DGS), split ring resonator (SRR) and photonic band-gap (PBG), have proven to be effective in suppressing spurious harmonics. These techniques either increase the complexity of fabrication or enlarge the component's size. It has been proven that a filter, incorporating two spur-lines at the input and output feed lines of the coupled ring, can increase the rejection band of the bandpass filter.[8] The ideas demonstrated in this article are to implement spur-line structures in the square ring resonator to suppress the spurious harmonics without altering the passband response of the filter.

DUAL-MODE, WIDEBAND MICROSTRIP BANDPASS FILTER

A novel bandpass microstrip filter, based on a ring resonator, is shown in ***Figure 1***. The input and output ports are directly connected to the ring resonator at 180° and 270°. Two stepped-impedance tuning stubs are implemented within the resonator at 0° and 90°, and a 0.5 by 0.5 mm perturbation

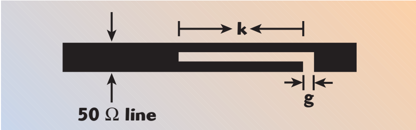

▲ *Fig. 3 Spur-line bandstop filter configuration.*

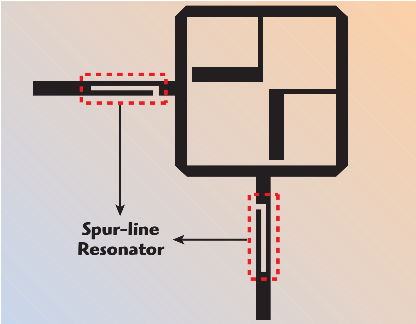

▲ *Fig. 4 UWB bandpass filter with input and output spur-lines.*

is positioned at 45°. The circumference l_r of the ring resonator is given by Equation 1, where n is the mode number and λ_g is the guided wavelength

$$l_r = n\lambda_g \qquad (1)$$

The ring resonator and the λ/8 stepped-impedance stubs are designed for a resonance frequency of 4.2 GHz and fabricated on an RT/duroid 6010.2 substrate with a thickness h = 25 mil and a relative dielectric constant ε_r = 10.2. The dimensions of the filter are l = 7.4 mm, m = 3.55 mm, n = 0.7 mm, t = 2.6 mm, w = 0.6 mm and p = 0.5 mm. The simulated results of the filter are shown in ***Figure 2***. The perturbation stubs can generate two transmission zeros, or dual modes, on either side of the passband within the 2.68 to 2.87 and 5.56 to 5.99 GHz bands. The filter has a 3 dB fractional bandwidth greater than 56 percent and an insertion loss better than 0.3 dB.

SPUR-LINE BANDSTOP FILTER CONFIGURATION

Figure 3 shows the configuration of the spur-line filter. The parameters k and g, the length of the spur and the gap, determine the resonant frequency of the spur-line bandstop filter. Based on the analysis introduced by Nguyen and Hsieh,[9] a spur-line bandstop filter on a homogeneous medium can support two quasi-TEM modes, that is an even and odd mode, and each mode propagates with a different phase velocity. The equivalent circuit model in matrix form can be

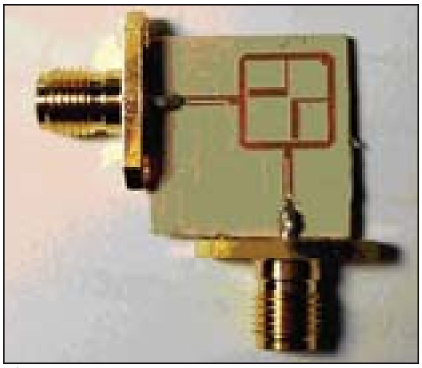

▲ *Fig. 5 The proposed UWB bandpass filter.*

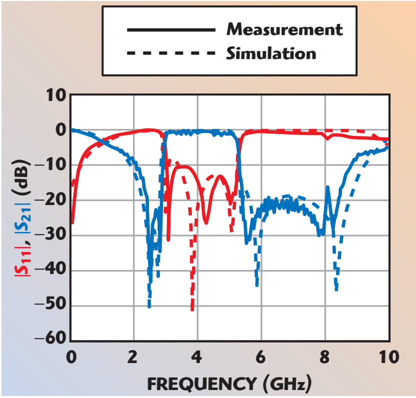

▲ *Fig. 6 Simulated and measured results of the UWB bandpass filter with spurious response suppression.*

constructed through manipulations of the impedance matrix of parallel-coupled transmission lines and termination conditions. It is proven that the filter type, either bandstop or bandpass, is mainly dominated by the odd mode of propagation, and the computations for the two parameters k and g are related by the effect of the odd mode fringing capacitances. The length of the spur-line is given by[8]

$$k = \frac{3\times10^8}{4f_0\sqrt{K_{effo}}} - \Delta k \qquad (2)$$

where the center frequency of the designed filter is f_0 and K_{effo} is the odd mode effective dielectric constant. The modifying term Δk is an effective length resulting from the effect of the gap g. In this case, k and g are 3.4 and 0.2 mm. This designed spur-line filter was embedded in the input and output microstrip lines of the ring resonator, as shown in ***Figure 4***. A new ultrawideband microstrip bandpass filter, based on a dual-mode ring resonator with spur-line structures placed at input and output ports, is created.

MEASUREMENTS

The overall size of the filter is 15.7 by 15.7 mm, and the prototype filter is shown in ***Figure 5***. The passband and stopband responses of the designed bandpass filter are shown in ***Figure 6***. The perturbation stubs can generate two transmission zeros or dual modes on either side of the passband within 2.70 to 2.89 GHz and 5.65 to 5.73 GHz. The filter has a 3 dB fractional bandwidth of 57 percent, an insertion loss better than 0.8 dB and a return loss greater than 10 dB in the passband from 3.1 to 5.6 GHz. The spurious response of the designed filter is effectively suppressed. The rejection of the spurious response from 5.8 to 8.5 GHz is successfully suppressed to a level lower than –20 dB through the effect of the input and output spur-lines.

CONCLUSION

The design for a UWB bandpass filter with spurious response suppression is proposed and shown in this article. Its characteristics are compact size, sharp rejection, low insertion loss and wide stopbands. The measured performance shows good agreement with the simulated results. The slight difference between the simulated and measured results may be due to a fabrication error, which can be improved by more precise fabrication technology. With the addition of the spur-line structures, another transmission zero can be created to suppress the spurious response without changing the prototype design. In addition, the maximum attenuation in the stopband of the proposed filter is more than 33 dB without degrading the performance of the bandpass filter. Specifically, the resonance frequency of the spur-line bandstop filter can be accurately and conveniently calculated. These features make spur-line bandstop filters more attractive in modern communication applications. ■

References

1. J.A. Curtis and S.J. Fiedziuszko, "Miniature Dual-mode Microstrip Filters," *1991 IEEE MTT-S International Microwave Symposium Digest*, Vol. 2, pp. 443–446.
2. J.S. Hong and M.J. Lancaster, "Bandpass Characteristics of New Dual-mode Microstrip Square Loop Resonators," *Electronics Letters*, Vol. 31, No. 11, May 1995, pp. 891–892.
3. J.S. Hong and M.J. Lancaster, "Microstrip Bandpass Filter Using Degenerate Modes of a Novel Meander Loop Resonator," *IEEE Microwave and Guided Wave Letters*, Vol. 5, November 1995, pp. 371–372.
4. L.H. Hsieh and K. Chang, "Dual-mode Quasi-elliptic-function Bandpass Filters Using Ring Resonator with Enhanced Coupling Tuning Stubs," *IEEE Transactions on Microwave Theory and Techniques*, Vol. 50, No. 5, May 2002, pp. 1340–1345.
5. L. Zhu, P. Wecowski and K. Wu, "New Planar Dual-mode Filter Using Cross-slotted Patch Resonator for Simultaneous Size and Loss Reduction," *IEEE Transactions on Microwave Theory and Techniques*, Vol. 47, No. 5, May 1999, pp. 650–654.
6. L.H. Hsieh and K. Chang, "Compact, Low Insertion Loss, Sharp Rejection and Wideband Microstrip Bandpass Filters," *IEEE Transactions on Microwave Theory and Techniques*, Vol. 51, No. 4, April 2003, pp. 1241–1246.
7. C.Y. Chen, C.Y. Hsu and S.F. Lin, "A Novel Compact Miniaturized Wideband Microstrip Bandpass Filters with Dual-mode Ring Resonators," *Microwave and Optical Technology Letters*, Vol. 45, No. 4, May 2005, pp. 312–315.
8. U. Karacaoglu, D. Sanchez-Hernandez, I.D. Roverson and M. Guglielmi, "Harmonic Suppression in Microstrip Dual-mode Ring Resonators Bandpass Filter," *1996 IEEE MTT-S International Microwave Symposium Digest*, Vol. 3, pp. 1635–1638.
9. C. Nguyen, C. Hsieh and D.W. Ball, "Millimeter-wave Printed Circuit Spur-line Filters," *1983 IEEE MTT-S International Microwave Symposium Digest*, pp. 98–100.

Chu-Yu Chen *received his BS degree in engineering science from National Cheng Kung University, Tainan, Taiwan, in 1990, and his MS degree in electrical engineering from the University of Detroit, MI, in 1995. From 1996 to 1999, he was a research and teaching assistant in the EMC laboratory of electrical engineering at Oakland University, MI, where he obtained his PhD degree. He is currently an assistant professor in the department of electronic engineering, Southern Taiwan University of Technology, Tainan, Taiwan. His research interests include electromagnetic compatibility, microwave circuit design and computational electromagnetics.*

Cheng-Ying Hsu *received his BS degree in information technology from Toko University, Chia-Yi, Taiwan, in 2004, and is currently working toward his MS degree in computer and communications at SUE-TE University, Kaoshiung, Taiwan. His research interests include RF/microwave passive components, with emphasis on high Q inductors and planar filters.*

MICROSTRIP LINE WITH A NOVEL BROADBAND PBG STRUCTURE

A new scalariform cross (a cross with a square in the middle) slot structure is proposed for a broadband photonic band-gap (PBG) microstrip line. Compared to other PBG structures of simple geometries, wider frequency stopbands, greater than 40 percent and with rejection of at least 35 dB, are achieved with this structure. The experimental and simulated results are in good agreement.

Photonic band-gap (PBG) structures were initially proposed in the optical component field. In the microwave field, PBG periodic structures suppress the propagation of electromagnetic waves whose frequencies are within certain bands. They allow shifting the rejected frequency band by simply changing the geometry parameters of the PBG element or the physical characteristics of the PBG structure. In recent years, because of these special properties, PBG structures have been widely used in the control of propagation of electromagnetic waves.

In the past few years, much research has been done in one- or two-dimensional PBG structures.[1–9] Most of the PBG structure elements are formed by simple geometries, such as a circle or a rectangle.[4,5] Because PBG structures are periodic, most of them will generate periodic band-gaps from higher order modes. Although the bandwidth of the main band-gap can be increased, the main band-gap is often not wide enough and the required bandwidth cannot be extended. This is due to an appreciable distance between the center frequencies of the periodic band-gaps. The relative bandwidth of the stopband can usually reach 30 percent.[1,7] In this article, a new photonic band-gap structure for microstrip lines is proposed. The periodic 2-D patterns, consisting of slots in the shape of crosses with squares in the middle (scalariform) etched in the ground plane of microstrip lines, can effectively increase the bandwidth of the stopband. The relative bandwidth can reach 40 to 50 percent. The proposed slot structure can easily be designed and fabricated using conventional printed circuit board technology.

Fig. 1 Ground plane of the microstrip line with slots etched with the proposed geometry.

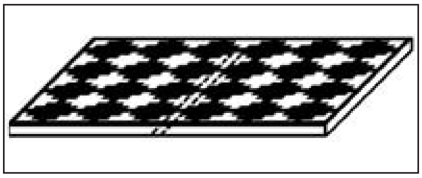

PBG STRUCTURE DESIGN

As is well known, if the period of the PBG elements is chosen to be half the guided wavelength at the center frequency of the stopband, the electromagnetic band-gap structure produces a stopband in which propagation is suppressed. The PBG structure is implemented by etching slots in the ground plane, as shown in ***Figure 1***. The dielectric constant of

FEI ZHANG, LINA SHI AND CHENGFANG LI
Wuhan University
Wuhan, China

the substrate is $\varepsilon_r = 10$ and its thickness is h = 0.8 mm. The length of every side of the cross-slot is kept constant and equal to 0.9 mm; the period is 5.4 mm. The microstrip line width is 1 mm for $Z_0 = 50\ \Omega$. The circuit simulation was performed using HFSS. To make a comparison, other structures composed of simple geometry patterns such as squares and crosses are also simulated, as shown in ***Figures 2*** and ***3***. All these PBG structures are composed of patterns of 7 × 7 elements.

In general, the stopband center frequency f_0 is a function of the period of the structure. The three structures are all based on the same substrates and have the same period. Consequently, in all three cases, the center frequency of the stopband is approximately 10 GHz. The magnitude and bandwidth of the stopband, however, depend on the geometry of the PBG pattern. The simulated performances for the three patterns are shown in ***Figures 4***, ***5*** and ***6***. The comparative data is listed in ***Table 1***.

It can be easily observed from the simulated results that the performance of the PBG structure with the proposed scalariform pattern is much

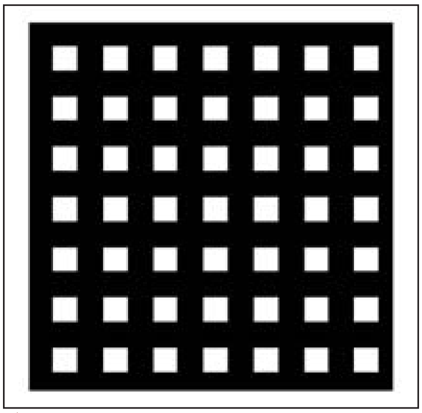

Fig. 2 Ground plane of the microstrip line with square slots etched.

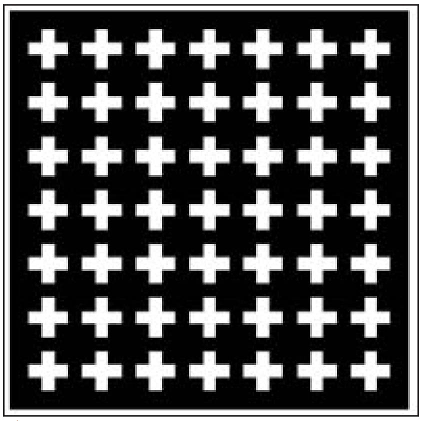

Fig. 3 Ground plane of the microstrip line with etched cross slots.

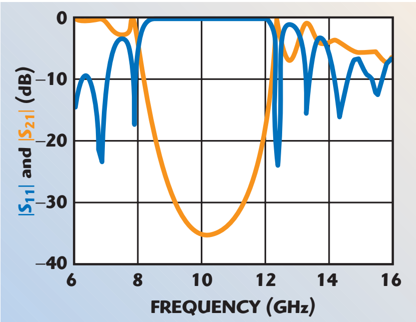

Fig. 4 Simulated S_{11} and S_{21} for the proposed PBG microstrip circuit.

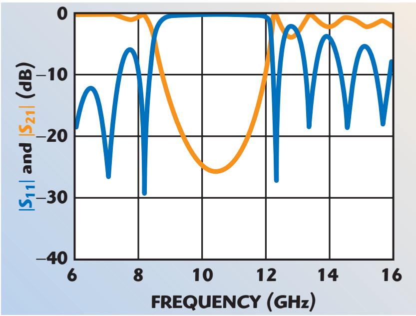

Fig. 5 Simulated S_{11} and S_{21} for a PBG microstrip line with square patterns.

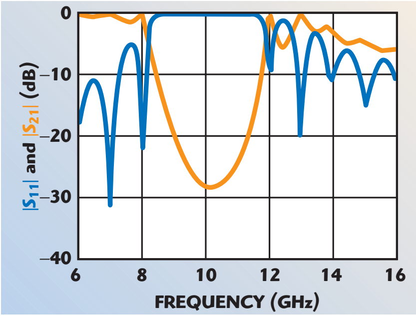

Fig. 6 Simulated S_{11} and S_{21} for a PBG microstrip line with cross patterns.

TABLE I

PERFORMANCE OF THE THREE PBG STRUCTURES

εr = 10, h = 0.8 mm	Period (mm)	f_0 (GHz)	Δf (3 dB) (GHz)	Relative Bandwidth (%)	Depth of Stopband (dB)
scalariform cross slot	5.4	10.3	4.35	42.2	–35
square slot	5.4	10.3	3.63	35.2	–26
cross slot	5.4	10.3	3.73	36.2	–28

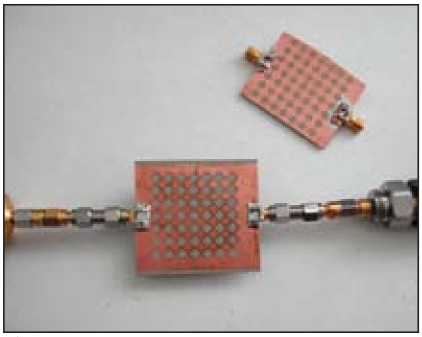

Fig. 7 A fabricated PBG microstrip sample.

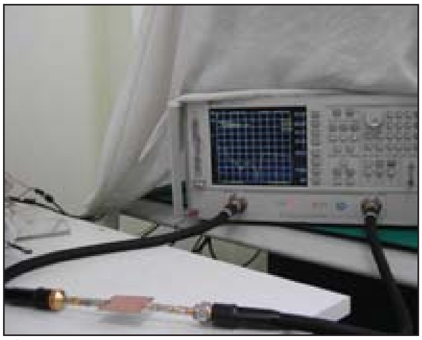

Fig. 8 The experimental setup.

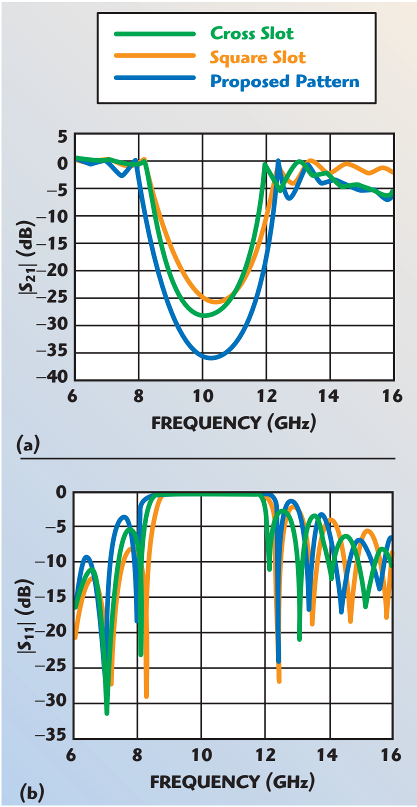

Fig. 9 Measured (a) S_{21} and (b) S_{11} performance of the three PBG patterned microstrip lines.

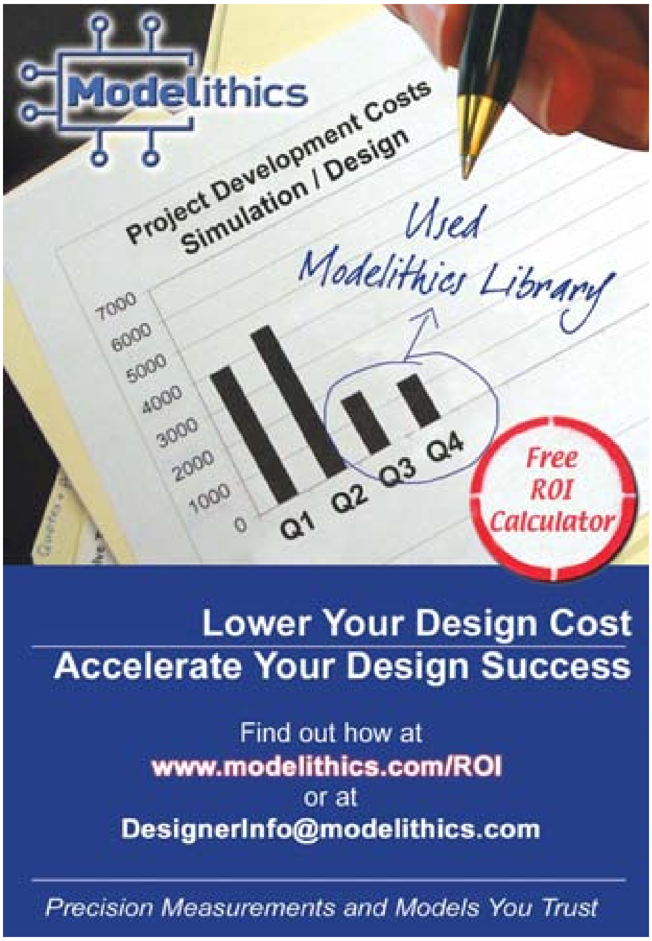

better than that of the PBG structures with square and cross patterns.

EXPERIMENT AND MEASUREMENTS

Experiments were performed to demonstrate the suppression of the propagation of electromagnetic waves. A fabricated PBG sample, with a pattern arrangement of 7 × 7 elements, is shown in ***Figure 7***. ***Figure 8*** shows the experimental setup used for the measurements. The two ends of the microstrip line are soldered to two SMA connectors. The results are shown in ***Figure 9***. The PBG sample with the proposed pattern has a rather wide bandwidth characteristic. The central frequency of the stopband is 10.5 GHz; the bandwidth is about 5 GHz. In the stopband, the rejection level can reach –47 dB. Outside the stopband, the return loss of the microstrip line is less than 1.5 dB. The measurement results agree well with the simulation results.

CONCLUSION

A novel microstrip line with a scalariform (cross plus square) slot PBG structure has been proposed. The new PBG structure can effectively increase the width of the stopband compared with some other PBG structures composed of simple geometry slots. Both the simulated and experiment results have shown that a wide stopband is achieved for this PBG structure. ■

References

1. V. Radisic, Y. Qian, R. Coccioli and T. Itoh, "Novel 2-D Photonic Band-gap Structure for Microstrip Lines," *IEEE Microwave and Guided Wave Letters*, Vol. 8, No. 2, February 1998, pp. 69–71.
2. H. Rong, X.X. Zhang and G.B. Xin, "2-D PBG Structure in Microstrip Line and Symmetrical Microstrip Line," *2000 Asia-Pacific Microwave Conference Digest*.
3. T.Y. Yun and K. Chang, "One-dimensional Photonic Band-gap Resonators and Varactor Tuned Resonators," *1999 IEEE International Microwave Symposium Digest*, Vol. 4, pp. 1629–1632.
4. D. Dawn, Y. Ohashi and T. Shimura, "A Novel Electromagnetic Band-gap Metal Plate for Parallel Plate Mode Suppression in Shielded Structures," *IEEE Microwave and Wireless Components Letters*, Vol. 12, No. 5, May 2002, pp. 166–168.
5. J.S. Sun and G.Y. Chen, "Microstrip Line with the PBG Structures," *Proceedings of the APMC2001*, Taipei, Taiwan, ROC.
6. H. Liu, Z. Li and X. Sun. "Compact Defected Ground Structure in Microstrip Technology," *Electronics Letters*, Vol. 41, No. 3, 2005.
7. J.M. Hickmann, D. Solli, C.F. McCormick, R. Plambeck and R.Y. Chiao, "Microwave Measurements of the Photonic Band-gap in a Two-dimensional Photonic Crystal Slab," *Journal of Applied Physics*, Vol. 92, No. 11, 2002.
8. F. Yun-qi, Z. Guo-hua and Y. Nai-chang, "A PBG Microstrip Line with Fractal Characteristics," *ACTA Electronic Sinica*, 2002.
9. V. Radisic, Y. Qian, R. Coccioli and T. Itoh, "Novel 2-D Photonic Band-gap Microstrip Structures," *Microwave and Optical Technology Letters*, Vol. 22, No. 9, 1999.

Fei Zhang *received his BSc degree in physics from Wuhan University, Wuhan, China, in 2002, where he is currently pursuing his PhD degree. His research interests include microwave/ semiconductor devices and RF circuits.*

Lina Shi *received her BSc degree in physics from Wuhan University, Wuhan, China, in 2002, where she is currently pursuing her PhD degree. Her research interests include photonic crystal materials and devices.*

Chengfang Li *received his BSc degree in physics from Wuhan University, Wuhan, China, in 1970, where he is currently a professor. His research interests include photonic crystal devices, negative refractive materials and infrared detection.*

SALVAN: CRADLE OF WIRELESS

How Marconi Conducted Early Wireless Experiments in the Swiss Alps

On September 26, 2003, the IEEE dedicated a "Historical Milestone," acknowledging some of the first wireless experiments conducted in 1895 by Guglielmo Marconi in Salvan, Switzerland, a picturesque resort in the Swiss Alps. This historical development had been described in detail by an elderly citizen, who had assisted Marconi during his short stay in Salvan.

In 1965, inhabitants of Salvan, Switzerland, located above Martigny in the Mont Blanc region, "remembered" that a senior citizen of their village had lived a very unusual experience seventy years before, when he was a young boy. A radio reporter was vacationing nearby, and Maurice Gay-Balmaz, by then 80 years old (see ***Figure 1***), told him how he had met a "nice young man," who had arrived with heavy equipment along the mule path ascending from the Rhone valley.[1] The recordings made at the time describe a crucial episode in the development of wireless communications, which was until then unknown to Marconi's "official" biographers.

Fig. 1 Maurice Gay-Balmaz.

AN OLD MAN TELLS AN OLD STORY

The young Gay-Balmaz, born in 1885, was playing near his home in Salvan, when he noticed some odd-looking bits and pieces lying in the grass. Seeing the boy's interest, Marconi, who was then a tenant in the uncle's house, supposedly said: "So, you're interested in that, are you, young'un? If you'd like to work with me, I'll take you on."[2] In this manner, ten-year-old Gay-Balmaz became Marconi's little helper, very excited at the idea of carrying such fascinating equipment. He enjoyed helping this kind and generous summer resident, a man very different from the area's customary tourist. Without realizing it, Gay-Balmaz was about to play a role in one of the most significant adventures of our time.[3]

Overlooking the village of Salvan is a flat-topped erratic rock called "Pierre Bergere" (The Shepherdess Stone) (see ***Figure 2***), on which Marconi installed his transmitter. His equipment consisted of a battery, a Ruhmkorff induction coil, a Righi spark generator and an antenna (see ***Figure 3***). A few meters away from the rock, the boy held a two-and-a-half-

FRED GARDIOL
Ecole Polytechnique Federale de Lausanne Switzerland
YVES FOURNIER
College de L'Abbaye Saint-Maurice, Switzerland

▲ *Fig. 2 The Shepherdess Stone in Salvan.*

▲ *Fig. 3 Reconstruction of Marconi's transmitter at the Salvan Marconi Museum.*

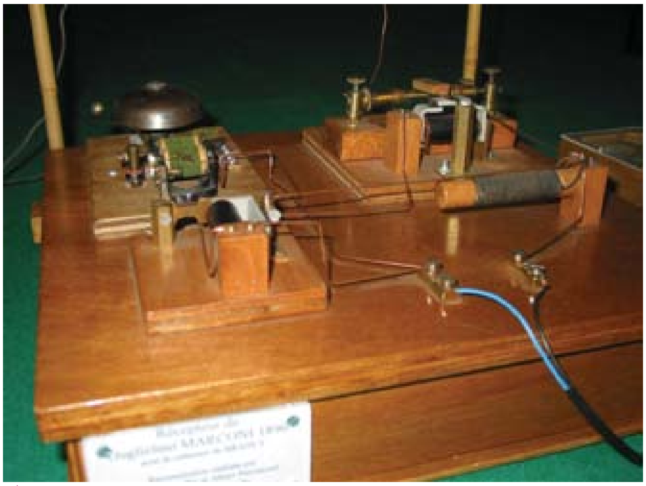

▲ *Fig. 4 Reconstruction of Marconi's receiver at the Salvan Marconi Museum.*

meter long pole, along which ran a metallic wire connected to a receiver, probably consisting of a Branly coherer, a battery and a bell (see ***Figure 4***). Actually, the Italian word for pole is "antenna." This term, introduced at the time by Marconi, has since been used worldwide to designate what was previously called an "aerial." Part of the equipment had been brought from Bologna by Marconi and his elder brother Alfonso, who by then had returned to Italy.

A lot of time and effort was needed to get the system to operate. Gay-Balmaz recalled the long waiting periods: "At first the bell would not ring, and then, after careful trials, evaluations and adjustments of his apparatus, it did ring at such a distance. Marconi's face was beaming, and he shouted to me 'it is fine, now it is starting to work!' He asked me to move farther, maybe a hundred meters away. And then it took some time, maybe half a day of trials before the bell rang again. But it did ring! And we went along in the same way."[2]

With a broken voice full of emotion, the old man showed the places where he had placed the receiver and described how the tests progressed. Soon, the distance became too large to talk or to shout to each other, and flags were used to exchange messages. Whenever the bell rang, the boy raised a red flag to show that the signal had been received, while a white flag meant "not yet, keep trying!" The receiver was moved farther and farther away from the Shepherdess Stone, the four or five initial meters soon becoming hundreds of meters, finally reaching a location at the top of the next village of "Les Marécottes," at a distance of roughly one and a half kilometers (see ***Figure 5***). The transmitter's location was not always visible from the receiver, and then Gay-Balmaz had to change his position in order to indicate the result of the test. The first transmission without direct visibility was thus realized in Salvan.

This last information is particularly significant because, at that time, people believed that electromagnetic waves could only propagate along straight lines — just like light — and therefore could not reach the other side of hills and mountains. It was also felt that the curvature of the earth would drastically limit the transmission length. But such beliefs had not been verified, and Marconi proved that they were incorrect.

After several weeks of testing, Marconi returned to Italy, leaving in Salvan only some copper wire forgotten in his room. But he did not forget his young helper, who received a letter from Italy. Gay-Balmaz remembers, "I did not realize that he would become so famous. So when he wrote inviting me to come to Rome for a few days, I did not even keep the letter. Alas, I was still very young, and my parents did not let me go." For the rest of his life, Gay-Balmaz resented this irrevocable decision. He became a carpenter and spent his whole life in and around Salvan, working as a general handyman in a sanitarium. He died in 1975 at the age of 90.

Marconi's life, on the other hand, was extremely active. A few months after the Salvan episode, a gunshot sounded in the grounds of Villa Griffone, near Bologna in Italy. It announced the successful transmission of a message over two and a half kilometers.[5] By then, flags were no longer sufficient for signaling. In 1896, Marconi filed patent No. 12039 in London, followed in 1897 by

1. Les Marécottes; 2. La Combaz; 3. Ladray; 4. Creté dy Serré; 5. Les Maraiches

▲ *Fig. 5 Panorama from the Shepherdess Stone, showing the places where Gay-Balmaz carried the receiver.*

the wireless transmission over all of fourteen kilometers, between Lavernock Point and Flat Holme Island in the Bristol Channel, officially recorded by the British Post Office.[6] A signal crossed the English Channel in 1899, and in 1901 Marconi managed the incredible feat of sending a wireless message across the Atlantic Ocean, from Poldhu in England to Signal Hill in Newfoundland.[7]

Marconi's realizations were acknowledged by the highest honors, among them a dozen "honoris causa" doctorates (quite a feat for a man who had failed the entrance exams for the University of Bologna) and many scientific awards throughout the world, including the Nobel Prize in physics in 1909. He kept traveling all around the globe and kept a close watch on the evolution of his commercial ventures, until a heart attack ended his activity in the early hours of July 20, 1937.[8] What followed is well known. Is it possible to imagine the world today without radio, television and cellular phones?

FUZZINESS OF HEARSAY HISTORY

For a historian, oral testimony like the one given by Gay-Balmaz always contains some elements of doubt. It is well known that memory does not register facts, but interpretations made by the observer. In addition, when a story is reported seventy years after the event, one may expect some inaccuracies. Independent testimony, or some written documents would be welcome, to complete and corroborate oral descriptions. Unfortunately, Marconi did not leave any report describing his experiments in Salvan, so that one can only rely on hearsay gathered many years later.[9] In his testimony, Gay-Balmaz recalled that he was about twelve years old, in which case the encounter should have taken place in 1897, but this cannot be true, because by then Marconi's waves were traveling over much longer distances. Gay-Balmaz also reports that Marconi was then around 26 or 27 years old,[1] which is some five or six years older than he actually was at the time. This is not too significant, perhaps, because it is notoriously difficult for young children to estimate the age of adults. The chronological sequence of events shows that Marconi's experiments in Salvan were made during the summer of 1895, but a discrepancy of several years in the testimony of Gay-Balmaz does not shed doubt upon its validity. Who can remember, within plus or minus one or two years, what was going on when he or she was ten years old?

Two articles[10,11] describe Marconi's stay in Salvan as shrouded in a thick veil of mystery; the first of which even wonders whether Gay-Balmaz might not have made up the whole story, supposedly to impress his wife. But the honesty of the old man was proverbial, and only someone who did not know him could shed any doubt on his testimony. Many inhabitants of Salvan told of this young gentleman, roaming around the rocky woods and steep meadows with a local boy, carrying odd machines, poles and flags, and the story remains part of the "collective memory" of the village. Gay-Balmaz's testimony is remarkably detailed and precise, describing in a plausible way how Marconi operated, and it provides interesting information about what took place at that time.[1] One should also note that, in the absence of written documents, Marconi's official biographers are faced with the very same situation concerning this part of his life. They must also rely on oral reports told much later by family members, servants or guests at the Villa Griffone. For instance, a servant remembered digging a hole in the ground to bury a large metal plate. It is known now that, among other things, Marconi discovered that by earthing his equipment he could lengthen the transmission range considerably. Marconi was a man of action, who did not take much time off to "look back" and to write his memoirs, so that some questions may remain forever unanswered.

THE BEGINNINGS OF RADIO

For a long time, a recurring question has been frequently asked, "Who actually invented radio?" To answer it properly, an indisputable manner of what is meant by 'invent' and by 'radio' should be defined. For reasons of national prestige, several countries claimed at various times that the sole and unique "inventor of radio" was one of their outstanding citizens. For many years, unfortunate priority quarrels poisoned the scientific community. Fortunately, these sterile disputes have somewhat quieted by now. The invention of radio, or rather its development, is a long adventure in which many scientists took part during the nineteenth and twentieth centuries. This saga was marked by many, more or less important, milestones. The existence of electromagnetic waves was first predicted by theory and then confirmed by experiment. It was then found that these waves could transmit messages, equipment was developed for this purpose and information was forwarded over increasingly longer distances, reaching by now the confines of the solar system. At first, the messages were primitive, made up of spark noise modulated by the dots and dashes of the Morse code. Later on, technical developments made possible the transmission of voice, music, images and, finally, of computer data. New technologies appeared: solid-state detectors, electron tubes, transistors, integrated circuits, masers, sophisticated transmission codes and so on.

It is generally accepted that the original "forerunner" of radio was the Danish physicist Hans Christian Oersted, who in 1820 showed that an electrical current could rotate the magnetized needle of a compass, demonstrating for the first time that electricity and magnetism are somehow related to each other. One year later, the French mathematician André Marie Ampère repeated and completed the experiment, and developed a theory to account for it. Michael Faraday (1791–1867) discovered magnetic induction and introduced the concept of lines of force. Since he was an experimental researcher without an academic background (like Marconi later on), however, this concept was disputed until the great physicist James Clerk Maxwell made use of it to establish his famous equations in 1864. Maxwell's theory predicted the existence of electromagnetic waves. It still had to be discovered whether these waves actually existed.[6] During the winter of 1886–1887, Heinrich Hertz, experimenting in Germany with spark generators and dipoles, detected for the first time the presence of electromagnetic waves and thus validated the theory developed by Maxwell in 1864. His detector had a very low sensitivity, so that the transmission range did not exceed a few meters. Hertz died in 1894 at the age of 34. Hertz's work had been closely monitored by Oliver Lodge, in England, who carried out a detailed study of tuned circuits. In 1893, he introduced in his receiver a "coherer" recently developed in France by Edward Branly, who noticed that the resistivity of iron filings decreased sharply when close to an electric spark discharge. Lodge could then transmit signals up to some tens of meters, which was sufficient for demonstrations to the Royal Institution and to his students. But he was a fundamental scientist and did not look for practical applications until Alexander Muirhead, a telegraph engineer, pointed out that waves could carry messages. The two collaborated later on to develop wireless systems. Lodge's main contribution was probably the memorial lecture presented at the Royal Institution in 1894, in which he described Hertz's work and some of his own experiments. This lecture, and several articles published shortly afterwards,[13,14] had a very strong impact. The whole world heard of developments that had remained mostly confidential until then, and scientists in many places started experimenting with electromagnetic waves, among them Augusto Righi at the University of Bologna.

Many other scientists developed interest in electromagnetism and obtained more or less conclusive results or filed patents, but did not contribute significantly to the development of wireless before Marconi's first successful transmissions.[15] A certain amount of technical background had been established at that time, in theory as well as in practice, but the spark of genius had yet to be fired. This was the situation encountered by Marconi when he started experimenting. People believed then that electromagnetic waves propagated along straight lines and traveled only over short distances. It was not obvious that they could be used in practical applications. In addition, telegraphic transmission across several continents and oceans had been available for some time. Why should one spend time and effort to develop another system, which, if it did work, would only duplicate an existing one? Apparently, no one had thought of the potential use of wireless transmission for maritime communications.

THEN MARCONI CAME

In 1894, Marconi was on vacation with his family in Andorno, near Santuario di Oropa in the Italian Alps. He learned of the death of Heinrich Hertz, and became fascinated by a technical article describing electromagnetic waves. Marconi had lived in Leghorn, the main port of central Italy, and right away foresaw that

▲ *Fig. 6 How the village of Salvan looked in 1937.*

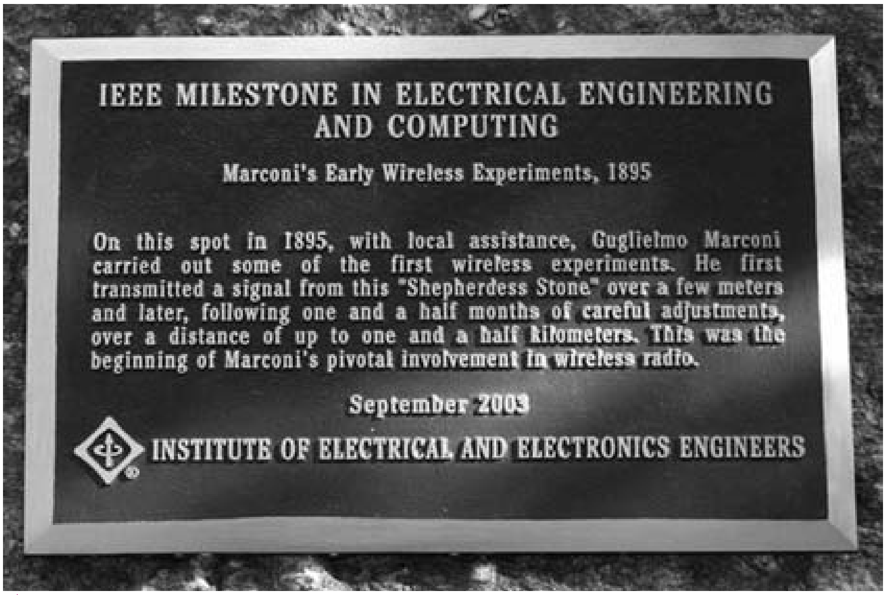

▲ *Fig. 7 IEEE milestone plaque placed on the Shepherdess Stone. (Photo by J.F. Zürcher)*

these waves would offer tremendous possibilities for maritime communications. He decided that he would "transmit a message without any metallic connection between transmitter and receiver." Marconi had seen Augusto Righi's equipment in the University of Bologna and probably started by repeating Hertz's experiments in the Villa Griffone attic. He increased the distance covered by the transmission across a room, then along a passageway, and then between the house and the surrounding fields. It must be realized that, at that time, he did not have technical manuals, nor suitable measuring instruments, neither analysis nor simulation tools, and could not call any specialized troubleshooter to repair defective equipment, all things taken for granted by engineers nowadays. It is hard to visualize what difficulties he encountered. He was on his own, a young beginner with a limited technical background, who had failed the entrance examinations for Leghorn Naval Academy and for the University of Bologna. In addition, he generally met with a climate of skepticism and incredulity, and even with hostility from his father, who did not approve of his son's manual activities. But from his youngest age, Marconi had been a genial tinkerer, interested in everything mechanical or electrical, and he possessed the exceptional practical sense and indomitable motivation that allowed him to carry on in the face of adversity and failure.[12] As Marconi kept increasing the transmission range, the attic in the family house became too small and he had to move his equipment into the garden, in full view of the whole family, servants and visitors. At first, he was pleased with the interest encountered, but later on he disliked the time-consuming interruptions. He looked for a quiet and remote place to pursue his experiments, and selected a "climacteric" alpine resort well known at that time: Salvan (see ***Figure 6***). He had only crude equipment to start his activity, and he wanted to avoid disturbance while adjusting it. Marconi already knew that his cut-and-try endeavors, if successful, would lead to a very significant breakthrough and he wanted to avoid any premature disclosure. Marconi's youngest daughter, princess Elettra Marconi-Giovanelli, visited Salvan in March 2001 and described how her father was looking for a quiet place, where nobody would understand what he was doing. As he said later on, "the idea was so elementary, so simple in logic, that it seemed difficult for me to believe that no one else had thought of putting it into practice. There must be many more mature scientists than myself who had followed the same line of thought and arrived at an almost similar conclusion."[16] In his biography, his

▲ *Fig. 8 Prince G. Marconi-Giovanelli, Prof. F. Gardiol, Princess E. Marconi-Giovanelli, Prof. J. Mosig, Prof. G. Falciasecca, Prof. Y. Fournier. (Photo by S. Vaccaro)*

daughter Degna indicates that her father was afraid that someone would discover his secret, as if a ghost was haunting him.[5] Marconi did not accept any limitation, and devoted his entire life to fulfilling the vision he had had in 1894 in Andorno, the validity of which he started to check the following year in the scenic surroundings of Salvan. In spite of the overall skepticism, he obstinately pursued an endeavor that went contrary to generally accepted beliefs, and was never discouraged by difficulties and failures. He succeeded in doing what many others had considered impossible. A key to his success is that he realized, quite early in his research, that his activity had to be self-supporting. Therefore, he set up a commercial wireless telegraph service that ensured his financial independence. In rather sharp contrast, several other researchers spent considerable time and effort locating and trying to convince sponsors, and some even died in abject poverty. As Marconi's daughter Elettra said,[4] "The village of Salvan can pride itself in having offered its ideal setting for the first stages of one of the most important discoveries of our time, wireless telegraphy."

IEEE HISTORICAL MILESTONE

Feeling that this major episode in the development of radio deserved more widespread recognition, the authors started the procedure to having the location "officially" acknowledged by the IEEE. The necessary documents were formulated and submitted to the IEEE History Center, where experts scrutinized them and gave a positive response. The History Committee of the IEEE acknowledged Marconi's early wireless experiments in Salvan as a "Historical Milestone" and a commemorative plaque (see ***Figure 7***) was dedicated on behalf of the IEEE by Raymond Findlay, IEEE Past President, on September 26, 2003, in the presence of both Princess Elettra Marconi-Giovanelli, youngest daughter of Guglielmo Marconi (see ***Figure 8***), and Pascal Couchepin, president of Switzerland.[17,18] The speakers recalled that Salvan had been the theatre of a major event in the history of electrical engineering and of mankind, as Marconi's discovery brought people closer together. Through his intelligence and doggedness of purpose, Marconi, father of wireless communications, provided an example of creativity and inventiveness to younger generations. Couchepin concluded hoping that this ceremony would prompt us to meditate on the importance of science and technical progress in our civilization. ■

References

1. A. Nusslé, Interview of Maurice Gay-Balmaz (84 years old) broadcast on July 22, 1968, by the French-speaking Swiss Radio (transcription by Y. Fournier).
2. Y. Fournier, "Salvan Following Marconi's Footsteps," *Salvan, Foundation Salvan Marconi*, preface by Princess Elettra Marconi-Giovanelli, Second Edition, 2000.
3. M.C. de Henseler, "On Marconi's Trail in Switzerland," *The Proceedings*, The Radio Club of America Inc., Spring 2001, pp. 22–24.
4. G. Pelosi, S. Selleri and B. Vallotti, "Antennæ," *IEEE Antennas and Propagation Magazine*, Vol. 42, No. 1, February 2000, pp. 61–63.
5. D. Marconi, *My Father Marconi*, Muller, 1962 (reprinted by Guernica Editions, 2002).
6. G.R.M. Garratt, *The Early History of Radio: From Faraday to Marconi*, The Institution of Electrical Engineers, London, England, 1994.
7. *From Semaphore to Satellite*, International Telecommunications Union (ITU), Geneva, Switzerland, 1965.
8. M.C. Marconi, *Marconi, My Beloved*, Dante University of America Press, Boston, MA, 1999.
9. R.W. Simons, "Guglielmo Marconi and the Early Systems of Wireless Communication," *GEC Review*, Vol. 11, No. 1, 1996.
10. P. Leggatt, "A Marconi Mystery," *Bulletin of the British Vintage Wireless Society*, Vol. 21, No. 2, Summer 1996.
11. P. Leggatt, "A Postscript to a Marconi Mystery," *Bulletin of the British Vintage Wireless Society*, Vol. 22, No. 3, Fall 1997.
12. W.P. Jolly, *Marconi*, Stein and Day, New York, NY, 1972.
13. O.J. Lodge, "The Work of Hertz," *Proceedings of the Royal Institution*, Vol. 14, 1894, pp. 321–349; also appeared in *The Electrician*, Vol. 33, 1894, pp. 153–155, 186–190, 204–205.
14. B.A. Austin, "Oliver Lodge, the Forgotten Man of Radio?" *The Radioscientist and Bulletin* (URSI, Ghent, Belgium), Vol. 5, No. 1, March 1994, pp. 12–16.
15. J.S. Belrose, "Reginald Aubrey Fessenden and the Birth of Wireless Telephony," *IEEE Antennas and Propagation Magazine*, Vol. 44, No. 2, April 2002, pp. 38–47.
16. Jacot and Collier, *Marconi, Master of Space*, Hutchinson, 1935.
17. www.ieee.org/organizations/history_center/milestones_photos/swiss_marconi.html.
18. F. Gardiol, "Inauguration of IEEE Marconi Milestone in Salvan, September 26, 2003," *IEEE Antennas and Propagation Magazine*, Vol. 45, No. 5, October 2003, pp. 84–85.

Fred Gardiol *graduated with a degree in engineering physics at the Ecole Polytechnique Federale de Lausanne (EPFL), Switzerland, in 1960. He received his MSEE degree in electrical engineering from the Massachusetts Institute of Technology in 1965 and his doctorate in applied science from Louvain University, Belgium, in 1969, where he became assistant professor. From 1970 to 1999, he was professor and director of the Laboratory of Electromagnetism and Acoustics (LEMA) at the Ecole Polytechnique Federale de Lausanne, Switzerland (Swiss Federal Institute of Technology). He retired at the end of 1999 and is now an honorary professor at EPFL.*

Yves Fournier *graduated in contemporary and Swiss history from Fribourg University in 1992. He also followed a course in public relations (organizational communication) at the University of Quebec, Canada. Author of numerous articles concerned with political ideology and international history, he has also been a scientific collaborator for the Dictionnaire Historique de la Suisse. His many cultural activities led him to pursue research in the history of science. He is now a history professor and member of the management team at the College de l'Abbaye in Saint-Maurice, Switzerland. He is also president of the Marconi Foundation, Salvan, Switzerland.*

INTEGRATED PASSIVE AND ACTIVE DEVICES USING CSP, DFN AND QFN PACKAGING FOR PORTABLE ELECTRONIC APPLICATIONS

Over the past five years, an explosion in growth of the portable electronics industry has provided numerous opportunities for manufacturers of RF components. Today, the designers of compact electronic systems, especially handheld/wireless devices, are faced with tightening board space constraints, thus driving the requirement for alternative integrated passive technologies. For a cell phone or PDA designer, success in the market comes from the ability to produce small handheld devices with long battery life in very high volumes. The handheld/wireless devices are attaining smaller practical size with miniaturization coming from the reduction in size of components and their associated packages. Functional integration and miniaturization is the key to this success.

To aid this miniaturization campaign, a new generation of integrated components has emerged, which offers the capability to integrate resistors, capacitors, inductors, diodes and transistors into a single monolithic device with minimal packaging overhead. By combining thin-film-on-silicon wafer fabrication technology with an advanced wafer-level chip scale packaging (CSP), dual flat no-lead (DFN) or quad flat no-lead (QFN) packaging process, component manufacturers can now provide designers with an integrated passive and active device solution that saves PCB real estate while at the same time offering remarkable electrical performance. This article discusses the thin-film-on-silicon technology used in the manufacturing of integrated passive and active devices in CSP, DFN and QFN packages. The article outlines typical functional applications including associated performance characteristics of line filtering, ESD protection, high speed bus termination, tunable filters and switching transistors.

IAN DOYLE
Bourns Electronics Inc.
Cork, Ireland

TABLE I

COMPARISON OF INSTALLED COST FOR A DISCRETE SOLUTION vs. INTEGRATED SOLUTIONS

DISCRETE SOLUTION BOM Costs	Component	Qty	Price (ea)	Subtotals	Total
	0402 resistor	12	$0.0029	$0.03	
	0402 capacitor	6	$0.0081	$0.05	
	SOT Zener 23	3	$0.0251	$0.08	$0.15
Placement Costs	All	21	$0.01	$0.21	$0.21
Total Installed Cost					$0.36
INTEGRATED SOLUTION BOM Costs	**Component**	**Qty**	**Price (ea)**	**Subtotals**	**Total**
	15 Bump CSP	1	$0.15	$0.15	$0.15
Placement Costs	15 Bump CSP	1	$0.01	$0.01	$0.01
Total Installed Cost					$0.16
INTEGRATED SOLUTION BOM Costs	**Component**	**Qty**	**Price (ea)**	**Subtotals**	**Total**
	12 Lead DFN	1	$0.15	$0.15	$0.15
Placement Costs	12 Lead DFN	1	$0.01	$0.01	$0.01
Total Installed Cost					$0.16

THIN-FILM-ON-SILICON TECHNOLOGY

Thin film passive components have been available to the electronic designer for many years. The thin film resistors are fabricated using a tantalum nitride (TaN) layer as the resistive material and an aluminum metal layer for interconnect and contacting purposes. The aluminum metal layer and tantalum nitride layers are uppermost in the resistor construction (except for the passivation layers), while the required resistor value is arrived at using the pattern geometry (R = ρL/W) as the primary design parameter. Thin film capacitors are normally fabricated using an aluminum metal layer as the top electrode providing low parasitic resistance and inductance values for the interconnect. A silicon nitride layer is used as the dielectric and the carrier silicon substrate as the bottom electrode plate. The thin film capacitor value (C = εA/d) represents the surface area of the top metal plate area over a lower silicon plate with a dielectric material between the plates. The thin film inductor can be constructed in a spiral or square layout where the inductor value is a function of the outer diameter, inner diameter, and number of turns and thickness of the metal layer. Inductors are fabricated using the top aluminum metal layer over a TaN layer. A lower aluminum metal layer provides the 'lead' into the inductor through a via-hole.

Thin film resistors, capacitors and inductors are renowned for their stability, temperature characteristics and reliability. Typical thin film resistor values are in the 10 Ω to 100 kΩ range with ±10 percent tolerance, capacitor values are in the range of 20 to 300 pF with ±20 percent tolerance, and inductors range between 1 and 15 nH, also with ±20 percent tolerance. These elements exhibit excellent performance over a broad frequency range.

Underneath the thin film layers, the silicon substrate can be used to integrate bipolar transistors and diodes of various types (Schottky, zener and varactor). These elements can be constructed on the silicon substrate using the material properties of the N or P silicon. With no board-level, copper-trace interconnections between these elements together with the most direct connection possible from component terminals to board pads, the behavior of these devices is easily controlled and highly repeatable.

CHIP SCALE PACKAGING

Given that thin-film-on-silicon integrated passive and active devices fundamentally form an integrated circuit (IC) or application-specific integrated circuit (ASIC), the package choice has, up to now, been restricted to SOIC, QSOP, TSSOP and the like. These packages have the disadvantage of being unwieldy for most space-sensitive applications and can often be counter-productive when compared to a discrete passive solution. Furthermore, the presence of bond wire parasitics renders such packages electrically unsuitable for high frequency applications. In the last few years, there has been somewhat of a revolution in the IC packaging world, where the birth of a generation of extremely space-efficient packaging solutions has been seen. Prominent among these is the wafer-level chip scale packaging process, which effectively allows individual die on silicon wafers to be "packaged" in

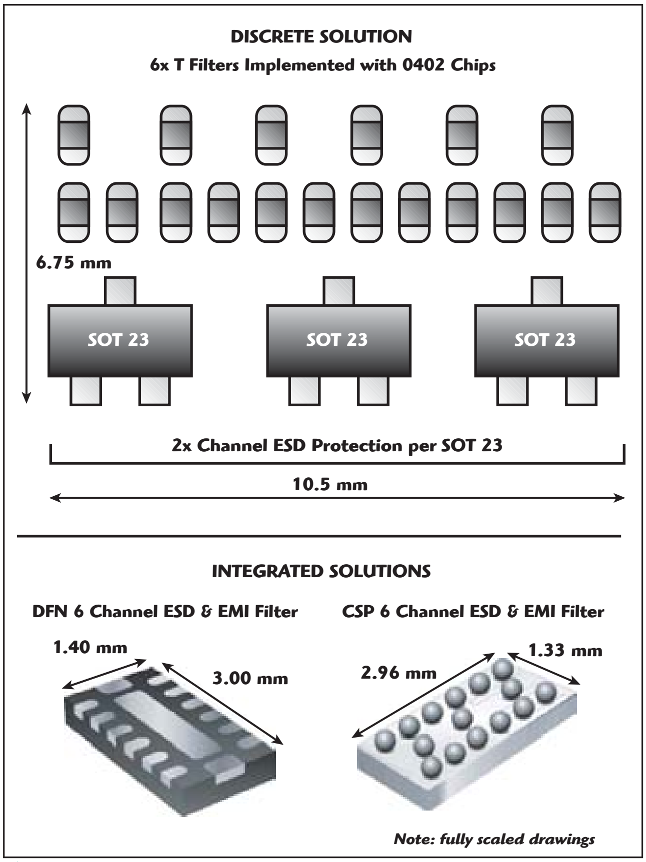

▲ *Fig. 1 Comparison of real estate usage with a discrete solution vs. integrated solutions.*

advance of the dicing operation. The CSP uses a dual-layer dielectric system of benzocyclobutene (BCB), where the BCB layers provide an additional passivation layer on the original die surface, a planarizing dielectric coating and the definition of the solder ball wettable area. The under bump metallization (UBM) pad is constructed by sputtering Al/NiV/Cu material on the wafer and, after etching, is only present in the pad areas. For RoHS Pb-free compliance, the solder bumps use an Sn 95.5/Au 3.9/Cu 0.6 alloy, so a solder ball is constructed on the pad and reflowed. Following singulation from the wafer, the resulting package can be considered as a "scaled-up flip-chip" component, which can be soldered directly to the printed circuit board using conventional SMT processing.

DUAL/QUAD FLAT NO-LEAD PACKAGING

Another low cost small size package that is available is the dual flat no-lead (DFN) package, which is a plastic leadless chip carrier with dual (two opposite) populated sides and an exposed thermal pad with a typical package height of 0.8 mm. All surface-mount contact pads have 100 percent Sn terminations and 0.5 mm contact pitch. This rectangular package conforms to the JEDEC package outline MO-229 and provides 4, 6 and 8 I/O options. For easier PCB routing and higher density of contact pads, the quad flat no-lead (QFN) package offers a plastic leadless chip carrier with quad (four opposite) populated sides and an exposed thermal pad with a typical package height of 0.75 mm. All surface-mount contact pads have RoHS Pb-free compliant 100 percent Sn terminations and 0.5 mm contact pitch. This square package conforms to JEDEC package outline MO-220 and provides 16 and 20 I/O options. For both package options, the singulated die is attached to the center paddle lead frame and then wire-bonded to the external I/O lead frames. The die and wire bonds are then over-molded to achieve the nominal height of 0.75 mm making them ideal for high volume SMT processing.

COST CONSIDERATION

Cost is a factor that will inevitably spring to mind in the context of integrated passive and active devices. After all, thin film passive component technology has traditionally been associated with such applications as precision instrumentation, high accuracy converters and ultra-low noise amplifiers. Here, the reader may be pleasantly surprised to learn that the installed cost of a well-designed integrated passive and active device can usually compare favorably with the discrete solution that it is intended to replace. The term "installed cost" is the key. When doing the math, it is important to consider that the cost of installation does not end at the bill of materials. The main elements of the total installed cost include the price of the discrete components, the placement cost, cost of procurement and storage. The placement costs for discrete chip and/or SOT components are nearly always significantly higher than the cost of the components themselves. With this in mind, the IPAD using CSP becomes a very attractive proposition, especially when one considers the electrical and mechanical performance advantages already discussed. The costs given in ***Table 1*** relate to the circuit in ***Figure 1***. From this example, it is clear that there is a potential savings of nearly $0.20 per part. Additional advantages include the use of less solder paste and a reduced number of solder joints (45 for the discrete solution and 15 for the CSP solution). Furthermore, the integrated passive and active devices are electrically tested during the manufacturing process, whereas the discrete solution can only be tested once it is assembled onto the PCB.

INTEGRATED PASSIVE AND ACTIVE DEVICE APPLICATIONS

ESD Protection

Many handheld devices have external ports, which are potential paths for ESD to enter the handheld device and damage the internal circuitry. A suitable solution for this type of problem, where board area is

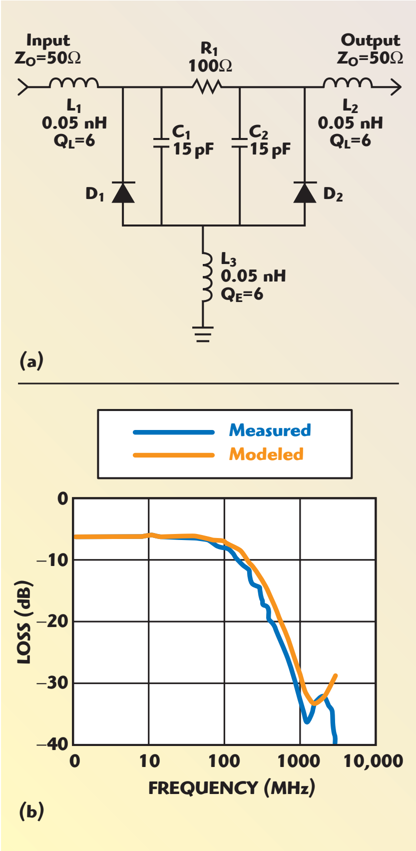

▲ *Fig. 2 ESD and EMI filter channel's (a) schematic and (b) modeled and measured performance.*

an issue, is an integrated passive and active device with ESD protection from contact discharges in excess of ±8 kV and air discharges of ±15 kV. For this and most handheld devices, the applicable test method is the IEC 61000-4-2 specification.

Line Termination

System bus speeds are increasing, making line termination a more important consideration. Transmission line effects, such as reflections, must be controlled to prevent misinterpretation of data or other malfunctions. Terminating bus lines using high speed Schottky diodes is an effective method in terms of both performance and cost.

ESD Protection and EMI Filters

Handheld devices, such as cell phones, often have data/audio ports, which are used to connect the device to external devices such as laptop computers and headsets. Cell phones by their nature generate RF noise and this noise can be coupled into the data/audio port. Combining ESD protection and a low pass filter will attenuate the RF noise, which may otherwise interfere with the internal baseband circuitry of the cell phone. For a GSM, CMDA or 3G cell phone, some devices can offer attenuation of 30 dB minimum from 800 MHz to 3 GHz. Typically, the low pass filter is used to protect data/audio ports on wireless devices and LCD screen interfaces. A typical schematic is shown in ***Figure 2***.

CONCLUSION

It is hoped that this article has shed some light on the capabilities of thin-film-on-silicon integrated passive and active devices. In particular, the intent was to demonstrate how the advent of wafer-level chip scale packaging (CSP), dual flat no-lead (DFN) and quad flat no-lead (QFN) packaging technology has made these versatile devices attractive to designers of miniature handheld wireless products by eliminating any disadvantages attributable to previous packaging forms. The integration of resistors, capacitors, inductors, diodes and transistors into single, ultra-miniature, monolithic packages has opened the door to a new level of component count reduction. This allows the bill of materials to shrink, pick and place cycles to decrease and overall product manufacturing costs to come down. In addition, manufacturers receive the advantage of reduced board real estate usage and improved electrical performance. ■

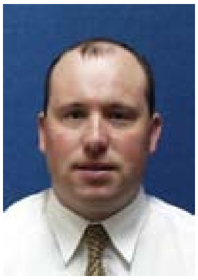

Ian Doyle *received his BEng degree from the Cork Institute of Technology, Ireland, in 1994. From 1994 to 1998, he was employed with M/A-COM Eurotec, Cork, Ireland, as a staff engineer, where he designed RF passive components for the broadband CATV and cellular base station markets. In 1998, he joined Bourns Electronics Inc., Cork, Ireland, as product line manager, where he is responsible for the product development of integrated passive and active devices, using a combination of thin-film-on-silicon substrates with CSP, DFN or QFN packaging technology.*

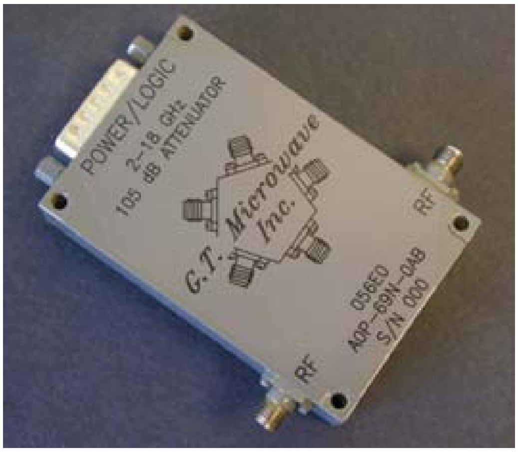

AN ULTRA-BROADBAND 2 TO 18 GHZ DIGITAL ATTENUATOR WITH HIGH RESOLUTION AND 105 DB DYNAMIC RANGE

The function of an attenuator is to reduce the amplitude level without substantially distorting the waveform of a microwave signal in the process. It contains a lossy element along the direction of the electromagnetic field vector, in order to dissipate the RF energy. This article describes a digital attenuator to adjust a signal to a desired amplitude level via an electronic command.

The theory of operation is to reduce the level of a known source of power by a predetermined amount expressed in decibels, which are obtained from the logarithm of the power ratio desired. The RF topology for this digital attenuator consists of a transmission line with diodes spaced optimally to cover the desired frequency range and digital-to-analog drive circuitry to control the variable analog attenuator.

The key component of the attenuator is the choice of diodes. It is an important design consideration. The diodes are mounted in a shunt configuration with and without Q spoiling networks. Diodes oriented in the same direction eliminate bi-directional currents for improved temperature compensation. Using chip diodes with a ribbon lead has its drawbacks. In a high frequency broadband application, the inductance of the ribbon lead adversely affects the attenuation and bandwidth. A beam-lead diode, installed using a proprietary technique, reduces the series inductance and provides a significant improvement in performance. To minimize the adverse effects from biasing, the network is buried as far as possible from the input and output ports.

In the RF design of a digital attenuator, the preferred transmission media is microstrip, which allows access to the circuitry while being measured. This provides for a more precise tuning capability. This technique yields an overall improvement in both optimization and performance. Even with the improvement in microwave performance, it is the control circuitry that provides the absolute accuracy for

G.T. MICROWAVE INC.
Randolph, NJ

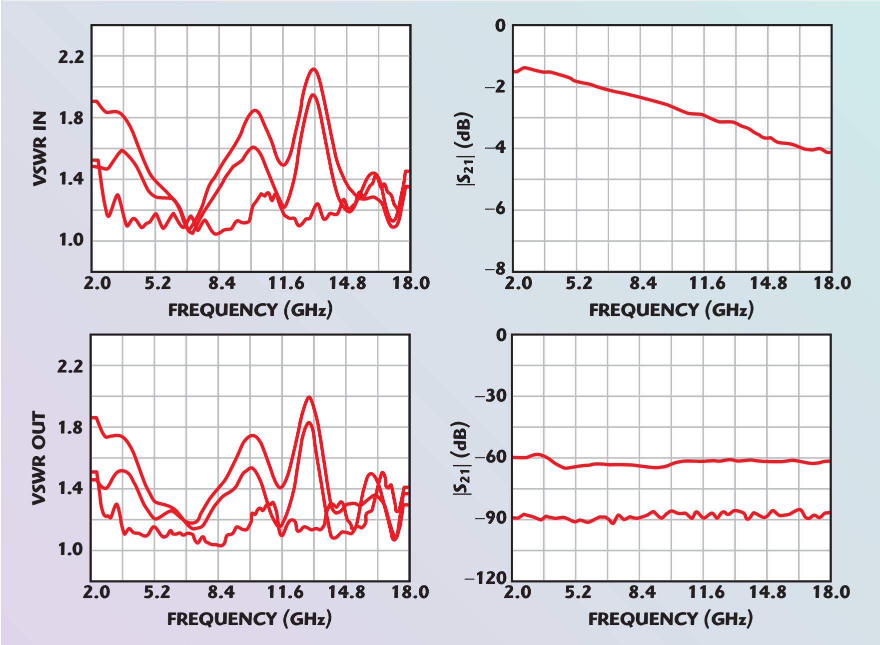

▲ *Fig. 1 Digital attenuator typical performance.*

the overall device. It has to be capable of canceling the nonlinear effect of the PIN diodes and provides a monotonic linear control of the input slope characteristic. In order to achieve the absolute accuracy required for the attenuator, the digital section has a 64K resolution capability to control and compensate the performance. For any desired resolution, the optimal performance values for each digital attenuator are stored in the driver's EEPROM, ready to be commanded from the external digital control input. This is accomplished by using a computer with I/O and IEEE controller cards, a G.T. Microwave proprietary program and a vector network analyzer. The computer's I/O port sets the external control input for the desired digital attenuation, then ramps the driver's 64K of resolution down the dynamic attenuation range, using another I/O port to an internal control input. While ramping the digital attenuator driver, the vector network analyzer measures the attenuation at each step and sends the data to the computer via the IEEE bus. When the optimal condition is determined, the computer programs the driver's EEPROM for the external control input count.

The digital attenuator described is optimized over a 9:1 bandwidth, 2 to 18 GHz with 105 dB of dynamic attenuation range and 0.03 dB resolution, 12 bits of TTL compatible binary logic, and is capable of switching between any state within 350 ns. The insertion loss is 5.0 dB, the attenuation flatness is ±1.0 dB to ±8 percent of the set attenuation value and the VSWR is 2.2. The digital attenuator envelope is 3.0" × 2.0" × 0.75". Using the techniques described herein, the test data shown in ***Figure 1*** illustrates the typical performance achieved.

This technology hosts a variety of products, which include, but are not limited to BPSK, QPSK and vector modulators, phase shifters and phase free attenuators. Models are offered with options that include digital control with up to 64K of resolution, linearized or any desired control input slope characteristic, narrowband optimized performance, temperature compensation, video filtering and sub-assembly integration.

New modulation techniques will demand a technology requiring a new generation of components. These components will need an improved performance at a lower cost. Industry can now welcome the arrival of ultra-broadband digital attenuators that will provide tomorrow's capability, at the leading edge in performance and available today.

G.T. Microwave Inc., Randolph, NJ (973) 361-5700, www.gtmicrowave.com.

RS No. 300

A DUAL-CHANNEL DIGITAL RECEIVER

A dual-channel, very high speed data acquisition and real-time digital signal processing module has been developed that is useful in applications such as electronic warfare (EW), radar and software-defined radios. The board incorporates two Atmel AT84AS008VGL, 2.2 Gsa/sec, 10-bit analog-to-digital converters and up to three Virtex-4 field programmable gate arrays (FPGA). The board also has two high speed serial (Hotlink) interfaces and a VME64 interface.

PRODUCT DESCRIPTION

The board incorporates two Atmel AT84AS008VGL A/Ds that feature a maximum sample rate of 2.2 Gsa/sec at 10-bits with a 3.3 GHz full power input bandwidth. Their spurious free dynamic range (SFDR) is 58 dBc (7.4 effective bits at F_S = 1.4 Gsa/sec, f_{IN} = 700 MHz). A companion device, the AT84CS001, demultiplexes the high speed, 10-bit LVDS A/D outputs onto a 40-bit, differential bus running at ¼ of the sample rate. The A/D's sampling delay and gain can be adjusted to support synchronizing and interleaving multiple A/D boards. The output of the demultiplexer is connected to a Virtex-4 using a 40-bit, differential bus and clock.

Also, on the new receiver board are sites for three Virtex-4 FPGAs. There is an XC4VSX55s directly connected to each A/D channel and also an XC4VLX200. High speed differential buses connect all three devices. The XC4VLX200 is used to implement the Hotlink and VME interfaces. A soft processor (CPU) is integrated into the XC4VLX200 for board level control and communication.

The CPU module is used to provide a user interface, local control, and to read and write from Flash. This module also provides an RS232 interface for test; a simple command set is used to configure the board and control data collection and processing. There are 64 Mbytes of flash memory that can be used to store FPGA configuration data.

LNX CORP.
Salem, NH

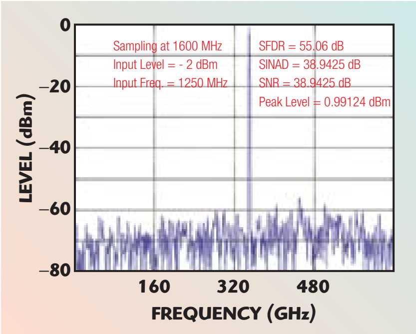

▲ *Fig. 1 Direct downconversion of a 1250 MHz signal sampled at 1600 Gsa/sec.*

The high speed serial links are implemented using the CYP15G0101-DXA HOTLink II™ transceiver from Cypress Semiconductor. It contains all of the logic to support the serialize/de-serialize (SERDES) function and clock recovery, and supports data rates from 200 to 1500 Mbaud. ***Figure 1*** displays a downconverted 1250 MHz signal, sampled at 1600 Gsa/sec showing the receiver's SFDR performance exceeding 55 dBc.

The VMEbus interface is designed to conform to the VME64x specification and requires the 160 pin connectors with the added ground pins and +3.3 V power pins. The interface was designed to support A32/D32 slave data transfer.

Typical power consumption is 60 W; all power is derived from the VME standard power supplies using on-board DC-DC converters. The board can be used in convection or conduction cooled applications and is rated for operation from –40° to +85°C.

ADDITIONAL CAPABILITIES

In addition, LNX can develop custom algorithms based on customer specifications as a result of the company's significant investment in system simulation, algorithm development and FPGA logic synthesis tools. These tools allow the company to develop and simulate fixed-point DSP algorithms in Matlab™ and automatically convert those algorithms into VHDL for synthesis and implementation on the FPGAs. This allows LNX engineers to rapidly develop, simulate and test new algorithms without having to manually convert new algorithms to VHDL or Verilog.

CONCLUSION

A very high speed data acquisition and real-time DSP processing platform has been introduced that is ideal for use with EW, radar and software-defined radio applications. With the company's in-house tools and capabilities, new receiver designs can be easily tailored, using lower cost design techniques as necessary to implement new requirements.

LNX Corp.,
Salem, NH (603) 898-6800,
www.lnxcorp.com.

RS No. 301

A HIGH PASS FILTER WITH A LIMITED REJECTION BAND

Most typical high pass filters pass frequencies above their specified cut-off frequency with little or no attenuation and then start to attenuate frequencies below the cut-off frequency in a continuous slope depending on the configuration of the filter. Little attention is paid to the characteristics of the stop band other than to make sure it is below a predetermined level. A new requirement was recently placed on the high pass filter's stop band performance to meet a specific military requirement. The new filter's attenuation band had to be controlled and set to a specific attenuation level. Thus, a relatively simple high pass filter suddenly became more complicated.

Fig. 1 The limited rejection high pass filter's insertion loss and return loss vs. frequency.

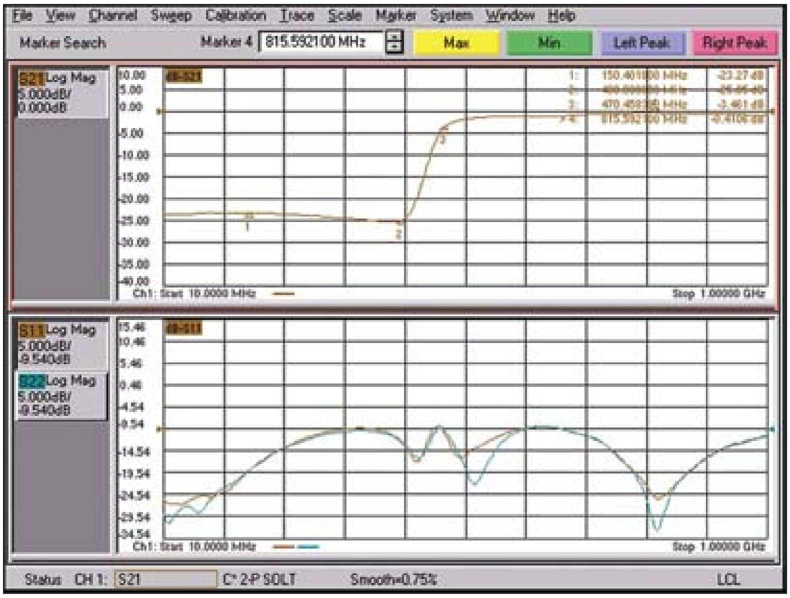

This particular filter was designed with a high pass band of 470 MHz to 1 GHz while the stop band is 10 to 470 MHz and has approximately –23 dB of rejection over the full stop band. In addition, the VSWR over the full 10 MHz to 1 GHz operating band was specified at 2.0:1 maximum.

The new filter is currently being used as a gain equalizer in a military aircraft system, providing gain correction over the full operating band. The particular system problem was that at frequencies below 450 MHz there was a specific amount of additional gain. This excess gain from 20 to 450 MHz had to be attenuated while not interfering with the gain level above 450 MHz.

The resulting filter's insertion loss and return loss is shown in ***Figure 1***. The actual specification for the military application was from 20 MHz to 1 GHz with an insertion loss meeting a particular specified profile, and with an input and output VSWR of 2.3 maximum over the entire 20 MHz to 1 GHz operating band. As can be seen in the data plots, the attenuation level in the stop band remained constant to within 2 dB and the VSWR easily remained 2:1 or below.

Although this particular filter was designed and delivered for a specific military requirement, the product design is easily adapted to similar frequency ranges and applications, military or commercial. Other frequency ranges and attenuation levels are available upon request.

Planar Filter Co.,
Frederick, MD (301) 662-5019,
www.planarfilter.com.

RS No. 302

EMC TEST SOFTWARE

The model SW1006 is the latest version of the company's radiated susceptibility, conducted immunity and precompliance emissions software. Model SW1006 automatically performs both calibration and immunity testing in full compliance with IEC 61000-4-3, 4-6, MIL-STD 461/462 RS103, CS114, RTCA/DO160 Section 20 specifications. The software also supplies the user with selectable test parameters and a "thresholding" mode for pre-compliance investigation of equipment susceptibility, as well as closed loop leveling. Pre-compliance emission testing can be done with the use of a spectrum analyzer and either a pre-amp or LISN. The SW1006 software is designed for use with the supplied NI PCI-GPIB interface card for instrument communication.

AR Worldwide RF/Microwave Instrumentation,
Souderton, PA (215) 723-8181, www.ar-worldwide.com.
RS No. 310

3D EM SIMULATOR

The Time Domain 3D EM simulator, CST MICROWAVE STUDIO®, is available in its new release, version 2006. Users can now benefit from a major re-design in the architecture and substantial new functionality. The most significant change is the use of the CST DESIGN ENVIRONMENT™ as a common access point to CST's solver technology. Structures are presented in 3D and schematic views and the comparison of models and co-simulation has been facilitated by a new multi-document interface.

CST of America Inc.,®
Wellesley Hills, MA (781) 416-2782, www.cst.com.
RS No. 311

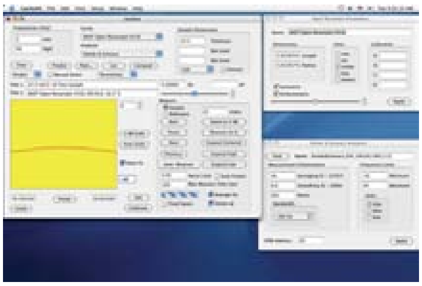

MATERIAL MEASUREMENT SOFTWARE

Cavity™ is a versatile software package for Microsoft Windows and Macintosh OS X that performs all of the major functions associated with collecting and processing data to determine material constitutive properties, such as permeability and permittivity from a variety of cavity types and resonators. The program controls common network analyzers made by Agilent, Anritsu and Rohde & Schwarz; the program leads the user through calibration and measurement steps. A variety of data processing options are available to determine mu, epsilon and other parameters.

Damaskos Inc.,
Concordville, PA (610) 358-0200, www.damaskosinc.com.
RS No. 312

PARAMETRIC PRODUCT SEARCH TOOL

The parametric product search tool is designed for the RF engineer to specify important product parameters and view the company's products that match a specific requirement in a specification-compliance format. Unlike conventional search engines which eliminate products that narrowly fall outside of specification, the parametric product search tool can show these products allowing the engineer to make intelligent design trade-off decisions to "fine tune" the requirement to specific needs. View this and other product software support tools including Product Cross Reference, PLL Phase Noise and Mixer Spur Chart Calculators on the company's site.

Hittite Microwave Corp.,
Chelmsford, MA (978) 250-3343, www.hittite.com.
RS No. 313

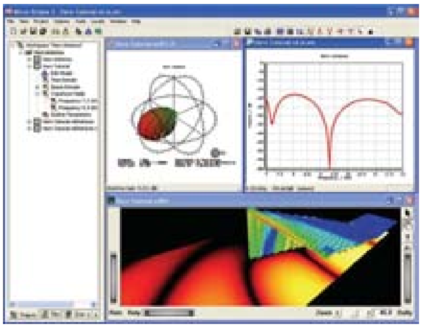

EM DESIGN SOFTWARE

Version 7 of the MicroStripes electromagnetic design simulation software for microwave and antenna design substantially increases the speed with which users can tune their designs. It automatically runs a series of simulations while varying one or more design parameters over a user-specified range. This feature is supplemented by improvements in the accuracy of the automatic meshing algorithm. Also, Version 7 enables users to inspect simulation results quickly by simply running the mouse over the graphical output. It uses the Transmission Line Matrix (TLM) method for solving Maxwell's equations, which when applied to antenna design solves for all frequencies of interest in a single calculation, capturing the full broadband response of the system in one simulation cycle.

Flomerics Ltd.,
Hampton Court, UK +44 (0) 20 8487 3000, www.flomerics.com.
RS No. 314

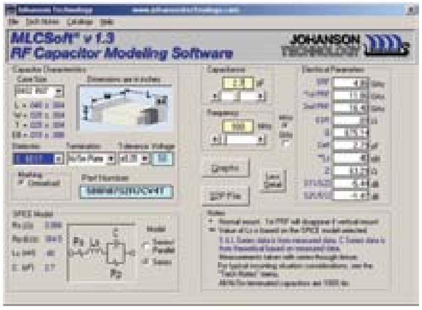

DESIGN SIMULATION SOFTWARE

JTIsoft® version 1.3 is comprised of two advanced design simulation software programs, MLCsoft® and MLIsoft®. It provides complete S-parameter and SPICE modeling data on the company's line of RF multilayer ceramic capacitors and inductors over the frequency range of 1 MHz to 20 GHz. In MLCsoft, the interface allows the user to select one of six MLCC sizes plus other part variables and displays the complete part number for accuracy when ordering. In MLIsoft, the user can select one of three MLCI sizes plus other part variables and display the complete part number for accuracy when ordering.

Johanson Technology Inc.,
Camarillo, CA (805) 389-1166, www.johansontechnology.com.
RS No. 315

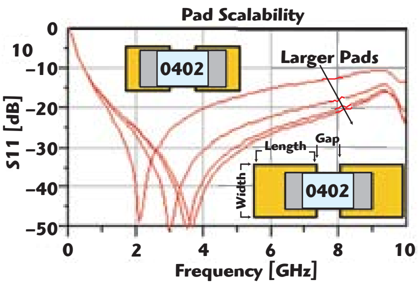

PAD SCALABLE MODELS

The CLR Library 4.0 is a substrate- and part value-scalable surface-mount model library that includes pad scalability on selected components. The company's Global Model™ has input parameters that allow users to specify custom pad dimensions to meet specific design requirements. The 4.0 version will include 13 new models expanding the total library to 61 Global Models. Additional models include 0201's, 0402's, 0603's, 0805's and DC blocking capacitors with vertical and horizontal orientation selection.

Modelithics Inc.,
Tampa, FL (813) 866-6335, www.modelithics.com.
RS No. 316

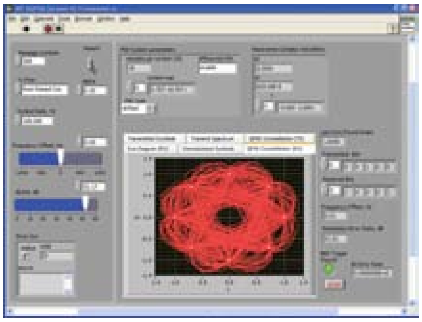

MODULATION TOOLKIT

This Modulation Toolkit 3.1 is a flexible, software-defined approach to RF and communication system design and test that builds on the LabVIEW intuitive dataflow-based programming model and transforms modular instruments into communication systems. The LabVIEW add-on includes software for signal generation, analysis, visualization and processing of standard digital and analog modulation formats including bit generation, encoding, interleaving and signal equalization. The toolkit provides ASK, FSK, MSK, PSK, PAM, QAM, AM, FM, PM and many of their derivatives – even generation and analysis of custom modulation formats. The Modulation Toolkit also comes standard with algorithms such as Reed-Solomon, Hamming, Golay and Convolution that improve transmission efficiency and noise immunity to serve countless communications applications.

National Instruments Corp.,
Austin, TX (800) 531-5066, www.ni.com/rf.
RS No. 317

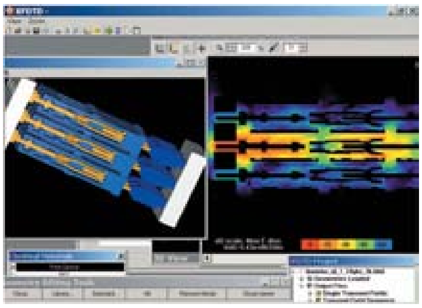

FULL-WAVE ELECTROMAGNETIC SOLVER

XFDTD, version 6.3, is now released and offers many new features and improvements, including enhanced PML boundary conditions, new multiple plane wave excitation, full 3D far zone plotting with extended data presentation, new CATIA interface, enhanced Pro-E and STEP interfaces, and greater flexibility in the adaptive meshing based on the Remcom FAST MESH algorithm. Further, a new Bio-Heat optional module is available for temperature rise due to SAR. Engineers, designers and scientists use the capabilities of XFDTD, a full-wave 3D electromagnetic simulation, in such applications areas as microwave, RF, antennas, scattering, biological EM, photonics, packaging, EMC and specialized materials.

Remcom,
State College, PA (814) 861-1299, www.remcom.com.
RS No. 318

EXPANDED PXI-BASED TEST SOLUTION

The new version 2.3 of the enhanced generic test software library (EGT-SL) for in-circuit tests, expands the company's Open Test Platform R&S CompactTSVP into a more powerful multi-purpose tester. The software provides a previously unavailable level of openness that lets users expand the test solution at any time by adding further test methods for new components. An automatic test generator and the intuitive graphical user interface enable users to implement error-free in-circuit test applications quickly without requiring much previous experience. Thus, the CompactPCI/PXI-based test platform makes it possible to perform configuration and function tests of electronic modules on one system.

Rohde & Schwarz GmbH,
Munich, Germany +49 89 4129-13779, www.rohde-schwarz.com.
RS No. 319

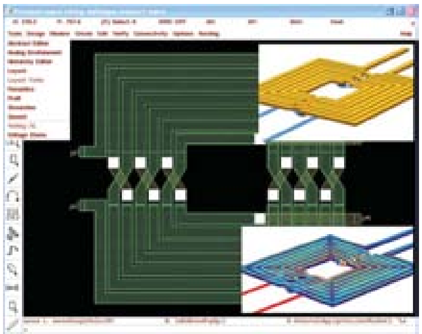

ELECTROMAGNETIC SOFTWARE

SONNET® Software's interface to the Cadence® Virtuoso® environment enables customers to use Sonnet Suites Professional™ completely within the Cadence environment. Sonnet uses layout cells to quickly and seamlessly extract EM analysis projects based on a user's Cadence technology files and process information. Model data views (including Broadband Spice extraction models) are automatically generated and installed in a library, available with a choice of circuit analysis tool. Sonnet Software Inc. is a member of the Cadence® Connections Program.

Sonnet Software Inc.,
North Syracuse, NY (877) 776-6638, www.sonnetsoftware.com.
RS No. 320

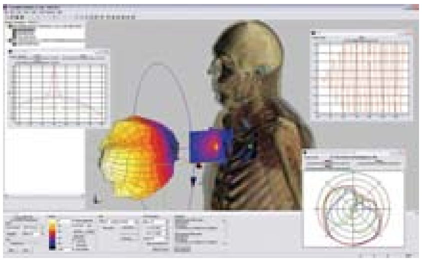

FAST EM SIMULATION

SEMCAD X Eiger is the latest release of the company's powerful EM TCAD package. Efficient and user-friendly, it is claimed to be the only one featuring Conformal and ADI in addition to conventional FDTD solvers, providing the right solution for any EM-related requirements. By offering 64-bit support of over one billion voxels and exclusively integrating the aXware hardware accelerators, real problems can be solved within only a few minutes by computing at up to 400 MCells/s. This EM simulation tool is suitable for the most complex EM challenges, including optimization and failure/safety evaluations of sensor systems as well as implants or transmitters operating inside or near the human body.

SPEAG, Schmid & Partner Engineering AG,
Zurich, Switzerland +41 (0) 44 245 9700, www.speag.com.
RS No. 321

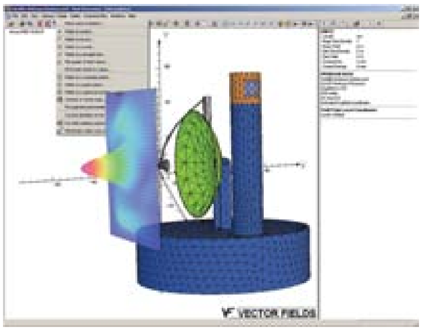

3D SOFTWARE

This recent version of the 3D software CONCERTO computes and predicts electromagnetic performance with confidence, giving users the ability to produce competitive and innovative products while keeping costs to a minimum. The diverse range of applications that can be analyzed with CONCERTO include antennas, waveguides, filters and cavities. This latest addition to CONCERTO is a Moment Method module that is ideal for antenna installed performance and radar signature prediction. Using the same geometric modeler, it complements the FDTD module that is recommended for component design.

Vector Fields Inc.,
Aurora, IL (630) 851-1734, www.vectorfields.com.
RS No. 322

ON-LINE CONFIGURATION TOOL

This on-line interactive design guide provides simple step-by-step instructions for configuring GORE™ High Flex Flat Cable or GORE Trackless Cable from standard components, with five-day lead times. This configurator simplifies the cable design process and generates a 3D downloadable CAD model via a quick, streamlined step-by-step procedure. Users can take an interactive tour to learn more about the configurator, and then proceed to design a cable and submit an RFQ using the simple step-by-step configuration tool.

W.L. Gore & Associates Inc.,
Elkton, MD (302) 292-5100, www.gore.com/designacable.
RS No. 323

NEW WAVES: RF Components and Systems

SP2T Terminated Switch

The model SWN-218-2DT option NS is a single-pole, two-throw, terminated switch module that offers an insertion loss of 1.2 dB typical, high isolation of 80 dB minimum and an integral TTL driver. This switch is designed for ultra-low video transient, high power and operation between 3.1 to 3.5 GHz.

American Microwave Corp., Frederick, MD (301) 662-4700, www.americanmicrowavecorp.com.

RS No. 216

RF Capacitor

The SQ series is a porcelain and ceramic dielectric multilayer capacitor chip that offers a new internal construction. These chips are ideal for RF and microwave applications ranging from 10 MHz to 4.2 GHz, including microwave RF/IF amplifiers, mixers, oscillators, low noise amplifiers and filter networks. Available in 1210 and 0605 sizes with voltages up to 500 VDC, the SQ series offers good stability under the stresses of changing voltage, frequency, time and temperature. Price: \$0.10 to \$0.75. Delivery: stock to six weeks.

AVX Corp., Myrtle Beach, SC (843) 448-9411, www.avx.com.

RS No. 217

Coaxial Adapter Kit

The EI2205-KIT is an adapter kit that includes reverse polarity and standard coaxial adapters in BNC, TNC, SMA, N, MMCX, UHF and RCA. These adapters are made of brass/stainless steel with gold plating. The kit comes with 40 adapters. High precision adapter kits are also available up to 40 GHz. These kits were designed to solve the problem of quick interconnection that sometimes develops in wireless design and development, standard and reverse polarity type connectors that are used in various telecommunication systems.

Electronika International Inc., Cleveland, OH (440) 743-7034, www.electronikainc.com.

RS No. 218

Dual Reject Filter

The model BPF2G-10 is a dual reject filter that offers two passbands: one at 1995 to 2130 MHz with rejection 1) at 1980 MHz and 2150 MHz: 10 dB minimum, 2) at 1950 MHz and 2180 MHz: 40 dB minimum, 3) at 1850 MHz and 2300 MHz: 60 dB minimum. Insertion loss is 0.9 dB maximum. The second passband is 2450 to 2494 MHz with rejection 1) at 2445 MHz and 2500 MHz: 10 dB minimum, 2) at 2420 MHz and 2540 MHz: 40 dB minimum. Insertion loss is 1.5 dB maximum. These filters operate in a temperature range from –30° to +50°C. Size: 4.640" × 4.570" × 1.28".

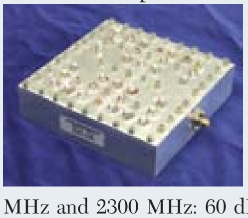

Filtel Microwave Inc., Ottawa, ON, Canada (613) 731-5882, www.filtel.com.

RS No. 219

Co-location Filter

The model 6FVSP-00078 is a co-location filter that is designed to minimize the interference between co-located Inmarsat and Iridium systems. Locations such as ships and aircraft have space at a premium creating interference between these two systems. This co-location filter has low insertion loss in the Iridium band while providing 40 dB of rejection in the adjacent Inmarsat transmission band. Independent tests have indicated that utilizing the company's filter reduces the required antennae spacing for acceptable operation of both systems from as much as 700 m to as few as 1 m, depending on application.

K&L Microwave, Salisbury, MD (410) 749-2424, www.klmicrowave.com.

RS No. 220

DPDT Switch

The model MASWSS0184 is an RoHS-compliant DPDT switch that maximizes system linearity performance while reducing DC power consumption. This high power switch is designed for 802.16 (WiMAX) and MESH network applications that require high power handling at P1dB of 40 dBm, low typical insertion loss of 1 dB and a high isolation of 30 dB. Typical applications for this product include two antenna solutions requiring diversity switching in linear systems, thus connecting the receiver and transmitter to both antennas. Size: 3 × 3 mm. Price: \$2.25 (10,000).

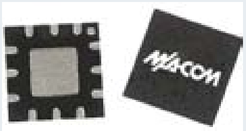

M/A-COM Inc., Lowell, MA (800) 366-2266, www.macom.com.

RS No. 223

High Power Splitter/Combiners

The VXL series of high power, 0° splitter/combiners are available in two-, three- and four-way configurations, and operate from 800 through 2500 MHz. This series exhibits low VSWR, high isolation and can handle up to 50 W CW of power. Delivery: stock to two weeks.

Vista RF Inc., Roseville, CA (916) 529-4799, www.vistarf.com.

RS No. 231

Hybrid Band Reject Filter

The model 6BRX-1575/X20-S is a hybrid band reject filter with bi-directional inputs. This filter features 65 dB of notch depth attenuation from 1565 to 1585 MHz. The typical 3 dB bandwidth is 150 MHz. The VSWR is 2.0 from DC to 2900 MHz excluding the notch area. Size: 1.50 × 0.750 × 0.40 excluding SMA female connectors.

Lorch Microwave, Salisbury, MD (410) 860-5100, www.lorch.com.

RS No. 222

Directional Couplers

These directional couplers provide a convenient and accurate means for sampling microwave energy, which is ideally suited for monitoring incident and reflected power. Directional couplers are offered in octave, broadband and high power models (100 W model shown). A wide range of dB values are available in many frequencies. SMA and N connectors are standard. Most items are in stock and ready for immediate delivery.

Microwave Communications Laboratories Inc., Saint Petersburg, FL (727) 344-6254, www.mcli.com.

RS No. 224

Low Pass Filters

The LFTC series of low pass filters operate in a frequency range from DC to 5400 MHz. The filters can handle more than 10 W and cover cut-off frequencies up to 6 GHz. This series is ideal for applications dealing with rejection of harmonics, intermods and avoiding unwanted signals from creeping into the system. Size: 0.15" × 0.15" × 0.028". Price: \$3.75 each (Qty. 10–49).

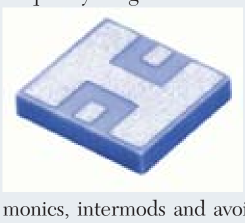

Mini-Circuits, Brooklyn, NY (718) 934-4500, www.minicircuits.com.

RS No. 225

Seven-channel Switch Filter Bank

The model 7SFB-0R258R3-5-15-SFF is a switch filter bank that features seven bandpass filter channels within the 0.25 to 8.30 GHz frequency range and maintains > 60 dBc rejection up to 20 GHz. Passband insertion loss is better than 5 dB. Switching speed is 0.8 µs maximum. The unit operates from +5 and –12 VDC supplies. Size: 2.6" × 2.5" × 0.41".

Planar Filter Co.,
Frederick, MD (301) 662-5019,
www.planarfilter.com.

RS No. 253

Quadrature Hybrid

The model QC-052-YR3 is a 3 dB quadrature hybrid that when a signal is applied to any port the hybrid will split that signal equally between the ports on the side away from the input with the port adjacent to and on the same side as the input port remaining isolated. The direct port and the coupled port will be 90° out of phase. This hybrid/coupler operates in a frequency range from 0.5 to 2 GHz. Size: 1.45" × 0.75" × 0.22" and the SMA connectors are removable for surface-mounting the hybrid.

Planar Monolithics Industries Inc.,
Frederick, MD (301) 631-1579,
www.planarmonolithics.com.

RS No. 226

End Launch Connectors

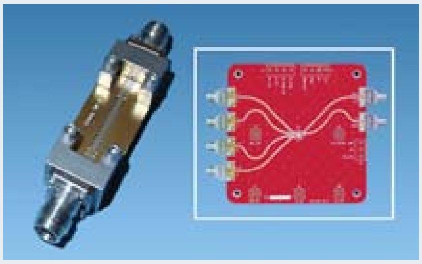

These end launch connectors are now available with SMA (27+ GHz), 2.92 mm (40+ GHz) and 2.40 mm (50+ GHz) male or female connectors. The connectors are shipped fully assembled. These connectors attach to boards using only two through holes and are intended for multi-layer boards with coplanar waveguide, but are also suitable for thinner microstrip boards. The connectors also offer low VSWR.

Southwest Microwave Inc.,
Tempe, AZ (480) 783-0201,
www.southwestmicrowave.com.

RS No. 229

Wideband Miniature Filter

The model 5BM-3.0G-2.0G-SX11 is a wideband miniature filter centered at 3 GHz with a minimum 1 dB passband of 2 to 4 GHz. This filter offers 0.8 dB of insertion loss, a VSWR of 2:1 (max.) and 40 dB of attenuation at 1 GHz and 5 to 10 GHz. This model is available with SMA or PIN connections. Size: 0.38" × 0.38" × 1.5".

Reactel Inc.,
Gaithersburg, MD (301) 519-3660,
www.reactel.com.

RS No. 227

Surface-mount Isolators/Circulators

The SLE series of low power surface-mount isolators/circulators operates from 380 to 2200 MHz. This device is miniature in size, which makes it a perfect fit for tomorrow's telecom applications. This device is also available in a circulator version. Both versions are available in tape and reel format for high speed automated assembly. Models are available in typical bandwidths of 5 percent with isolation > 17 dB and insertion loss < 0.8 dB.

Renaissance Electronics Corp.,
Harvard, MA (978) 772-7774,
www.rec-usa.com.

RS No. 228

In-phase Power Divider

The model SPC-PD2-CP-860 (PD2-860) is a high isolation, two-way, in-phase power divider with a minimum isolation of 40 dB. Power handing capability is 20 W. Operating frequency is from 800 to 950 MHz. Insertion loss is less than 0.5 dB, and amplitude and phase balance is less than 0.2 dB and 3 degrees, respectively. Impedance is 50 Ω. Connector type is SMA/Female, but other connector types are available. Size: 0.44" × 1.5" × 2". Delivery: two to four weeks.

SPECOL Inc.,
Landing, NJ (973) 770-3454,
www.specolinc.com.

RS No. 230

Front-mount Bulkhead Jacks

The N series of front-mount bulkhead jacks is designed for RG-316, LMR-100, RG-188 and RG-174. These are robust connectors that operate from DC to 12.4 GHz. Typical applications include Fleet Management Systems, Wi-Fi, WiMAX and WLAN.

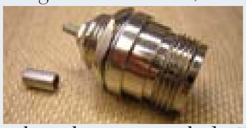

Lighthorse Technologies Inc.,
San Diego, CA (858) 292-8876,
www.rfconnector.com.

RS No. 221

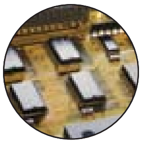

AMPLIFIERS

High Power Amplifier

The model SSPA 1.2-1.4-500-RM is a high power, rack-mounted, L-band, solid-state power amplifier (PA) that operates over the 1215 to 1400 MHz L-band radar band. This rack-mounted PA was designed for high power L-band radar applications. The peak RF power is 55 dBm minimum. Power flatness across the entire band is ±0.5 dB typical. Minimum small-signal gain is 54 dB. Input VSWR is 2.0 maximum and output VSWR is 2.0 maximum. Noise figure is 10 dB maximum. Harmonics are –30 dBc maximum.

Aethercomm Inc.,
San Marcos, CA (760) 598-4340,
www.aethercomm.com.

RS No. 232

High Power Amplifier

The model AMP2G18-20-27P is a broadband high power amplifier that operates in a frequency range

from 2 to 18 GHz with a minimum of 20 dB gain. Gain flatness is better than ±1.75 dB with typical values of ±0.75 dB. This amplifier features a P1dB of at least +27 dBm and VSWR is typically better than 2.0. The AMP2G18-20-27P is equipped with SMA(f) input and output connectors and draws less than 750 mA in DC current. Input voltage is 12 V.

Amplical Corp.,
Verona, NJ (201) 919-2088,
www.amplical.com.

RS No. 233

Broadband Amplifier

The model 800A3 is a broadband amplifier featuring a switchable transformer that allows users to select an output impedance to match the load tolerance. Model 800A3 drives loads without mismatch at 12.5, 25, 50, 100, 150, 200 and 400 Ω. This 800 W, 10 kHz to 3 MHz amplifier is ideal for applications that require high voltage and high impedance, such as chemistry, physics and ultrasonic cleaning. A modified version of the 800A3 allows users to select higher output impedances up to 2000 W.

AR Worldwide RF/Microwave Instrumentation,
Souderton, PA (215) 723-8181,
www.ar-worldwide.com.

RS No. 234

High Power Amplifier

The model XP1017 is a gallium arsenide (GaAs) monolithic microwave integrated cir-

cuit (MMIC) two-stage high power amplifier that integrates an on-chip temperature-compensated output power detector. Using 0.15 micron gate length GaAs pseudomorphic high electron mobility transistor (PHEMT) device model technology, this device covers the 30 to 36 GHz frequency bands and delivers 33 dBm OIP3 and 16 dB small-signal gain. The balanced design and Lange couplers help achieve good input and output match. This amplifier is well suited for millimeter-wave point-to-point radio, LMDS and SATCOM applications.

Mimix Broadband Inc.,
Houston, TX (281) 988-4600,
www.mimixbroadband.com.

RS No. 235

Low Noise Amplifier

The model LNA2-40DB-1.7DB is a low noise amplifier that offers 35 dB typical gain from 7

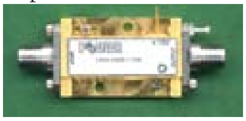

to 9 GHz. The gain flatness is better than ±1.5 dB, noise figure is < 2.5 dB and the OP1dB > 10 dBm. This amplifier offers an in/out VSWR of 2.0 maximum and the current is 150 mA at +12 VDC maximum. Up to 75 dB gain is available.

Planar Electronics Technology,
Frederick, MD (301) 662-5019,
www.planarelectronicstechnology.com.

RS No. 236

GaN Power Amplifier

These GaN HEMT power amplifiers are designed for WiMAX manufacturers in the US,

Europe, Canada and Korea. These transistors offer high power, high efficiency, high linearity, wide bandwidth, wide supply voltage and low cost at 2.7 W per 1 mm. The 2, 10, 20 W GaN HEMT power transistors are already in production and the OFDM 30 to 39 dBm, 20 to 40 dB gain hybrid power amplifiers and modules were just released for the 2.6 and 3.6 GHz WiMAX market.

RFHIC,
Suwon, Korea +82-31-250-5011,
www.rfhic.com.

RS No. 237

Two-stage Drive Amplifier

The model AH212 is a high dynamic range, 1 W, two-stage drive amplifier, housed in a low cost SMT lead-free/green/RoHS-compliant SOIC-8 package. The InGaP/GaAs HBT is able to achieve good performance for various narrowband-tuned application circuits, featuring 25 dB gain, +46 dBm OIP3 and +30 dBm of compressed 1 dB power. This device operates over the 1800 to 2200 MHz frequency band and provides good in-band gain flatness.

WJ Communications Inc.,
San Jose, CA (408) 577-6200,
www.wj.com.

RS No. 239

RF Power Amplifier

The model SM5759-37HS is a GaAs FET amplifier that is designed for various ISM band

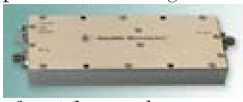

applications. The unit operates from 5.7 to 5.9 GHz with a P1dB of +37 dBm and an OIP_3 of +50 dBm. Small-signal gain is 37 dB with a flatness of ±0.5 dB across the band. Standard features include a single +12 VDC supply, thermal protection with auto reset and over/reverse voltage protection. Size: 4.7" × 2" × 0.54".

Stealth Microwave Inc.,
Trenton, NJ (609) 538-8586,
www.stealthmicrowave.com.

RS No. 238

DEVICES

P-band Transistors

The model 0910-60M, model 0910-150M and model 0910-300M are high power transistors

that cover the frequency for P-band radar applications from 890 to 1000 MHz with a pulsed output power of 60, 150 and 300 W, respectively. These transistors are designed to handle medium pulse widths of 150 µs with a duty cycle of 5 percent minimum.

Advanced Power Technology RF,
Santa Clara, CA (408) 986-8031,
www.advancedpower.com.

RS No. 240

Noise Diodes

The NW-diode series of broadband noise diodes offers a symmetrical white Gaussian

noise voltage distribution while maintaining a flat power spectral density versus frequency response. This series covers the frequency range of 0.1 Hz to 11 GHz with high output ENR. The series is available in an axial leaded version for audio frequency applications, a low cost surface-mount version for higher frequency coverage and a ceramic package for high microwave frequency operation.

NoiseWave Corp.,
East Hanover, NJ (973) 386-1119,
www.noisewave.com.

RS No. 241

INTEGRATED CIRCUIT

Ultrawideband Chipset

The WQST110 and WQST101 ultrawideband (UWB) chipset is a commercially-available, high performance silicon chipset that delivers wireless communication speeds up to one gigabit-per-second. This wireless CMOS integrated circuit combines a baseband PHY, MAC engine, high speed security processor, quality of service manager and a variety of host interfaces, all in one highly-integrated design. Designed to optimize the UWB system bill of materials, the WQST110 contains a complete high speed USB subsystem including controller and transceiver, removing any additional USB component cost. The WQST110 eliminates the need for expensive external memory, and the chip's architecture provides good power control and management for longer battery life in mobile devices. This IC also implements a tightly-coupled interface with the WQST101 RF transceiver.

WiQuest Communications Inc.,
Allen, TX (214) 547-1600,
www.wiquest.com.

RS No. 242

SOURCES

Voltage-controlled Oscillator

The model HMC588LC4B is a wideband HBT MMIC voltage-controlled oscillator (VCO) that operates in a frequency range from 8 to 12.5 GHz. This VCO incorporates the resonator, negative resistance device and varactor diode. This fully integrated MMIC VCO provides an output tuning range of 8 to 12.5 GHz, high output power of +5 dBm and low SSB phase noise of –93 dBc/Hz at 100 kHz offset. This VCO is ideal for industrial/medical test and measurement equipment, military communications, electronic warfare and electronic countermeasures applications.

Hittite Microwave Corp.,
Chelmsford, MA (978) 250-3343,
www.hittite.com.

RS No. 243

Voltage-controlled Oscillator

The model V418ME03 is a high performance voltage-controlled oscillator that operates in a frequency range of 390 to 406 MHz within 0.5 to 4.5 VDC tuning range making it ideal for quick integration into PLLs where the error voltage can be taken directly from the IC's charge pump circuitry. This compact performer exhibits a spectral purity of –119 dBc/Hz, typically, at 10 kHz from the carrier while preserving precious battery life. The V418ME03 consumes only 14 mA, typically, while operating from a 4.7 VDC supply. Size: 0.50" × 0.50" × 0.13". Delivery: stock to four weeks.

Z-Communications Inc.,
San Diego, CA (858) 621-2700,
www.zcomm.com.

RS No. 244

TEST EQUIPMENT

RF Design Kit

This radio frequency design methodology kit is targeted to address key challenges in wireless design. It leverages the latest technologies for intelligently managing parasitic extraction and linking system-level design with IC implementation, and accurately, yet rapidly, verifying complete wireless designs that span digital, analog and RF. The kit includes an 802.11 b/g WLAN transceiver reference design, a full suite of RF verification IP, test plans and applicability training on the RF design and analysis methodologies. It focuses on front-to-back RF IC design and addresses behavioral modeling, circuit simulation, layout, parasitic extraction and resimulation, and inductor synthesis.

Cadence Design Systems Ltd.,
Bracknell, UK +44 (0) 1344 360 333,
www.cadence-europe.com.

RS No. 247

Bit Error Ratio Tester

The model N4903A is a high performance serial bit error ratio tester with advanced jitter generation capabilities for jitter-tolerance testing (J-BERT) of serial gigabit devices up to 12.5 Gb/s. This model provides a complete jitter-tolerance test solution for fast, high quality characterization of next generation serial devices. The next generation of high speed serial bus standards with data rates of 5 Gb/s and beyond is expected by 2006. The increasing speed will cause significant signal integrity and jitter issues during the design and test of next generation serial bus devices.

Agilent Technologies Inc.,
Palo Alto, CA (800) 829-4444,
www.agilent.com.

RS No. 245

Handheld with HSDPA/WCDMA Capability

A High Speed Downlink Packet Access (HSDPA) testing capability for the UMTS Master MT8220A analyzer is claimed to make it the first portable handheld test instrument that can verify Node B transmitter performance — helping to ensure the successful deployment and installation of HSDPA mobile networks. When equipped with the HSDPA option, the analyzer can make all the measurements listed in the 3GPP specification for HSDPA base station performance testing. Field technicians and wireless engineers can quickly check base station performance using any of the three options: RF measurement, demodulation and over the air (OTA). All key RF measurements, including band spectrum, channel spectrum, spectral emission mask and ACLR, can now be made on HSDPA signals.

Anritsu Ltd.,
Luton, UK +44 (0)1582 433 433,
www.anritsu.com.

RS No. 246

Calibration Kit

This line of (TNC) TNCA calibration kits fully comply with the interface requirements of MIL-STD-348A. These kits are mode free to 20 GHz and exhibit good performance. MIL-STD-348A is the direct replacement for the now obsolete MIL-C-39012 and is typically used by the US Armed Forces — Army, Navy and Marine Corps. TNCA is similar to the MIL-C-87104/2 "AFTNC" typically used by the Air Force. However, mating the TNCA male connector to the AFTNC female connector could result in a non-contacting condition or "gap" fit between outer conductors.

Maury Microwave Corp.,
Ontario, CA (909) 987-4715, www.maurymw.com.

RS No. 248

Grandmaster Clock

The XLi IEEE 1588 Grandmaster Clock with GPS reference is a protocol that enables accurate synchronization over Ethernet LANs and offers users the ability to synchronize clocks within better than one hundred nanoseconds accuracy, with only a network connection. The company's first deployment of the IEEE 1588 protocol is in its versatile XLi GPS time and frequency system. IEEE 1588 enables sub-microsecond time-of-day synchronization between clocks over standard Ethernet LAN infrastructure. High accuracy time distributed over standard Ethernet LAN infrastructure offers benefits in the areas of cable infrastructure cost savings; improved accuracy for distributed measurements and processes; improved control system techniques; and leveraging the innovation/investment wave of network centric technology and solutions.

Symmetricom Inc.,
San Jose, CA (978) 927-8220, www.symmttm.com.

RS No. 250

EMF Measurement Option

The 9102 handheld spectrum analyzer with the 9131 EMF measurement option is an easy and lightweight test solution that allows network operators, broadcast stations, regulation authorities and engineering offices to test the actual radiation against defined limits. Several antennas for different purposes are optionally available and the analyzer includes all the control and calculation software without the need for an external computer. The electromagnetic field measurement can be displayed in volts per meter (V/m) and in watts per square meter (W/m^2) over a frequency range from 100 kHz to 4 GHz.

Willtek Communications GmbH,
Ismaning, Germany +49 (0) 99641 200, www.willtek.com.

RS No. 251

WLAN Application Firmware

With the R&S FSL-K91 option, the company has developed a WLAN application firmware solution for the R&S FSL spectrum analyzer. It features an I/Q demodulation bandwidth of 20 MHz, a displayed average noise level of –152 dBm (1 Hz) and a total measurement uncertainty of under 0.5 dB. With the new option, the R&S FSL can now perform all spectrum and modulation measurements on signals in accordance

with the IEEE 802.11 a/b/g/j WLAN standards. Thus, the compact, all-purpose analyzer fulfills the measurement requirements in the production of WLAN instruments.
Rohde & Schwarz GmbH & Co. KG, Munich, Germany +49 89 4129-13779, www.rohde-schwarz.com.

RS No. 249

Noise Figure and Gain Test Set

The SNG series of noise figure and gain test sets are configured to provide automatic noise and gain measurement of amplifiers or receivers in the frequency range of 26.5 to 140 GHz in seven overlapping waveguide bands. These test sets combine high performance broadband solid-state noise sources with full waveguide band down converters (STS Series) extending the Agilent 8970A/B noise figure meters to the millimeter-wave frequency range. A signal generator with output frequencies from 8 to 20 GHz, such as an Agilent 8350B/83550A or 83751B is required by the down converter unit as an LO.
WiseWave Technologies Inc., Torrance, CA (310) 539-8882, www.wisewave-inc.com.

RS No. 252

Microwave Journal CALL FOR PAPERS

To see one's work in print is the rightful reward of every creative engineer and scientist. The editors of *Microwave Journal* invite you to submit your technical manuscripts for consideration to be published in one of our upcoming issues. Technical articles, application notes and tutorial articles based on the monthly editorial themes are encouraged. Editorial themes include wireless, radar and antennas; RF components and systems; test, measurement and CAD; amplifiers and oscillators; semiconductors, MMICs and RFICs; satellite and mm-wave applications; communications and wireless applications; passive components; and control devices and modulation.

Design features should contain new and innovative technical ideas of practical use and interest to our predominantly engineering readers. Papers should be 14 to 16 double-spaced pages and contain 8 to 12 visual aids in the form of sketches, graphs, photographs or tables.

Papers should be submitted to the attention of the Technical Editor and will be reviewed promptly by our Editorial Review Board prior to acceptance. Articles outside of the monthly themes also will be encouraged.

SEND ALL MATERIAL TO:

Microwave Journal
685 Canton Street
Norwood, MA 02062
(781) 769-9750
Fax (781) 769-5037
e-mail:
fbashore@mwjournal.com

NEW LITERATURE

DATA SHEET

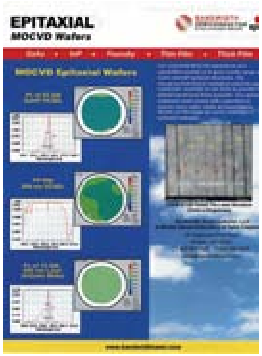

This data sheet provides complete detail on the company's epitaxial MOCVD wafers that are designed for defense and commercial markets. The growth area is class 10,000 and houses production and small volume reactors. Reactors are outfitted to grow InP- and GaAs-based materials on 2 to 4 inch diameter wafers with the highest precision available.

Bandwidth Semiconductor LLC,
Hudson, NH (603) 689-1225,
www.bandwidthsemi.com.

RS No. 200

PRODUCT BROCHURE

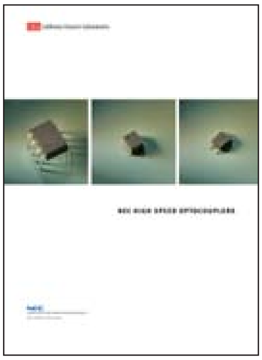

This brochure and selection guide provides a complete overview of the company's high speed optocouplers that feature speeds up to 25 Mbps, operating temperatures to 100°C, dual 3.0/5.5 V operation and output current as low as 3 mA. The brochure also characterizes the isolation requirements of various applications and recommends the optocouplers that best meet these requirements.

California Eastern Laboratories,
Santa Clara, CA (408) 919-2500,
www.cel.com.

RS No. 202

QUICK REFERENCE GUIDE

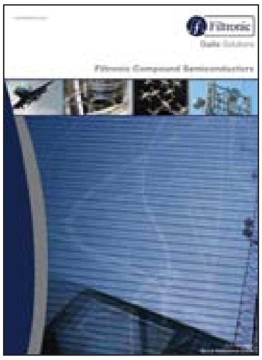

The new autumn 2005 edition Quick Reference Guide now consists of two separate brochures, one for the discrete/MMIC product line and one for the switch product line. The discrete catalog features several new broadband MMICs, and its new line of packaged C-band amplifiers. The switch catalog also includes several new switch products for WLAN/WiMAX applications.

Filtronic Compound Semiconductors Ltd.,
Newton Aycliffe, County Durham, UK
+44 (0) 1325 306 880, www.filtronic.com.

RS No. 201

RF/MICROWAVE CAPABILITIES BROCHURE

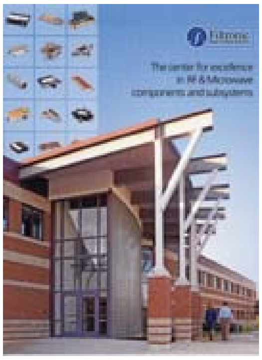

This RF and microwave capabilities brochure highlights the company's new state-of-the-art manufacturing facility and heritage passive component products. It also features the company's capabilities in filter and switch filter technology along with its ability to serve higher levels of custom integrated multi-function assemblies.

Sage Laboratories Inc.,
Hudson, NH (603) 459-1600,
www.sagelabs.com.

RS No. 203

POWER AMPLIFIERS DATA SHEET

This data sheet provides complete detail on the company's 25 to 35 W Ku-band power amplifiers, the MPC2-1220 series. A product photograph, description, performance features, electrical and mechanical specifications, and outline drawings are also provided.

Sophia Wireless Inc.,
Chantilly, VA (703) 961-9573,
www.sophiawireless.com.

RS No. 204

WIRELESS PRODUCTS CATALOG

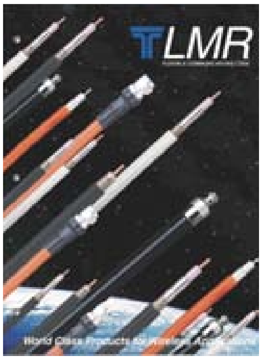

The 2006 11th edition of the LMR® wireless products catalog includes the entire range of LMR cables including LMR-DB, LMR-FR, LMR-PVC, LMR-MA, LMR-Ultraflex, LMR-W, LMR-LLPL and LMR-75 as well as TCOM® (low PIM cable), FBT® low loss, high power cables and T-RAD™ leaky feeder cables. The latest connectors, accessories and installation tools have also been added.

Times Microwave Systems,
Wallingford, CT (203) 949-8400,
www.timesmicrowave.com.

RS No. 205

Phaselock Techniques, Third Edition

Floyd M. Gardner
Wiley-Interscience • 447 pages; $84.95
ISBN: 0-471-43063-3

To order this book, contact:
John Wiley & Sons Inc.
One Wiley Drive
Somerset, NJ 08875
(800) 225-5945

The first edition of this book was published in 1966 and the second in 1979. Phaselock was an unimaginably exotic subject in 1966, with limited applications and few practitioners. Now phaselocking is a mature subject. This book reexamines the traditional phaselock topics in greater depth than previously. In addition, much new material has been included, some of it never published. Examples of additions include revised and expanded material on transfer functions, two chapters related to phase noise, two chapters related to digital phaselock loops, a chapter on charge-pump phaselock loops, expanded material on phase detectors and a chapter on anomalous phaselocking. As in earlier editions, only minimal space has been devoted to circuits. The book is concerned with underlying principles, which remain valid despite technology advances, not with implementations, which change drastically as technology changes. Several parts of the second edition have been omitted: the chapters on optimization and synchronization, and the mathematical appendix. Formal optimization has not proved to be as important to design as was earlier anticipated; instead, a designer is much more likely to perform a trade-off among the few parameters available in a practical phaselock loop. The mathematical appendix has been omitted on the premise that the level of mathematics presented should be comfortable for all electrical engineering graduates. Synchronization, a major discipline of its own, was deemed to have grown too large to cover adequately in a book on phaselock loops. Simulation is another absent topic. Information presented in several chapters is based on simulation. Simulation is crucial for design and verification of integrated circuits. However, this topic is too extensive and deserves a separate book of its own.

RF Systems, Components and Circuits Handbook, Second Edition

Ferril A. Losee
Artech House • 500 pages; $119, £68
ISBN: 1-59693-010-1

To order this book, contact:
Artech House
685 Canton St.
Norwood, MA 02062
(781) 769-9750 ext. 4030
or 46 Gillingham St.
London SW1V 1HH, UK
+44 (0) 207-8750

Since the first publication of this book, in 1997, there have been many changes in the RF field. The goal of this second edition is to add as much new material and to be as up-to-date as possible. It is organized in two parts. Part I, which comprises Chapters 1 through 10, covers RF systems. Important topics include telephone systems, wireless communication systems; global positioning systems (GPS); radar systems; radio frequency signal propagation; RF noise; signal modulation techniques; RF subsystems; modulators and demodulators; and block diagrams of communications systems.

Part II, which comprises Chapters 11 through 19, covers RF components and circuits. Important topics include transmission lines and transmission line devices; waveguides and waveguide-related systems; antennas; lumped constant components and circuits; RF transformer devices and circuits; piezoelectric, ferromagnetic and acoustic wave devices and circuits; semiconductor diodes and their circuits; bipolar and field-effect transistors and their circuits; and vacuum tubes and microwave tubes. An effort has been made to better consolidate subject material. For example, nearly all the material on telephone systems is found in Chapter 1 rather than in a number of chapters. Nearly all the material on radar is found in Chapter 4 rather than being disseminated in a number of chapters. Chapter 3 presents new material on global positioning satellite systems. Chapter 7 includes new material on direct-sequence spread spectrum systems and Chapter 13 includes new material on microstrip patch antennas. One way to make the book interesting and easy to understand is to make use of many illustrations and figures. In this second edition, there are 163 figures in Part I and 196 figures in Part II.

Advertising Index

RS No.	Advertiser	Page No.	Phone	Fax	Web Address
1	AA MCS	167	+33(0)8 11 09 76 76	+33(0)1 76 91 50 31	http://mwj.ims.ca/7956-1
2	Advanced Control Components Inc.	139	732-460-0212	732-460-0214	http://mwj.ims.ca/7956-2
3	Advanced Power Technology RF	96	408-986-8031	408-986-8120	http://mwj.ims.ca/7956-3
4	Advanced Switch Technology	179	613-384-3939	613-384-5026	http://mwj.ims.ca/7956-4
5	Aeroflex	57	516-694-6700	516-694-2562	http://mwj.ims.ca/7956-5
6	Aeroflex/Inmet, Inc.	115	734-426-5553	734-426-5557	http://mwj.ims.ca/7956-6
7	Aeroflex/Weinschel, Inc.	153	800-638-2048	301-846-9116	http://mwj.ims.ca/7956-7
8	Aethercomm	61	760-598-4340	760-598-4342	http://mwj.ims.ca/7956-8
	Agilent Technologies, Inc.	81,143	800-829-4444	415-857-5518	www.agilent.com
9	American Microwave Corporation	109	301-682-6038	301-662-4938	http://mwj.ims.ca/7956-9
10,11	American Technical Ceramics	72,144	631-622-4700	631-622-4748	http://mwj.ims.ca/7956-10
12	Ametek Specialty Metal Products	142	203-949-8837		http://mwj.ims.ca/7956-12
13	AML Communications Inc.	51	805-388-1345	805-484-2191	http://mwj.ims.ca/7956-13
14	Anaren Microwave	107	800-411-6596	315-432-9121	http://mwj.ims.ca/7956-14
15	Ansoft Corporation	87	412-261-3200	412-471-9427	http://mwj.ims.ca/7956-15
16	Applied Wave Research, Inc.	154	310-726-3000		http://mwj.ims.ca/7956-16
17,18	AR Worldwide	30–31,52	215-723-8181	215-723-5688	http://mwj.ims.ca/7956-17
19	Artech House	178	800-225-9977	781-769-6334	http://mwj.ims.ca/7956-19
149	Auriga Measurement Systems, LLC	169	978-441-1117	978-441-2666	http://mwj.ims.ca/7956-149
20	Avtech Electrosystems	136	800-265-6681	613-226-2802	http://mwj.ims.ca/7956-20
21	Cernex, Inc.	18	408-541-9226	408-541-9229	http://mwj.ims.ca/7956-21
22	Chelton Microwave	6	603-775-5200	603-775-5201	http://mwj.ims.ca/7956-22
23	Ciao Wireless, Inc.	32	805-389-3224	805-389-3629	http://mwj.ims.ca/7956-23
24	COM DEV Saw Products	28	647-887-SAWS	519-622-1691	http://mwj.ims.ca/7956-24
25	CPI Beverly Microwave Division	17	978-922-6000	978-922-2736	http://mwj.ims.ca/7956-25
26	Crane Aerospace & Electronics	54	480-961-6269		http://mwj.ims.ca/7956-26
27	CST of America, Inc.	25	781-416-2782	781-576-5702	http://mwj.ims.ca/7956-27
28	CTIA Wireless 2006	159	202-736-3664	202-785-0721	http://mwj.ims.ca/7956-28
29	CTT Inc.	55	408-541-0596	408-541-0794	http://mwj.ims.ca/7956-29
30	Daico Industries, Inc.	53	310-507-3242	310-507-5701	http://mwj.ims.ca/7956-30
31	Damaskos Inc.	179	610-358-0200	610-558-1019	http://mwj.ims.ca/7956-31
32	Dielectric Laboratories Inc.	65	315-655-8710	315-655-0445	http://mwj.ims.ca/7956-32
33	Elisra Electronic Systems Ltd. (Microwave Division)	27	972(3)617-5655	972(3)617-5299	http://mwj.ims.ca/7956-33
34	EMC Technology Inc.	15	772-286-9300	772-283-5286	http://mwj.ims.ca/7956-34
35	Emhiser Micro-Tech	78	775-345-0461	775-345-1152	http://mwj.ims.ca/7956-35
36	Empower RF Systems, Inc.	63	310-412-8100	310-412-9232	http://mwj.ims.ca/7956-36
37	Endwave Defense Systems	23	408-522-3180	408-522-3181	http://mwj.ims.ca/7956-37
38	ET Industries	122	973-394-1719	973-394-1710	http://mwj.ims.ca/7956-38
39	EuMW 2006	168	+ 44 20 7596 8742	+ 44 20 7596 8749	http://mwj.ims.ca/7956-39
40	Filtronic Compound Semiconductors, Inc.	149	408-850-5740	831-621-8074	http://mwj.ims.ca/7956-40
41	G.T. Microwave Inc.	58	973-361-5700	973-361-5722	http://mwj.ims.ca/7956-41
42	GGB Industries, Inc.	3	239-643-4400	239-643-4403	http://mwj.ims.ca/7956-42
43	Herley Industries, Inc.	94	781-729-9450	781-729-9547	http://mwj.ims.ca/7956-43
44	Herotek, Inc.	92	408-941-8399	408-941-8388	http://mwj.ims.ca/7956-44
45	Huber + Suhner AG	79	+41 (0)71 353 41 11	+41 (0)71 353 45 90	http://mwj.ims.ca/7956-45
	IEEE ICUWB 2006	170			www.ICUWB2006.org
	IEEE MTT-S International Microwave Symposium	185	781-769-9750	781-769-5037	www.ims2006.org
	IEEE Radio and Wireless Symposium	183	781-769-9750	781-769-5037	www.radiowireless.org
46	Insulated Wire Inc.	161	203-791-1999	203-748-5217	http://mwj.ims.ca/7956-46
47	Integra Technologies, Inc.	66	310-606-0855	310-606-0865	http://mwj.ims.ca/7956-47
48	International Manufacturing Services, Inc.	42	401-683-9700	401-683-5571	http://mwj.ims.ca/7956-48
49	Isola Corp.	110	800-845-2904		http://mwj.ims.ca/7956-49
50,51,52	J microTechnology	179	503-614-9509	503-531-9325	http://mwj.ims.ca/7956-50
53	Jacket Micro Devices, Inc.	68	404-526-6046		http://mwj.ims.ca/7956-53
54	JFW Industries, Inc.	113	317-887-1340	317-881-6790	http://mwj.ims.ca/7956-54
55	K&L Microwave, Inc.	7	410-749-2424	443-260-2268	http://mwj.ims.ca/7956-55
56	LNX Corporation	105	603-898-6800	603-898-6860	http://mwj.ims.ca/7956-56
57	Locus Microwave, Inc.	24	814-861-3200	814-861-5195	http://mwj.ims.ca/7956-57
58	Lorch Microwave	35	800-780-2169	410-860-1949	http://mwj.ims.ca/7956-58

ADVERTISING INDEX

RS No.	Advertiser	Page No.	Phone	Fax	Web Address
59	M/A-COM, Inc.	11	800-366-2266	978-442-5350	http://mwj.ims.ca/7956-59
60	Marki Microwave, Inc.	108	408-778-4200	408-778-4300	http://mwj.ims.ca/7956-60
61,62	Matrix Systems Corporation	176	818-222-2301	818-222-2304	http://mwj.ims.ca/7956-61
63	Maury Microwave Corporation	9	909-987-4715	909-987-1112	http://mwj.ims.ca/7956-63
64	MECA Electronics, Inc.	62	973-625-0661	973-625-9277	http://mwj.ims.ca/7956-64
65	Micro Lambda Wireless, Inc.	36	510-770-9221		http://mwj.ims.ca/7956-65
66	Microlab/FXR, (a Wireless Telecom Group Company)	19	973-386-9696	973-992-0513	http://mwj.ims.ca/7956-66
68	Micronetics	135	603-579-0900	603-882-8987	http://mwj.ims.ca/7956-68
69	Microwave Communications Laboratories Inc. (MCLI)	13	800-333-6254	727-381-6116	http://mwj.ims.ca/7956-69
	Microwave Journal	180–181,182	800-225-9977	781-769-5037	www.mwjournal.com
70	Mimix Broadband, Inc.	COV 3	281-988-4600	281-988-4615	http://mwj.ims.ca/7956-70
71,72,73, 74,75,76, 77,78,79, 80,81,82	Mini-Circuits	4–5,16,29, 39,40,75, 98–99,117,123, 137,175,187	718-934-4500	718-332-4661	http://mwj.ims.ca/7956-71
83	Mini-Systems, Inc.	148	508-695-0203	508-695-6076	http://mwj.ims.ca/7956-83
84,85	MITEQ Inc.	44–45,141	631-436-7400	631-436-7430	http://mwj.ims.ca/7956-84
86	Modelithics, Inc.	122	888-359-6359	813-558-1102	http://mwj.ims.ca/7956-86
87	Narda Microwave-East, an L3 Communications Co.	93	631-231-1700	631-231-1711	http://mwj.ims.ca/7956-87
88	Narda Microwave-West, an L3 Communications Co.	71	916-351-4500	916-351-4550	http://mwj.ims.ca/7956-88
89	Networks International Corporation	82	913-685-3400	913-685-3732	http://mwj.ims.ca/7956-89
90	Nexyn Corporation	88	408-982-9339	408-982-9275	http://mwj.ims.ca/7956-90
92	NoiseWave Corp.	8	973-386-1119	973-386-1131	http://mwj.ims.ca/7956-92
93	OML Inc.	147	408-779-2698	408-778-0491	http://mwj.ims.ca/7956-93
150	Pascall Electronics Limited	171	+44(0) 1983 817300	+44(0) 1983 564708	http://mwj.ims.ca/7956-150
94	Peak Devices, Inc.	67	978-422-7641	978-422-0011	http://mwj.ims.ca/7956-94
95	Picosecond Pulse Labs Inc.	59	303-209-8100	303-447-2236	http://mwj.ims.ca/7956-95
96	Planar Monolithic Industries, Inc.	111	301-631-1579	301-662-2029	http://mwj.ims.ca/7956-96
97	Prewell Corporation	116	82-31-420-8362	82-31-420-8301	http://mwj.ims.ca/7956-97
98	QuinStar Technology, Inc.	74	310-320-1111		http://mwj.ims.ca/7956-98
67	Radio Freeq	166	866-MYFREEQ		http://mwj.ims.ca/7956-67
99	Radio Research Instrument Co., Inc.	152	203-753-5840	203-754-2567	http://mwj.ims.ca/7956-99
100	Reactel, Incorporated	14	301-519-3660	301-519-2447	http://mwj.ims.ca/7956-100
151	REMEC Defense & Space	64	858-560-1301		http://mwj.ims.ca/7956-151
101,102	Renaissance Electronics Corporation	34,104	978-772-7774	978-772-7775	http://mwj.ims.ca/7956-101
103	RF & Hyper Europe 2006	189	33 (0)1 49 68 51 00	33 (0)1 44 78 99 49	http://mwj.ims.ca/7956-103
104	RF Connectors, Division of RF Industries	136	800-233-1728	858-549-6340	http://mwj.ims.ca/7956-104
105	RF Micro Devices	20–21	336-678-5570	336-931-7454	http://mwj.ims.ca/7956-105
106	RFHIC	173	82-31-250-5011	82-31-250-5089	http://mwj.ims.ca/7956-106
107	RLC Electronics, Inc.	125	914-241-1334	914-241-1753	http://mwj.ims.ca/7956-107
108	Rogers Corporation	91	480-961-1382	480-961-4533	http://mwj.ims.ca/7956-108
109	Rohde & Schwarz GmbH	49	+49-1805-124242	+49-89-412913777	http://mwj.ims.ca/7956-109
110	Rosenberger	50	+49-8684-18-0	+49-8684-18-499	http://mwj.ims.ca/7956-110
111	S.M. Electronics	69	800-715-4396		http://mwj.ims.ca/7956-111
112	San-Tron Inc.	COV 2	978-356-1585	978-356-1573	http://mwj.ims.ca/7956-112
113	Schmid & Partner Engineering AG	97			http://mwj.ims.ca/7956-113
91	SciTech Publishing, Inc.	179	866-510-4724		http://mwj.ims.ca/7956-91
114	Sector Microwave Industries, Inc.	179	631-242-2300	631-242-8158	http://mwj.ims.ca/7956-114
115	Sirenza Microdevices	73	303-327-3030		http://mwj.ims.ca/7956-115
116	Skyworks Solutions, Inc.	43	781-376-3000		http://mwj.ims.ca/7956-116
117	Spectrum Elektrotechnik GmbH	127	+49-89-3548-040	+49-89-3548-0490	http://mwj.ims.ca/7956-117
118	Special Hermetic Products, Inc.	38	603-654-2002	603-654-2533	http://mwj.ims.ca/7956-118
119	Spinner GmbH	151	+49 89 12601-257	+49 89 12601-287	http://mwj.ims.ca/7956-119
120	SSI Cable Corporation	134	360-426-5719	360-426-5912	http://mwj.ims.ca/7956-120
121	State of the Art, Inc.	80	800-458-3401	814-355-2714	http://mwj.ims.ca/7956-121
122	Stealth Microwave, Inc.	76	888-772-7791	609-538-8587	http://mwj.ims.ca/7956-122
123	StratEdge Corporation	90	858-569-5000	858-560-6877	http://mwj.ims.ca/7956-123
124	SV Microwave, Inc.	85	561-840-1800	561-842-6277	http://mwj.ims.ca/7956-124
125	Swift & Associates	133	818-989-1133	818-989-4784	http://mwj.ims.ca/7956-125

ADVERTISING INDEX

Visit Microwave Journal *on the Web at* **www.mwjournal.com**

Visit mwjournal.com/info and enter RS# to request information from our advertisers

Microwave Journal

MARCH 2006 ISSUE

Synthetic Instruments: A New Horizon

Anechoic Chamber Measurement Improvement

RWS 2006 Wrap-up

SALES REPRESENTATIVES

microwave journal

CARL SHEFFRES, PUBLISHER

ED JOHNSON, ASSOCIATE PUBLISHER

KEN HERNANDEZ, TRAFFIC ADMINISTRATOR

Eastern and Central Time Zones
Chuck Curley
Eastern Reg. Sales Mgr.
685 Canton Street
Norwood, MA 02062
Tel: (781) 769-9750
FAX: (781) 769-5037
ccurley@mwjournal.com

Michael Hallman
Eastern Reg. Sales Mgr.
4 Valley View Court
Middletown, MD 21769
Tel: (301) 371-8830
FAX: (301) 371-8832
mhallman@mwjournal.com

Eastern and Central Time Zones
Ed Johnson
Associate Publisher
PO Box 5962
Ocala, FL 34478-5962
Tel: (352) 620-2442
FAX: (352) 620-2443
ejohnson@mwjournal.com

Pacific and Mountain Time Zones
Wynn Cook
Western Reg. Sales Mgr.
PO Box 23200
San Jose, CA 95153
Tel: (408) 224-9060
FAX: (408) 224-6106
wcook@mwjournal.com

International Sales
Richard Vaughan
International Sales Manager
Tel: +44 207 596 8742
rvaughan@horizonhouse.co.uk

Michel Zoghob
Deputy Publisher
Tel: +44 207 596 8741
mzoghob@horizonhouse.co.uk

46 Gillingham Street
London SW1V 1HH, England
Tel: +44 207 596 8740
FAX: +44 207 596 8749

Germany, Austria, and Switzerland (German-speaking)
Juergen Wissling
Wissling Marketing Services
Riedstrasse 5
72813 St. Johann-Wuertingen
Germany
Tel: +49 7122 828140
FAX: +49 7122 828145
jwissling@horizonhouse.com

Israel
Oreet Ben Yaacov
Oreet International Media
15 Kineret Street
51201 Bene-Berak, Israel
Tel: +972 3 570 6527
FAX: +972 3 570 6526
obenyaacov@horizonhouse.com

Korea
Young-Seoh Chinn
JES Media International
2nd Floor, ANA Bldg.
257-1, Myungil-Dong
Kangdong-Gu
Seoul, 134-070 Korea
Tel: +82 2 481-3411
FAX: +82 2 481-3414
yschinn@horizonhouse.com

Singapore
Hoong-Mun Koo
Publicitas
02-01 Wellington Bldg.
20 Bideford Road
Singapore 229921
Tel: +65 6836 2272
FAX: +65 6735 9653